

**‘Studying the Interactions of Cytotoxic
T Cells with Neurons *in vivo*’**

Doctoral Thesis

In partial fulfillment of the requirements for the degree

‘Doctor rerum naturalium’

in the Molecular Medicine Study Program

at the Georg-August University Göttingen

submitted by

Mario Kreutzfeldt

born in Bonn, Germany

Göttingen, January 2013

Members of the Thesis Committee

Supervisors

Prof. Dr. W. Brück

Department of Neuropathology

University of Göttingen (Medical Faculty)

and

Prof. Dr. D. Merkler

Department of Pathology and Immunology

University of Geneva

Second member of the Thesis Committee

Prof. Dr. J. Wienands

Department of Cellular and Molecular Immunology

University of Göttingen (Medical Faculty)

Third member of the Thesis Committee

Prof. Dr. M. Simons

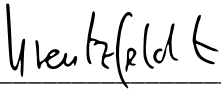
Max-Planck-Institute of Experimental Medicine

Max-Planck-Institute Göttingen

Date of Disputation: 12 March 2013

Affidavit

Here, I declare that my doctoral thesis entitled “Studying the interactions of Cytotoxic T Cells with Neurons *in vivo*” has been written independently with no other sources and aids than quoted.



(Mario Kreutzfeldt)

Göttingen, January 2013

List of publications

Kreutzfeldt M., D. D. Pinschewer, A. Bergthaler, M. Fernandez, W. Brück, K. Steinbach, M. Vorm, R. Coras, I. Blümcke, W. V. Bonilla, T. Misgeld, M. Kerschensteiner and D. Merkler. "Interferon- γ receptor – STAT1 signaling in neurons accounts for CD8⁺ T cell-mediated dendrite and synapse loss in inflammatory central nervous system disease." In Revision

Bonilla, W. V., A. Frohlich, K. Senn, S. Kallert, M. Fernandez, S. Johnson, **M. Kreutzfeldt**, A. N. Hegazy, C. Schrick, P. G. Fallon, R. Klemenz, S. Nakae, H. Adler, D. Merkler, M. Lohning and D. D. Pinschewer (2012). "The alarmin interleukin-33 drives protective antiviral CD8⁺ T cell responses." Science 335(6071): 984-989.

Manrique-Hoyos, N., T. Jurgens, M. Gronborg, **M. Kreutzfeldt**, M. Schedensack, T. Kuhlmann, C. Schrick, W. Bruck, H. Urlaub, M. Simons and D. Merkler (2012). "Late motor decline after accomplished remyelination: impact for progressive multiple sclerosis." Ann Neurol 71(2): 227-244.

Ghosh, A., N. Manrique-Hoyos, A. Voigt, J. B. Schulz, **M. Kreutzfeldt**, D. Merkler and M. Simons (2011). "Targeted ablation of oligodendrocytes triggers axonal damage." PLoS One 6(7): e22735.

Nikic, I., D. Merkler, C. Sorbara, M. Brinkoetter, **M. Kreutzfeldt**, F. M. Bareyre, W. Bruck, D. Bishop, T. Misgeld and M. Kerschensteiner (2011). "A reversible form of axon damage in experimental autoimmune encephalomyelitis and multiple sclerosis." Nat Med 17(4): 495-499.

Flatz, L., T. Rieger, D. Merkler, A. Bergthaler, T. Regen, M. Schedensack, L. Bestmann, A. Verschoor, M. Kreutzfeldt, W. Bruck, U. K. Hanisch, S. Gunther and D. D. Pinschewer (2010). "T cell-dependence of Lassa fever pathogenesis." PLoS Pathog 6(3): e1000836.

TABLE OF CONTENT

AFFIDAVIT	I
LIST OF PUBLICATIONS	II
ABSTRACT	V
ZUSAMMENFASSUNG	VI
LIST OF FIGURES	VII
LIST OF TABLES	VIII
ABBREVIATIONS	IX
INTRODUCTION	1
CNS AS AN IMMUNE PRIVILEGED ORGAN	1
THE MAJOR HISTOCOMPATIBILITY COMPLEX AND ANTIGEN PRESENTATION	3
THE LYMPHOCYTIC CHORIOMENINGITIS VIRUS	6
VIRUS INFECTIONS IN THE CNS AND AUTOIMMUNITY	7
CHORIOMENINGITIS	8
INTRACEREBRAL INFECTION OF LCMV IN NEONATE MICE	9
THE VIRAL DÉJÀ VU MODEL	10
AIM OF THE STUDY	11
MATERIAL	14
HUMAN TISSUE SAMPLES	14
VIRUSES	15
LIST OF MATERIALS	16
BUFFER AND MEDIA COMPOSITIONS	21
METHODS	23
RESCUE OF LYMPHOTITIC CHORIOMENINGITIS VIRUS FROM CDNA	23
FOCUS FORMING ASSAY	24
CELL CULTURE	25
VIRUS PROPAGATION	25
CONCENTRATION OF VIRUSES	25
VIRAL DÉJÀ-VU	25
CREATION OF BONE MARROW CHIMERIC MICE	26
NEUTRALIZATION OF IFN- γ	26

TISSUE ASSERVATION USING 'HOPE' FIXATION	26
TRANSCARDIAL PERFUSION OF MICE	27
RUNNING WHEEL	27
FLOW CYTOMETRY OF BLOOD AND BRAIN TISSUE	27
IMMUNOHISTOCHEMISTRY	28
RNA EXTRACTION	29
QUANTITATIVE REAL-TIME PCR	29
PLASMID PREPARATIONS	29
QUANTIFICATION OF CEREBRAL CD8 ⁺ CELL INFILTRATES	29
QUANTIFICATION OF INFLAMMATORY INFILTRATES AND P-STAT1 ⁺ NEURONS AND DENSITOMETRY	30
GENERATION OF CD8 ⁺ DENSITY MAP OF RE BIOPSY	30
STATISTICAL ANALYSIS	31
RESULTS - AIM 1	33
RESULTS - AIM 2	42
DISCUSSION	51
SUMMARY	57
REFERENCES	XII
ACKNOWLEDGEMENTS	XXIII

Abstract

The central nervous system (CNS) is considered as largely isolated from the immune system – a status referred to as “immune privilege”. But CNS-tissue is constantly surveyed by immune cells and can under certain circumstances, such as viral infections, become a target of inflammatory responses. Cytotoxic T cells (CTLs) combat viruses in peripheral organs as well as the CNS and can contribute to inflammation-induced tissue damage. This concept drives the viral déjà vu mouse model, where defined sequences of lymphocytic choriomeningitis virus (LCMV) infections cause severe CNS inflammation. The CTL response targets viral epitopes of persistently infected neurons that are shared by the used viruses.

To better understand the requirements and consequences for CTL:neuron interactions *in vivo*, different epitope mutants of the immunodominant LCMV epitopes NP396-404 and GP33-41 with different affinities to MHC class I were tested for their contribution in déjà vu disease. While the CTL response against the LCMV nucleoprotein epitope NP396-404 was shown to be pivotal for viral déjà vu disease, the co-expression of high affinity GP33 mutant epitopes did indeed aggravate disease but could not induce viral déjà vu disease in the absence of NP396-404.

Furthermore, the molecular mediators and structural consequences of CTL attack on neurons were investigated by using bone marrow chimeras of CTL effector molecules and their receptors. CTL-derived Interferon- γ (IFN- γ) was identified as key mediator of CTL-induced synapse loss (“deafferentation”) in virus-infected neurons. Deafferentation was found to correlate with clinical disability and depend on the activation of the JAK–STAT1 pathway by IFN- γ -receptor signaling in target neurons. A similar IFN- γ signature was found in human neurons affected by Rasmussen’s encephalitis, a CTL-mediated autoimmune disease.

These results provide important insights into the molecular mechanisms operating at the immunological synapse between CTL and neuron in inflammatory diseases of the CNS.

Zusammenfassung

Das Zentralnervensystem (ZNS) wird als weitgehend vom Immunsystem isoliert angesehen – ein als „Immunprivileg“ bezeichneter Status. Dennoch überwachen Zellen des Immunsystems fortwährend das ZNS-Gewebe, welches unter bestimmten Umständen (z.B. Virusinfektionen) Ziel der Immunabwehr werden kann. Zytotoxische T-Lymphozyten (CTL) bekämpfen Viren in peripheren Organen sowie ZNS und können zu entzündungsinduzierten Gewebeschädigungen beitragen. Dieses Konzept bildet die Grundlage des in Mäusen etablierten viralen-Déjà-vu-Modells, in welchem konzertierte Infektionen mit dem Lymphozytäre-Choriomeningitis-Virus (LCMV) eine schwere ZNS-Entzündung auslösen. Ziel der induzierten CTL-Reaktion sind dabei Epitope auf persistent infizierten Neuronen, welche den verwendeten Viren gemeinsam sind.

Um die *in vivo* Voraussetzungen und Konsequenzen von CTL-Neuron-Interaktionen besser zu verstehen, wurden Varianten der immundominanten LCMV-Epitope NP396-404 sowie GP33-41 mit variierenden Affinitäten für MHC-Klasse-I auf ihren Beitrag zur Déjà-vu-Erkrankung hin getestet. Während sich die CTL-Reaktion gegen das LCMV Nukleoproteinepitop NP396-404 als ausschlaggebend für die Erkrankung erwies, verstärkte die Koexpression von GP33-Varianten hoher MHC-Klasse-I Affinität die Erkrankung. Deren alleinige Expression hingegen reichte jedoch nicht aus um die Déjà-vu-Erkrankung in Abwesenheit von NP396-404 auszulösen.

Des Weiteren wurden die Effektormoleküle und strukturellen Konsequenzen des CTL-Angriffs auf Neurone untersucht. Unter zu Hilfenahme von Knochenmarkchimären von CTL-Effektormolekülen und deren Rezeptoren, konnte CTL-produziertes Interferon- γ (IFN- γ) als Schlüsselmolekül für CTL-induzierten Synapsenverlust (Deafferenzierung) in Virus-infizierten Neuronen identifiziert werden. Dabei korrelierte die Deafferenzierung mit klinischen Symptomen und beruhte in betroffenen Neuronen auf einem via IFN- γ -Rezeptor aktiviertem JAK-STAT1 Signalweg. Eine gleichartige IFN- γ -Signatur wurde in humanen Neuronen von Rasmussen-Enzephalitis-Patienten, eine CTL-induzierte Autoimmunerkrankung, gefunden,.

Diese Ergebnisse geben wichtige Einblicke in die molekularen Mechanismen an immunologischen Synapsen zwischen CTL und Neuronen in entzündlichen Erkrankungen des ZNS.

List of Figures

Figure 1: Schematic comparison of the human and mouse MHC locus.	3
Figure 2: Schematic of the TCR-peptide-MHC complex.	5
Figure 3: Appearance and genomic organization of LCMV.	6
Figure 4: Schematic setup of the viral déjà vu model.	10
Figure 5: S-Segment organization in wild type and re-combinant LCMV.	12
Figure 6: Schematic description of the algorithm utilized to create a CTL density map of a Rasmussen encephalitis brain biopsy.	32
Figure 7: GP33 epitope alone does not cause viral déjà vu disease.	35
Figure 8: GP33 epitope mutants with increased H-2D ^b binding capacity.	36
Figure 9: GP33 epitopes with higher affinity to H-2D ^b do not cause viral déjà vu disease	38
Figure 10: NP396 epitope induces viral déjà vu disease which can be influenced by GP33.	39
Figure 11: Viral déjà vu disease is not influenced by higher numbers of GP33 specific CTLs.	40
Figure 12: Neuronal loss is only observed in late stages of viral déjà vu disease.	43
Figure 13: Deafferentiation in viral déjà vu disease requires CTL contact with infected neurons.	44
Figure 14: Viral déjà vu disease depends on non-hematopoietic IFN- γ receptor.	45
Figure 15: STAT1 upregulation, phosphorylation and nuclear translocation reflect the neuronal signature of IFN- γ signaling.	47
Figure 16: Antibody-mediated block of IFN- γ signaling protects from viral déjà vu disease and neuronal deafferentation.	48
Figure 17: RE biopsies are characterized by widespread CD8 T cell infiltrates and clusters of cortical P-STAT1 ⁺ neurons.	49
Figure 18: Neuronal STAT1 phosphorylation and reduced synaptic boutons in CD8 ⁺ T cell clusters of human Rasmussen encephalitis.	50

List of Tables

Table 1: LCMV-epitope variants of NP396-404 and GP33-41 and MHC class I affinity.	13
Table 2: Clinical data of Rasmussen Encephalitis patients included in the study.	14
Table 3: DNA-Plasmid concentrations for LCMV production.	23
Table 4: qPCR protocol for NP and GAPDH.	29

Abbreviations

adT	–	Adoptive Transfer
APC	–	Antigen Presenting Cell
ARM	–	Amstrong Strain
BBB	–	Blood Brain Barrier
BHK	–	Baby Hamster Kidney
C9I	–	Cysteine to Isolycine Substitution at Position 9
C9M	–	Cysteine to Methionine Substitution at Position 9
CCL	–	Chemokine Ligand
CCR	–	Chemokine Receptor
CD	–	Cluster of Differentiation
Cl.13	–	Clone 13 Strain
CNS	–	Central Nervous System
CTL	–	Cytotoxic T Lymphocyte
DAB	–	3,3'-Diaminobenzidine
DCN	–	Deep Cerebral Nucleus
EBV	–	Epstein-Barr-Virus
ER	–	Endoplasmatic Reticulum
FCS	–	Fetal Calf Serum
FFA	–	Focus Forming Assay
GP	–	Glycoprotein
HHV	–	Human Herpes Virus
HRPN	–	Horseradish Peroxidase
IFN	–	Interferon
IFNGR	–	Interferon-g receptor
IGR	–	Intergenic region
IHC	–	Immunohistochemistry
INDG	–	VSV Indiana G
JAK	–	Janus Kinase
LCMV	–	Lymphocytic Choriomeningitis Virus
Mb	–	Mega base
MC57	–	Mouse Fibrosarcoma Cell Line 57
MHC	–	Major Histocompatibility Complex
MOI	–	Multiplicity of Infection
MS	–	Multiple Sclerosis
N5S	–	Asparagine to Serine Substitution at Position 5
NP	–	Nucleoprotein
pMHC	–	MHC with bound Peptide
P-STAT	–	Phosphorylated STAT1
p0	–	Postnatal day 0
PBS	–	Phosphate Buffered Saline

PFU	–	Plaque Forming Units
PKO	–	Perforin Knock-out
Pol-I	–	DNA Polymerase-I
qPCR	–	Quantitative Real-Time Polymerase Chain Reaction
RE	–	Rasmussen's Encephalitis
rLCMV	–	Recombinant LCMV
RT	–	Room Temperature
STAT	–	Signal Transducer and Activator of Transcription
TAP	–	Transporter associated with Antigen Processing
TLR	–	Toll-like Receptor
TNF	–	Tumor Necrosis Factor
V3A	–	Valine to Alanine Substitution at Position 3
VSV	–	Vesicular Stomatitis Virus
VZV	–	Varicella Zoster Virus
wt	–	Wild type

Introduction

CNS as an immune privileged organ

The brain is a vital organ with complex anatomy. It is comprised of many different specialized cell types and areas. The most prominent cell type within the central nervous system (CNS) is the neuron. Neurons form a complex network with their processes and conduct information via chemical and electrical synapses. A single human brain consists of ca. 100 billion neurons. Each neuron forming in average 100 synapses to other neurons leading to a total number of approximately 1×10^{13} synapses each of which can be remodeled, strengthened or weakened, a process which is called synaptic plasticity. But despite all the inherent plasticity and flexibility, neurons are quite sensitive to changes in their surrounding milieu or disturbances of their healthy steady state by e.g. injuries or infections. Since neurons are postmitotic cells integrated in a complex neuronal network that developed in an activity dependent (experience-driven) manner, they are difficult to replace and might be irreversibly lost. Cumulative loss of neuronal function on a sub-cellular level or neurons itself can lead to severe impairments to the point of death. Given the essential functions of the CNS tissue with neurons as its centerpieces, fighting infections within the CNS is a delicate balance between resolving infection on the one hand and immune mediated tissue damage on the other hand. Additionally, the brain's enclosure within the bones of the skull also greatly limits the tolerance for swelling (e.g. brain edema) and accumulation of (immune) cells within the CNS, as e.g. during inflammatory reactions of the CNS. In spite of the earlier believe that adaptive inflammatory immune responses are limited within the CNS (referred to as "immunoprivileged organ") by an intact blood-brain barrier (BBB) or not supported due to the absence of lymphatic vessels immune competent resident macrophages or dendritic cells, it became evident that the CNS is clearly immune competent. This is, amongst others, reflected in the high threshold for T-cells to engage their target cells within the CNS parenchyma (Tian, Rauvala, and Gahmberg 2009), making it a highly specialized organ for dealing with immune reactions. But the CNS can communicate injury to peripheral parts of the immune system. Spinal chord injury as well as local cytokine administration for example, has been shown to induce chemokine production in the liver (Campbell et al. 2005).

The BBB, as phenomenon first observed by Paul Ehrlich in 1885 (Ehrlich 1885) and extended by Edwin Goldmann in 1913 (Goldmann 1913) separates the blood stream from

the CNS parenchyma. The BBB is made up by endothelial cells forming tight junctions within capillaries of CNS vessels enforced by a surrounding basal lamina and astrocytic end feet coming from the brain's side, the glia limitans. Due to its anatomy, the BBB limits the free exchange of macromolecules but allows free exchange of small hydrophobic molecules like hormones or gas. Importantly, it restricts the access of pathogens (bacteria, worms) to the CNS, a feature of utmost importance to protect from fatal infections even without an adaptive immune system, which is evolutionarily younger than the BBB. Similar barriers exist in the choroid plexus within the ventricles (blood-cerebrospinal-fluid barrier) or in form of the blood-retinal barrier. While the BBB forms a barrier for macromolecules or some pathogens, immune cells can traffic through the BBB. In- and outward lymphocyte trafficking via the choroid plexus has been described and this route is implicated in immune surveillance of the CNS and depends on the CCR6:CCL20 axis (Ransohoff, Kivisäkk, and Kidd 2003; Reboldi et al. 2009). Peripherally activated immune cells can enter the CNS during inflammatory reactions via activated BBB endothelial cells and detect their matching antigens (Ransohoff, Kivisäkk, and Kidd 2003). Interestingly, CD4 and CD8 T cell populations differ in their distribution patterns, as might the underlying trafficking mechanisms. But both populations seem to require a peripheral priming to be able to access the CNS.

As mentioned earlier, the CNS lacks lymphatic vessels. In the periphery, soluble antigens are constantly transported from the interstitial fluid via lymphatic vessels towards secondary lymphatic tissues where they are taken up by professional antigen presenting cells (APCs, e.g. dendritic cells, macrophages, B-cells). APCs present the antigens to B- and T-cells in context of co-stimulatory molecules leading to induction of an adaptive immune response after the recognition of the presented antigen by these cells. So far, drainage of soluble antigens from the brain parenchyma to the cervical lymph nodes has been observed (Cserr and Knopf 1992), in contrast to the migration of APCs from the brain parenchyma to cervical lymph nodes. The most important non-professional APCs within the brain parenchyma are CNS-resident microglia and astrocytes, which possess low expression of MHC and co-stimulatory molecules (Farina, Aloisi, and Meinl 2007; Hanisch and Kettenmann 2007).

Recently it has been demonstrated that neurons can actively regulate immune responses by manipulating local APCs via contact dependent and independent mechanisms. Interestingly, many cell surface molecules involved in neuronal structure and function are involved in these processes. And at sites of neurogenesis and high plasticity (e.g. subventricular zone or dentate gyrus), these immunoregulatory and neuroprotective

mechanism seem to be more pronounced. As a result of this active maintenance of CNS immune regulation, defects on the CNS as well as on the side of the immune system could lead to lower thresholds for infections or proinflammatory responses with pathological outcome, e.g. autoimmune diseases (Carson et al. 2009).

The Major Histocompatibility Complex and antigen presentation

The body commonly encounters allogeneic and xenogeneic entities, e.g. mutated proteins, foreign cells or pathogens. Hence, it is under constant immune surveillance by the immune system. To efficiently perform this task, the immune system needs to discriminate between the body's own ('self') and foreign ('non-self') antigens. This function has been attributed to the genes of the 'major histocompatibility complex' (MHC). In 1916, Little and Tyzzer performed tumor transplants between different mouse strains. They observed that some strains allowed tumor growth while others rejected the tumor (Little and Tyzzer 1916). In the 1940s, Medawar grafted rabbit tissue and observed an inflammatory response in rejected grafts (Medawar 1948). But it was Zinkernagel in the 1970s, who demonstrated that the immune reaction not only depends on the antigen but also on the type of MHC molecule presenting this antigen (pMHC) to cytotoxic T cells (CTLs), a mechanism known as MHC-restriction (Zinkernagel and Doherty 1974) and responsible for tissue rejection. The 4 megabases (Mb) spanning locus of the major histocompatibility complex (MHC) is located on chromosome 6 in humans and chromosome 17 in mice. It consists of many different genes (polygenic) that are highly polymorphic and clustered into three different sub-groups, class I, class II and class III. (Fig. 1). MHC class I and class II loci comprise genes involved in antigen processing and presentation, whereas class III encodes other immune related proteins like components of the complement cascade as well as immune signaling and heat shock proteins.

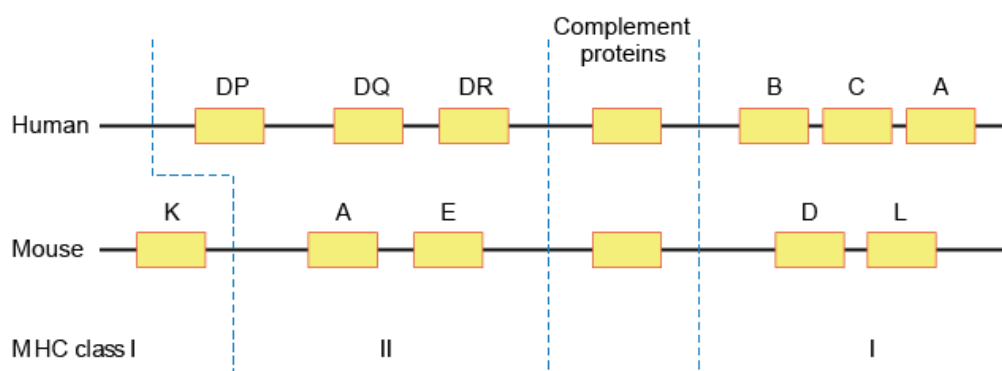


Figure 1: Schematic comparison of the human and mouse MHC locus. The main genes of each class are shown (Penn 2002).

The complexity of MHC-genes results in the expression of unique sets of MHC molecules in each individual from both inherited alleles. Since these molecules are crucial for the presentation of self and non-self peptide sequences (epitopes) to CD4⁺ and CD8⁺ T cells, differences in the MHC-peptide binding pocket sequence lead to different affinities to peptide sequences of the same protein. This explains why the effectiveness of immune responses can differ greatly on an individual level, a phenomenon known as herd immunity. As mentioned before, MHC class I and MHC class II pathways are responsible for antigen processing and presentation. MHC class I is expressed by all nucleated cells and mainly presents peptides from inside a cell (endogenous antigens) to cytotoxic T cells which detect the MHC class I with their CD8 co-receptor and the peptide in the binding pocket with their T cell receptor (TCR). These are the basic prerequisite for interactions of CTLs with their target cells (Fig. 2). Under physiological conditions, the majority of MHC class I presented peptides are self-peptides. The peptide processing for MHC class I takes place in the cytoplasm by the proteasome. These peptides are transported into the endoplasmatic reticulum (ER) by TAP (transporter associated with antigen processing) and subsequently loaded onto MHC class I. Reactive T cell clones with a very high affinity for self-peptides or the MHC molecule itself are deleted during T cell development in the thymus in a process called negative selection, while weak interactions with self-pMHCs are required for CTL survival. Hence, activation of T cells by self-pMHC is tightly controlled during ontogeneity. If a cell expresses foreign proteins during e.g. a virus infection, viral epitopes are presented by MHC class I and can be detected by the corresponding TCR of the CTLs. It has been a matter of discussion if neurons are capable of MHC class I expression and thus epitope presentation. New data has clearly demonstrated that neurons express low levels of MHC class I under steady-state conditions and can upregulate MHC class I expression under inflammatory conditions *in vitro* (Medana et al. 2001; Meuth et al. 2009) as well as *in vivo* (Scheikl et al. 2012). The recruitment of activated CTLs into the CNS can also be observed in viral infections, paraneoplastic disorders (Albert and Darnell 2004) and other autoimmune diseases like multiple sclerosis (Friese and Fugger 2005; Hauser et al. 1986) or Rasmussen encephalitis (Bien et al. 2005). In all settings, CTLs are thought to contribute to neuronal damage and functional deficits. *In vitro*, MHC class I expression can be induced by treating electrically silenced neurons with IFN- γ (Meuth et al. 2009). When loading these neurons with antigenic peptides, the cells are readily killed by activated epitope-specific CTLs. Independent of the function of MCHI in the immune system, its expression on neurons is crucial for normal CNS development (Corriveau, Huh, and Shatz 1998) and

regulation of synapses (Glynn et al. 2011). The MHC class II molecule is mainly expressed by professional APCs and thymus stromal cells. Peptides presented by MHC class II are taken up via endocytosis (exogenous antigens) by professional antigen presenting cells like macrophages, dendritic cells or B cells and recognized by TCRs of T helper cells and CD4 as their co-receptor (Fig. 2).

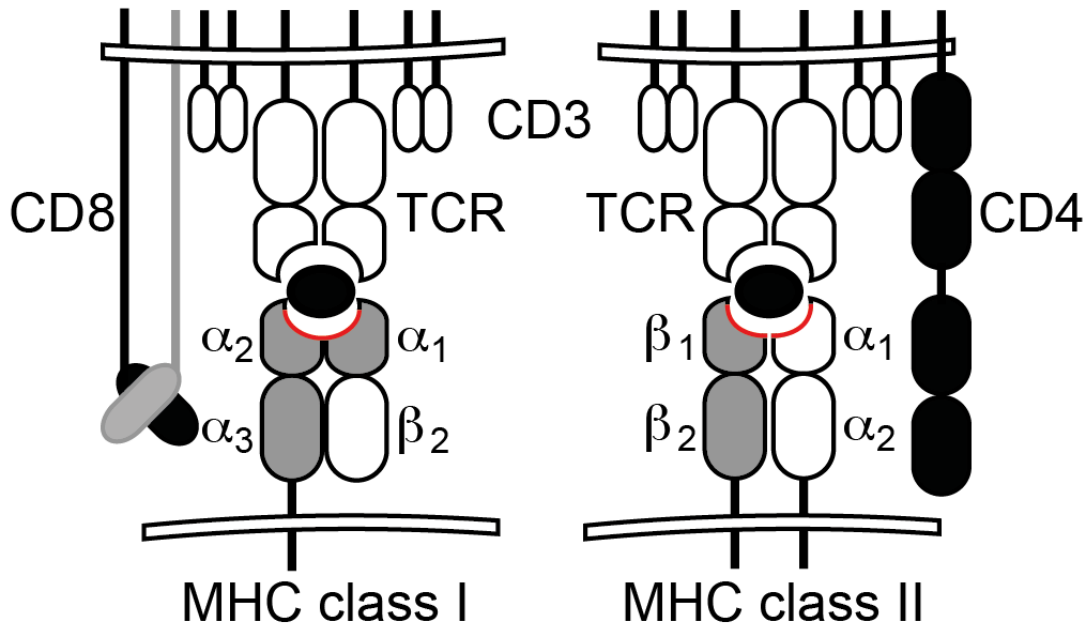


Figure 2: Schematic of the TCR-peptide-MHC complex.

MHC class I presented peptide recognized by CD8⁺ T cell (left) and MHC class II presented peptide recognized by CD4⁺ T cell (right)

The peptide loading onto MHC class II takes place in the endosomal compartment. Moreover, presentation of exogenous antigens via MHC class I by a process named cross-presentation has been described (Rock and Shen 2005). Not every peptide can be loaded on MHC class I or II, respectively. MHC class I has a closed binding cleft and therefore the peptides are limited to a length of 8-10 amino acids (Rammensee, Friede, and Stevanović 1995). In contrast, the sides of the MHC class II binding cleft are open allowing binding of longer peptide chains of 13-17 amino acids. In addition, antigenic peptides must have compatible amino acids to stably interact with the charged anchor residues at specific locations within the binding pocket of the MHCs. Naïve T cells migrate through the peripheral lymphoid tissues sampling the pMHC complexes found on APCs. If a naïve T cell encounters its specific antigen, it stops migrating and starts to proliferate, a process called 'clonal expansion'. After this expansion, the now fully activated effector T cell clones reenter the circulation ready to detect and act on target cells displaying the matching pMHC complex. In this event, CTLs mobilize different effector functions.

Cytotoxicity is mediated by perforin/granzymeB and Fas/FasL (CD95/CD95L) interactions (Stinchcombe and Griffiths 2007) inducing caspase-mediated apoptosis in target cells. CTLs also secrete cytokines including interferon- γ (IFN- γ) and tumor necrosis factor α (TNF- α). To which extend these effector functions contribute to tissue damage depends greatly on the target cell type and tissue (Guidotti et al. 1996; Kägi et al. 1996; Medana et al. 2000). It has been shown *in vitro* that CTLs can attack neuronal somata (Manning et al. 1987) and axons (Medana et al. 2001). Additionally, cultured neurons are sensitive to lysis or silencing by perforin (Meuth et al. 2009; Rensing-Ehl et al. 1996).

The Lymphocytic choriomeningitis virus

The lymphocytic choriomeningitis virus (LCMV) is a prototypic member of the arenaviridae family. This family divides into two serogroups, 'old world' and 'new world'. Members of each family are classified by their genetic differences and geographical distribution. The 'old world' viruses are found in the eastern hemisphere (Europe, Asia, Africa) and the 'new world' in the western hemisphere (South America, United States of America). LCMV, although existing in both areas, is classified as an 'old world' virus. It was 1934 during a meningitis epidemic in St. Louis (USA) that LCMV was first isolated and described by Charles Armstrong, who also named the hitherto unknown virus. Today, many different strains of LCMV are described, e.g. Armstrong, Clone-13, Traub and WE. Characteristic of this class of viruses is their enveloped capsid (Fig. 3A) and bisegmented negative single stranded RNA genome. LCMV's larger genome segment is called L, with 7.2kb, coding for the polymerase L and a small accessory protein Z. The 3.4kb small genome segment codes the glycoprotein precursor protein GPC and nucleoprotein NP. The genes on each segment are encoded with opposite polarities, called ambisense orientation, and separated by an intergenic region (IGR), which forms hairpin structures (Fig. 3B) and likely plays a role in transcription termination (Pinschewer, Perez and De la Torre 2005).

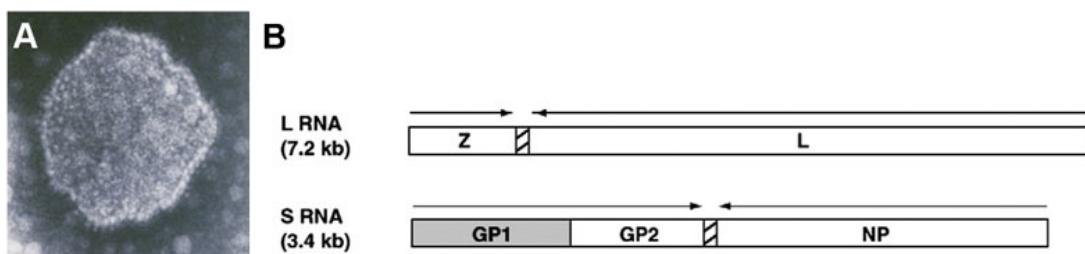


Figure 3: Appearance and genomic organization of LCMV.

(A) Single LCM virion recorded by electron microscopy. (B) Schematic genome organization of LCMV (modified from Oldstone and Campbell 2011).

LCMV is a natural pathogen of rodent populations and a minor human pathogen with a prevalence of 2 to 5 percent (Stephensen et al. 1992). In most cases, human LCMV infections are resolved clinically inapparent, with a mortality of less than 1% (Warkel et al. 1973). Infected adult individuals can, nevertheless, show signs of general malaise (e.g. fever, headache) and in rare cases seizures and fatal meningitis develop. Congenital infections by LCMV can be abortifacient or the virus can act as a teratogen (Barton and Mets 2001).

Virus infections in the CNS and autoimmunity

In many inflammatory diseases of the CNS, CTLs contribute to neuronal damage leading to permanent neurological deficits (Neumann et al. 2002). Due to the aforementioned immunological particularities of the CNS and especially neurons, e.g. low MHC class I expression (Joly, Mucke, and Oldstone 1991), neuronal FasL expression (Medana et al. 2001), TGF- β expression (Liu et al. 2006), little antigen drainage and slow proinflammatory response, this compartment is used by pathogens to evade detection by the immune system. Many different viruses have been described to infect neurons, specifically members of the Herpes, Paramyxo- and Arenavirus families (Brown et al. 1979; Joly, Mucke, and Oldstone 1991; ter Meulen et al. 1984; Sequiera et al. 1979). It has been demonstrated that in *in vivo* infection models of herpes simplex virus, Borna disease virus and Theillers murine encephalitis virus (Chevalier et al. 2011; Khanna et al. 2003), CTLs specifically interact with infected neurons and contribute to disease and neuronal damage (McDole et al. 2010).

Virus infections of the CNS can have different, but not mutually exclusive, consequences: disease, persistence or clearance. Using LCMV infection in mice is a good model to study these phenomena, because it allows driving the outcome in either direction, dependent on the choice of strain, timing, dosis and infection route used. If LCMV infects cells of the CNS, it does so in a non-cytolytic fashion. Viral clearance is CTL mediated, but B and CD4⁺ T cells are important to sustain the antiviral CTL response (e.g. by maintaining splenic integrity). The antiviral CTLs infiltrate the brain parenchyma, a process strictly dependent on the expression of CXCL10 in the brain parenchyma and CXCR3 on the infiltrating cells (Christensen et al. 2004) and clear LCMV from infected neurons probably in a non-cytopathic fashion, since no neuronal dropout can be observed in infected animals (Oldstone 1985). Apart from their essential role as antiviral effector cells, CTLs play a major role in autoimmune diseases like MS (Friese and Fugger 2005; Neumann et al. 2002; Steinman 2001; Willing and Friese 2012). They have been shown to be the

predominant cell type causing damage during relapses and chronic phases of MS. The axonal damage correlates with CTL numbers found in acute MS lesions (Bitsch et al. 2000; Kuhlmann et al. 2002). Furthermore, CD8⁺ cells were found in apposition to demyelinated axons (Neumann et al. 2002), pointing to a directed effect of CTLs on oligodendrocytes and that demyelination is not caused by bystander damage due to general inflammation. The fact that viruses can persist non cytolytically in neurons (Cao, Oldstone, and De La Torre 1997) allows to speculate that certain viruses may be involved in disorders of the CNS with unclear etiology, one of which is Rasmussen encephalitis. RE is a CTL-mediated autoimmune disease that manifests in early childhood and characteristically affects only one cerebral hemisphere, leading to hemiparesis, seizures and loss of cognitive functions. The CNS-infiltrate is dominated by putatively antigen-specific CTLs in close association with CNS neurons (Schwab et al. 2009), histologically closely resembling the CTL infiltrates in the viral déjà vu model.

Choriomeningitis

As mentioned in the previous chapter, LCMV was originally isolated from patients suffering from meningitis. LCMV can be found in ependymal cells, the choroid plexus and in meningeal regions. Since the virus itself is non-cytolytic in mice, the observed disease is induced by the antiviral immune response against infected cells. Intracerebrally infected adult mice develop acute fatal meningitis with nausea and seizures within 6-8 days after infection, a disease that is driven by the antiviral adaptive immune response and ultimately leads to death (Andersen, Marker, and Thomsen 1991; Camenga, Walker, and Murphy 1977; Zinkernagel and Doherty 1974).

It has been shown that virus specific cytotoxic T cells (CTL) are pivotal for disease precipitation as thymectomized mice are protected (Rowe, Black, and Levey 1963). Activated CTLs are recruited into the CSF and engage infected cells in a MHC class I restricted manner. Until now it is unknown which parts of the antiviral effector mechanisms leads to death of the host. Thus far, perforin (Storm et al. 2006), granzyme B (Zajac, Dye, and Quinn 2003), Fas/FasL interactions and TNF- α (Leist and Zinkernagel 1990) were found dispensable for disease. IFN- γ -deficient mice also succumb to disease, but longer survival after infection with a visceral strain was observed. Nonetheless, antiviral-CTL responses in the meninges are considered to lead to lethal disease. Recently it has become evident that antiviral CTLs not only locate to the meninges but also within the CNS-parenchyma in a CXCR3 and CCR5 dependent manner (Christensen et al. 2006). This population seems to be crucial for disease precipitation, since mice in which

CTLs are unable to invade into the CNS parenchyma (CXCR3-deficient) are protected from choriomeningitis induced death. In general it is believed that infected CNS endothelium expresses MHC class I and presents antigen to virus specific CTLs, which enter preferentially at these sites. Consequentially, CTLs release proinflammatory cytokines or lyse the endothelial or astrocytic cells directly in a perforin dependent manner, which in turn increases the blood brain barrier (BBB) permeability (Pinschewer et al. 2010). The importance of TCR-specificity has been demonstrated using LCMV-ARM i.c. infected OT-I mice, possessing endogenous CTLs with a TCR only reactive against an unrelated ovalbumin epitope. In these mice no acute meningitis is observed but after transfer of only 1000 CD8⁺ T cells specific for an epitope in LCMV-GP (GP33-41) lethal disease is induced (McGavern and Truong 2004). This experiment demonstrated clearly the importance of virus specific CTLs for the observed immunopathology and that antigen unspecific bystander T cells contribute only to a minor extend or not at all. LCMV infections can have many different outcomes depending on the route of infection, time point and virus strain used. During this work two main routes of infection, intracerebral in neonates (p0) followed by intravenous infection in adult mice, were used. They will be described in more detail in the following sections.

Intracerebral infection of LCMV in neonate mice

Shortly after the original discovery of LCMV, it was seen that the virus could persist in any organ, including the CNS, when hosts get infected in utero or within the first 24 hours after birth (Traub 1936). When neonate mice get experimentally infected i.c., around 90% of the inoculum leaks into the periphery leading to general infection of different organs in the case of LCMV-ARM. Due to the thymus' involvement, anti-viral T cells with high specificity get clonally deleted in these mice. Using neonatally infected ARM carrier mice, a mutated form of LCMV-ARM could be isolated, called LCMV clone 13 (Cl. 13). Coinfection experiments demonstrated that Cl.13 is far more potent in replicating within the periphery of carrier mice then LCMV-ARM but was outcompeted by it during CNS coinfections. Hence, LCMV-Cl.13 is referred to as viscerotropic and LCMV-ARM as neurotropic, respectively. Interestingly, only two amino acid changes cause the strain differences between LCMV-ARM and Cl.13, namely GP1: F260L (Matloubian et al. 1990; Salvato et al. 1991) and L: K1076Q (Matloubian et al. 1993). Other mutations in GP1: N176D (Sullivan et al. 2011) and L: K1079Q (Bergthaler et al. 2010) have been shown to have minor effects on virus replication and persistence.

The viral déjà vu model

The viral déjà vu model (Fig. 4) allows the study of CTL-mediated neuronal damage *in vivo* (Merkler et al. 2006). If attenuated, genetically modified recombinant LCMV (rLCMV/INDG) (Fig.5) is used to infect neonate mice intracranially (i.c.), the virus persists selectively in CNS neurons (Merkler et al. 2006; Pinschewer et al. 2003). No LCMV is detectable within oligodendrocytes, astrocytes, microglia and endothelial cells. The virus gets cleared from the periphery by the innate immune system in an IFN- α dependent manner (Merkler et al. 2006). Importantly, rLCMV/INDG is non-cytolytic and these mice do not develop spontaneous disease. The antiviral CTL populations are neither primed nor deleted. When referring to this kind of persistently infected mice, the term ‘carrier mice’ will be used. Upon reinfection (challenge) of carrier mice in adulthood with wild type LCMV (LCMVwt) i.v., the mice elicit a strong antiviral immune response with the kinetics of a primary response (Merkler et al. 2006). Within 7-10 days, rLCMV/INDG carrier mice suffer from severe CNS inflammation, which is not observed after LCMVwt infection of non-carrier mice. The infiltrating cells are predominantly CD8⁺ T cells, numerous found in apposition to LCMV⁺ neurons.

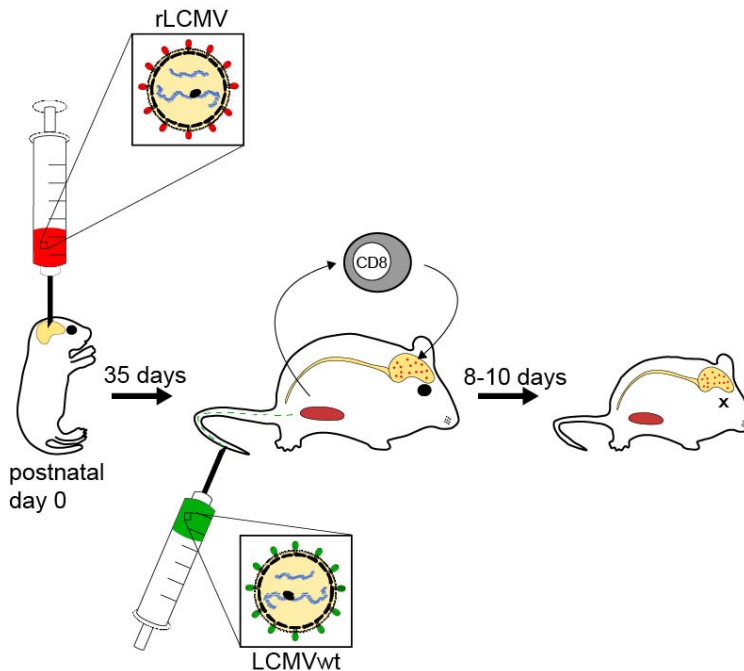


Figure 4: Schematic setup of the viral déjà vu model. Newborn C57Bl/6 mice are infected with attenuated rLCMV intracerebrally within the first 24h after birth. After 35 days the mice receive a second infection intravenously with wildtype LCMV. This infection elicits a strong antiviral CTL response. Since the predisposing and challenging virus share some epitopes, antiviral CTLs infiltrating the brain detect their cognate antigen presented by MHC class I on neurons and lead to disease.

Aim of the study

In the context of very low MHC class I expression on neurons, the molecular prerequisites for neurons to present endogenous non-self peptides on MHC class I *in vivo* are vaguely understood. It is not clear if neurons can effectively present CTL-epitopes and if so, which implications for the neuron result from a possible CTL attack. The interplay between infections, raised immune responses and possibly unknown neuroprotective strategies employed by the CNS are subject of active investigations. CTLs play a key role in these processes but the consequences of CTL-mediated damage on infected neurons remains unknown. By implementing the viral déjà vu model, which is well suited to investigate CTL-neuron interactions *in vivo*, this study addresses the following questions:

Aim 1: What are the qualitative requirements for peptide/MHC-specific interactions of CTL with neurons *in vivo*?

Question 1-1:

Is the epitope-specific pMHC recognition by CTL-TCRs operative on LCMV-infected neurons? If so, LCMVwt induced NP396 specific CTLs should be unable to sense virus in neurons infected with virus carrying the NP396 → N5S mutation, leading to loss of MHC class I binding and déjà vu disease should be prevented.

Question 1-2:

Can déjà vu disease be precipitated by CTLs against LCMV epitopes with moderate MHC class I binding affinities, e.g. GP33-41, or is high affinity MHC binding necessary for disease initiation?

Aim 2: What are the consequences of non-cytolytic CTL engagement for LCMV infected neurons

Question 2-1:

Which subcellular changes can be observed in virus infected neurons that are targeted by virus specific CTLs?

Question 2-2:

Which of the known CTL effector mechanism are required to induce neuronal pathology and disease *in vivo*?

Ad aim 1

To investigate the influence and dependency of the viral déjà vu disease on epitopes with high, intermediate or low/no affinities to MHC class I, different LCMV epitope mutants were created using a reverse genetic approach (Flatz et al. 2006; Pinschewer et al. 2003). This work focused on manipulating the two immunodominant epitopes NP396-404 and GP33-41 (Gairin et al. 1995; Kotturi et al. 2008), both of which are presented by the same MHC molecule H-2D^b. To minimize the influence of other epitopes contained in LCMV-GP the original LCMV/INDG virus was adapted. Instead of using the wild type VSV-GP, the leader sequence of LCMV-GP carrying the GP33 epitope was fused to VSV-GP (Fig. 5).

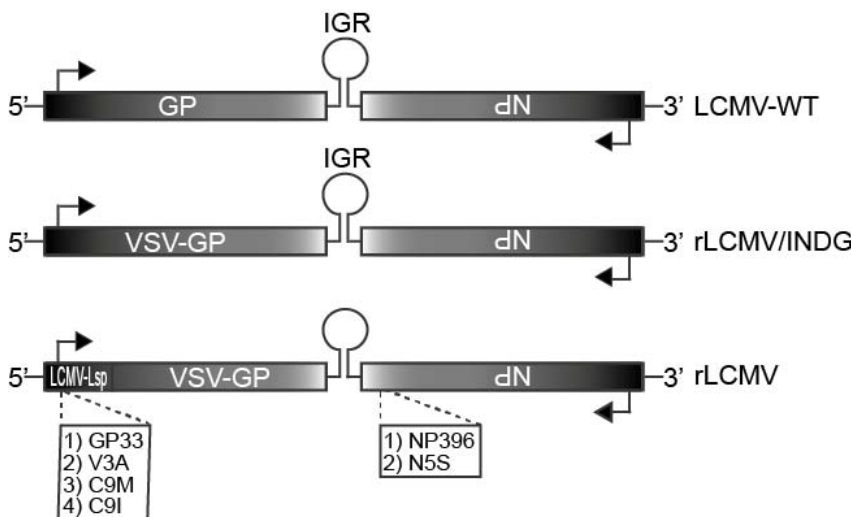


Figure 5: S-Segment organization in wild type and recombinant LCMV. S-Segment of LCMV-WT (top), reverse genetically engineered rLCMV with complete VSV-GP (middle) and mutant epitopes within the Nucleoprotein (NP) and glycoprotein (GP)(bottom).

The S-Segment of LCMV carries 2 genes in ambisense orientation separated by an IGR. Each gene carries H-2b restricted MHC class I immunodominant epitopes, here NP396 on NP and GP33 in GP. The sequences of both epitopes were modified to change the anchor residues of the peptide to MHC class I, thus altering the affinity to MHC class I. Loss of binding mutants: N5S, V3A. Enhanced affinity mutants: C9M, C9I.

The individual amino acid substitutions within the sequences of the immunogenic peptides increased or decreased their affinity to H-2D^b (Table 1). By establishing carrier status in mice using the different rLCMV epitope mutants and inducing déjà vu disease by infecting the carrier mice with LCMVwt, the influence and contribution of each epitope to the déjà vu disease could be addressed.

Table 1: LCMV-epitope variants of NP396-404 and GP33-41 and MHC class I affinity.

Epitope	Variant	Peptide Sequence	MHC class I affinity
NP396-404	Wild type	FQPQNGQFI	High ⁽¹⁾
	N5S	FQPQ[S]GQFI	Non-binding ⁽²⁾
GP33-41	Wild type	KAVYNFATC	Intermediate ⁽¹⁾
	C9M	KAVYNFAT[M]	High ⁽³⁾
	C9I	KAVYNFAT[I]	High ⁽⁴⁾
	V3A	KA[A]NFATC	Non-binding ⁽⁵⁾

1 (Van der Most et al. 1998); 2 (Pinschewer, personal communication); 3 (Gairin et al. 1995);

4 (Utzschneider and Zehn, unpublished); 5 (Boulter et al. 2007)

Ad aim 2

Alongside CTL-induced neuronal cell death, non-cytolytic effector molecules could lead to subcellular changes in neurons during viral déjà vu disease. The subcellular consequences of CTL attack were addressed histomorphologically, focusing on dendrite morphology and synaptic input of LCMV/INDG infected neurons in the déjà vu setting. To address the contribution of different CTL effector molecules to putative subcellular alterations on non-hematopoietic cells in the viral déjà vu model IFNGR^{-/-}, TNFR1/2^{-/-} and FAS^{-/-} carrier mice were lethally irradiated and syngeneic C57Bl/6 bone marrow transplanted. These bone marrow chimeras allowed dissecting the contributions of multiple CTL effector molecules individually by comparing the observed phenotypes to wild type C57Bl/6 mice after viral déjà vu.

Material

Human tissue samples

Human brain biopsies from patients with Rasmussen encephalitis (Table 2) were obtained from the department of Neuropathology at the Universitätsklinikum Erlangen. Their use for scientific purposes was in accordance with institutional ethical guidelines and was approved by the ethics committee of the University of Göttingen (Germany).

Table 2: Clinical data of Rasmussen Encephalitis patients included in the study

Patient ID (1)	Gender	Age at surgery (years)	Age at onset of epilepsy (years)	Duration of epilepsy (years)	Localization	Side of resection	Seizure type (2)
A	female	15	6	9	frontal, temporal	left	Aura, Myoclonia, SPS
B	male	8	6	2	temporal	left	EPC
C	male	9	5	4	frontal	left	SPS, CPS
D	female	3	2	1	temporal	left	EPC
E	female	42	33	9	temporal	right	SPS
F	female	7	n.a.	n.a.	frontal, temporal	left	n.a.

- 1 Patient ID (biopsy number): A (N574/07); B (N356/07); C (N814/11); D (N211/06); E (N1193/08) ; F (N948/08)
- 2 CPS=complex partial seizure; EPC=epilepsia partialis continua; SPS=simple partial seizure; sGTCS=secondary generalized tonic clonic seizure. n.a.=not analyzed

Mice

C57Bl/6 wild type, TCR327xLy5.1xRAG1^{-/-} (Pircher et al. 1989) and mice deficient for perforin (PKO) (Kägi et al. 1994), TNF receptor 1 and 2 (TNFR1/2^{-/-}) (Peschon et al. 1998), Fas (FAS^{-/-}) (Adachi et al. 1995) or interferon-gamma receptor (IFNGR^{-/-}) (Huang et al. 1993) were used. All transgenic lines were on C57Bl/6 H-2D^b background. Animals were bred at either the “Zentrale Tierexperimentelle Einrichtung” Göttingen or the animal facilities of the “Centre Medical Universitaire” Geneva and housed under P2 conditions. All experiments were approved and authorized by the cantonal veterinary office of Geneva (Switzerland) and performed in accordance with the Swiss law for animal protection or at the university of Göttingen with the authorization by the district government in Braunschweig in accordance with the German law for animal protection.

Cell lines

Baby hamster kidney (BHK) fibroblast cell lines BHK-21 (ATCC CCL-10) and BHK-21 clone 23 (Sigma-Aldrich) were used to rescue and propagate LCMV. MC57G (ATCC CRL-2295) and HEK-293 (ATCC CRL-1573) cells were used for viral titer measurement.

Viruses

All virus work was performed under biosafety level 2 laboratory conditions and approved and authorized by the German and Swiss authorities, respectively.

List of Materials

<u>Material</u>	<u>Reference</u>	<u>Manufacturer</u>
<u>Bacteria</u>		
DH5alpha	18265-017	Invitrogen
<u>Enzymes</u>		
GoTaq DNA Polymerase	M3175	Promega
IQ SYBR Green Supermix	170-8882	BioRad
iScript cDNA Synthese Kit	170-8891	BioRad
Pfu Turbo DNA Polymerase	600250	Agilent
Phusion Hot Start Polymerase	M0530S	NEB
Proteinase K	19131	Qiagen
rAPid alkaline phosphatase	4898133001	Roche
T4 DNA Ligase	M0202S	NEB
Trypsin-EDTA	25300054	Invitrogen
<u>Antibodies</u>		
CD3 rat anti human (clone MCA1477)	MCA1477T	AbD Serotec
CD8 rat anti mouse (clone YTS169)	ab22378	Abcam
CD8 mouse anti human (clone C8/114B)	GTX72053	Dako
Cy2, Cy3, Cy5-secondary antibodies	–	Jackson Immuno
NeuN (Clone A60)	MAB377	Chemicon Intl.
Goat anti rat IgG peroxidase coupled	112-035-003	Dianova
Synaptophysin mouse anti rat (SY38)	M077601	Dako
LCMV-NP (clone VL4, polyclonal rat sera)	–	Non-commercial
P-STAT1 (Tyr 701) rabbit	9167S	Cell Signaling
Horseradish peroxidase (Rat IgG1)	BE0088	BioXcell
Murine-IFN-gamma (clone XMG1.2)	BE0055	BioXcell
<u>Antibodies for Flow Cytometry</u>		
B220 PerCP (clone RA3-6B2)	553093	BD Pharmingen
B220 PerCP/Cy5.5 (clone RA3-6B2)	45-0452-82	eBioscience
CD127 PE (clone A7R34)	12-1271-82	eBioscience
CD44 APC/Cy7 (clone IM7)	103028	Biolegend
CD45.2 APC (clone 104)	17-0454-82	eBioscience
CD62L PE/Cy7 (clone MEL-14)	104418	Biolegend
CD8a FITC (clone 53-6.7)	553030	BD Pharmingen

Material

CD8a Pacific Blue (clone 53-6.7)	100725	Biolegend
KLRG-1 FITC (clone 2F1)	11-5893-82	eBioscience
<u>iTAg MHC Tetramers</u>		
H-2 D ^b LCMV (FQPQNGQFI) APC	T03029	Beckman Coulter
H-2 K ^b LCMV (AVYNFATC) PE	T03016	Beckman Coulter
H-2 K ^b LCMV (KAVYNFATC) APC	T03003	Beckman Coulter
H-2 K ^b LCMV (KAVYNFATC) PE	T03001	Beckman Coulter
<u>Kits</u>		
Avidin-Biotin Block	X0590	Dako
BD FACS lysing Solution	349202	BD
Gel Extraktion Kit	28706	Qiagen
M.O.M. Kit	2202	Biozol
pGEM-T Vector System I	A3600	Promega
Plasmid Midi Kit	12143	Qiagen
Plasmid Mini Kit	27104	Qiagen
<u>Buffer and Media</u>		
DMEM	61965-059	Gibco
DMEM w.o. phenol red	31053-044	Invitrogen
DMEM (powder)	52100-039	Gibco
DMEM (high glucose)	31966047	Invitrogen
DMEM (no glucose)	11966025	Invitrogen
Fluorescence mounting medium	S3023	Dako
DePex mounting medium	18243	Serva
Immu-Mount	9990402	Thermo
Fetal bovine serum (FCS)	S0115	Biochrom
Glucose powder	15023-021	Gibco
HEPES 1M	15630-056	Gibco
MEM	31095052	Invitrogen
Na-Pyruvate MEM (100mM)	11360039	Invitrogen
Opti-MEM	11058-021	Gibco
Phosphate buffered saline (PBS)	L182-50	Biochrom
S.O.C. Medium	15544-034	Invitrogen
Sodium Pyruvate, 100mM	11360-039	Gibco
<u>Solutions and solvents</u>		
A.bidest (for molecular biology)	T143-3	Roth

Material

Acetone	176800025	Acros Organics
Chloroform	7331.2	Roth
Ethylenediaminetetraacetic acid (EDTA)	8043.3	Roth
Ethanol	1009832500	Merck
Ether	8810.1	Roth
Heparin	H1027-50KU	Sigma
Isopropanol	8187662500	Merck
Peresal	PLH6	Ecolab
Trizma-base	T1503	Sigma
Trizol	15596-026	Invitrogen
Xylol	1086611000	Merck

Chemicals

Agarose	V3125	Promega
Agarose (Low Melting Point Agarose)	15517-022	Invitrogen
Ammonium nickel (II) sulfate hexahydrate	574988-100G	Sigma-Aldrich
Bacto Agar	212750	BD
Bacto Tryptone	211705	BD
Bacto Yest Extract	212750	BD
BD Micro-Fine+ 0.3ml syringes	230-4533	BD
BD Micro-Fine+ 0.5ml syringes	037-7614	BD
Citric acid	1002440500	Merck
DAB	D-5637	Sigma
DAPI	D1306	Invitrogen
Desomed Rapid AF	DT-311-005	Desomed
Dimethylsulfoxid (DMSO)	D2650-100ML	Sigma
DNA ladder, 100bp	25-2021	peqlab
DNA ladder, 1kb	25-2231	peqlab
DNA loading Dye, 6x	98-0034	peqlab
dNTP Mix, 2.5mM	R725-01	Invitrogen
EDTA	8043.3	Roth
Eosin-G	1159350025	Merck
Ethidium bromide	15585-011	Invitrogen
Glutamin	25030	Gibco
Glycerol ultra	G6279	Sigma
Glycose	49161	Fluka
HOPE I	HL001R500	DCS Diagnostics
HOPE II	HL002C001	DCS Diagnostics

Material

Hydrochloric acid (25%)	1003122500	Merck
Hydrogen peroxide	H1009-100ML	Sigma-Aldrich
IPTG (1g)	15529019	Invitrogen
L-Glutamine 200mM (100x)	25030024	Invitrogen
Lipofectamine Transfection Reagent	18324-012	Invitrogen
Luxol Fast Blue (Solvent blue38)	80140	Clin-Tech
Mayers Hemalaun	1092490500	Merck
Methocel	64620	Sigma
Neurotrace	N-21479	Invitrogen
Paraffin (low melting point)	PL003S2K	DCS Diagnostics
Paraformaldehyde (PFA)	1040051000	Merck
Penicilline /Streptomycine	12140-122	Gibco
Percoll	17-0891-01	GE Healthcare
Puromycin	QLL 3368B	Invitrogen
Rnase Zap	34022090	Ambion
SYBR-safe	S33102	Invitrogen
Sodium Azide Tablets	106687	Merck
Triton X-100	807423	ICN Inc.
Trizol	15596-026	Invitrogen
Tryptose	T8782-500G	Sigma
Tween-20	8221840500	Merck
X-Gal	10651745001	Roche
<u>Consumables</u>		
24 well plates	92424	Milian
6 well plates	92006	Milian
96 well plates (qPCR)	72.1978.202	Sarstedt
96 well plates (U-bottom)	6018111	Ratiolab
Adhesive sealing tape	951999	Sarstedt
Amicon Ultra-15 (100 kDa)	UFC910024	Millipore
Animal lancet for use on mice	-	MEDpoint
Autoclavable bags	AP-10-00618	Uniequip
Cell culture flask, T150	90151	Milian
Cell culture flask, T75	90076	Milian
Cell strainer, 70 µm	352350	BD
CryoTube, 1ml	377224	Nunc
Diethyl Polycarbonate (DEPC)	D5758-25ML	Sigma-Aldrich
FACS tubes, 5ml, polystyrene	2110554	BD

Material

Microscope cover slips	C10143263NR2	Thermo Scientific
Multiply- μ Strip Pro 8-strip	72.991.002	Sarstedt
Parafilm	P1150-2	Pechiney
Phenol red	32661	Riedel-de Haen
Pipet filter tips, 100 μ l	70.760.212	Sarstedt
Pipet filter tips, 10 μ l	4AJ-9409145	Ratiolab
Pipet filter tips, 1ml	70.762.100	Sarstedt
Razor blades	62-0167	GEM
RNA-later	AM-7021	Ambion
Round bottom tube, 14ml	352059	BD
Safe-Lock Eppendorf tubes, 0.5ml	22600001	Eppendorf
Safe-Lock Eppendorf tubes, 1.5ml	22600028	Eppendorf
Safe-Lock Eppendorf tubes, 2ml	22600044	Eppendorf
Serological pipette, 10ml	4488	Corning
Serological pipette, 25ml	86.1685.001	Sarstedt
Serological pipette, 2ml	SER-2ML-SI	Axygen Scientific
Serological pipette, 5ml	4487	Corning
Stainless Steel Beads	69989	Qiagen
Superfrost Plus slides	4951PLUS	Thermo Scientific
Syringe 10ml, luer-lock	300912	BD
Test tubes, 15 ml	352096	BD
Test tubes, 50ml	352070	BD
TissueTek	4583	Sakura

Machines

Fluorescence Microscope	BX50	Olympus
Gallios flow cytometer		Beckman Coulter.
Microwave		Bosch
Mirax MIDI Slide Scanner	-	Zeiss
Perfusion pump	MCMS/CA4/8	Ismatec
Pannoramic 250 Flash		3DHistech
Rotarod	7650	Ugo Basile
Running Wheel System	-	Custom-built

Software

Adobe Illustrator CS6	CS6	Adobe
-----------------------	-----	-------

Adobe Photoshop CS5	CS5	Adobe
AnalySIS	2.11	Olympus
CellSense Dimension	1.7.1	Olympus
Definiens	2.04	Definiens
Office for Mac	2011	Microsoft
Pannoramic Viewer	1.15	3DHistech
Prism	5.05d	Graphpad

Instruments

Acryl Matrix: Mouse 1mm coronal	BS-5000C	Braintree Scientific
Ear puncher	3104605	Ebeco

Buffer and Media Compositions

1% Ammonium nickel sulfate solution

Ammonium nickel (II) sulfate hexahydrate	0.1 g
Distilled water	10 ml

BHK21 culture medium

DMEM	412 ml
FCS	50 ml
Hepes (1M)	5 ml
Na-Pyruvat (100mM)	5 ml
Glucose (20%)	13 ml
Glutamine	5 ml
Tryptose (50%)	10 ml

DAB color reaction solution

3,3'-Diaminobenzidine (DAB)	25 mg
PBS	50 ml
Hydrogen peroxid (30%)	30 µl
Ammonium nickel sulfate solution (1% solution)	2.5 ml

FACS-buffer

PBS	500 ml
FCS	10 ml
EDTA (0.5mM, pH 8)	2 ml
Sodium azide	0.25 g

MC57 culture medium

MEM	500 ml
-----	--------

Pen/Strep	5 ml
Glutamine	5 ml
FCS	25 ml

4% Paraformaldehyde solution

FPA	40 g
10x PBS	100 ml
Distilled water	9000 ml
Adjust to pH 7.3	

Tris-EDTA buffered saline

Trizma-base	1.21 g
EDTA (1M)	1 ml
Distilled water	1000 ml
Adjust to pH 9	

Methods

Rescue of Lymphotitic choriomeningitis virus from cDNA

All viruses used in the experiments were generated using a DNA plasmid rescue system described by Bergthaler and Flatz (Flatz et al. 2006), employing cationic lipid-mediated transfection reagent Lipofectamine. The positively charged head-group of the lipid can spontaneously aggregate with the anionic phosphate backbone of DNA, forming a positively charged transfection complex, which can interact with the negatively charged cell membrane by fusion or endocytosis resulting in the release of the genetic material into the cytoplasm. Finally, the DNA must end up in the nucleus for successful gene expression and recovery of viable virus.

Here, 4 different plasmids were transfected into BHK cells to generate LCMV. Two of these plasmids provide the minimal transacting factors for LCMV replication, the nucleoprotein (NP) and viral RNA-dependent RNA polymerase (L) and carry a RNA-Polymerase-II promoter sequence, so the encoded genes can be directly transcribed into mRNA and translated into protein by the host cell. The other two plasmids provide the two viral genome segments (S-and L-segment), flanked by RNA-polymerase I (Pol-I) promoter and terminator sequences. Products of Pol-I lack a polyA tail and provide the template for viral genome replication by the viral polymerase L.

Protocol:

For the rescue, 6×10^5 cells per well were seeded in a 6 well plate. The next day, plasmid/lipofectamin transfection mix (Table 3) was prepared by adding each plasmid into 100 μ l Optimem and slowly adding 100 μ l Lipofectamine-Opimem-Mix (12 μ l Lipofectamine + 88 μ l Optimem) to the plasmids.

Table 3: DNA-Plasmid concentrations for LCMV production

Pol-II-pC NP (helper plasmid)	0.8 μ g
Pol-II pC L (helper plasmid)	1 μ g
Pol-I S (viral genome)	0.8 μ g
Pol-I-L (viral genome)	1.4 μ g

This mix was incubated for 30-45 minutes after which 800 μ l Optimem was added and applied on cells with 80% confluence. After 5 hours, the transfection mix was removed and 2 ml prewarmed BHK medium was added. After 72 h, the supernatant was removed

and the cells transferred into a 75 mm² flask with 20 ml of BHK medium. After additional 48 h incubation, the supernatant was harvested, centrifuged down once for 5 min at 1200 rpm, transferred into a clean tube and aliquoted. The virus was titrated by using the 'focus forming assay' and stored at -80 °C.

Focus Forming Assay

The Focus Forming Assay (FFA) is a method to determine the titer of a given LCMV sample and is based on the Plaque Forming Assay, a method used to determine titers of lytic viruses. Since LCMV is non-lytic the titer is determined by visualizing foci of infected cells with anti-nucleoprotein (NP) antibody VL4 and the avidin-biotin technique with 3,3'-diaminobenzidine (DAB) as chromogen. Nevertheless, the convention of using the term "plaque forming units" (PFU) instead of "focus forming units" to describe the titer was retained.

Protocol:

First, MC57 cells were adjusted to a density of 8×10^5 cells/ml and kept on ice until usage. Using a 96-well U-bottom plate, the rows 2-11 were prefilled with 130 μ l of MEM/2%FCS/PSQ. To achieve serial dilution of the virus sample, 200 μ l of the sample was added to row 1 and 60 μ l of the sample was transferred into the next row successively until row 12. The pipet tips were exchanged every 3 dilution steps. The 200 μ l (2x100 μ l) from the dilutions of row 11, 9, 7,5,3 and 1 were transferred into rows 1-6 of a 24-well plate, thus covering 10x serial dilutions of up to 10^{-5} . Next, 200 μ l MC57 cells were added into each well and spread out using a '+' shaped movement with the plate. The plate was left in a CO₂ incubator at 37°C for 2-4 hours before 200 μ l of DMEM-overlay (2x DMEM/10% FCS/2x Glutamine/2x Penicillin and Streptomycin) was added and the plates were incubated for 2 more days. For the staining, the overlay was discarded 200 μ l 4% paraformaldehyde (PFA) in PBS was added into each well and incubated at room temperature (RT) for 30 minutes to fix the cells and inactivate the virus. The PFA was discarded and 200 μ l TritonX solution was added for 20 minutes at RT. After discarding the TritonX solution, 200 μ l of PBS/5% FCS was added for 1h to block non-specific binding of antibodies. The blocking solution was replaced by 200 μ l VL4 monoclonal antibody diluted 1:30 in PBS/2% FCS. After washing two times with PBS, 200 μ l peroxidase-conjugated secondary antibody diluted 1:200 in PBS/2% FCS was added to the cells and incubated for 1 h. After washing two times with PBS, 400 μ l color reaction was added to the cells for 10-15 minutes and the reaction was stopped by

flicking off the color reaction and washing with tap water. To calculate the titer of the measured LCMV-aliquot, all foci in a well were counted. Since every focus corresponds to one infectious particle, the number has to be multiplied by the well's corresponding dilution and by the factor five, because only 200 µl of the original sample were used for the dilutions. A typical titer of wild type LCMV (e.g. LCMV-Armstrong) was in the range of 10^6 to 10^7 PFU/ml.

Cell culture

The BHK and MC57 cell lines were cultivated at 37°C and 5% CO₂ until reaching 80-90% confluence. At this point, cells were washed with PBS and incubated with 1 ml Trypsin-EDTA for 10min. Trypsinisation was stopped by adding 10 ml of FCS containing medium. 500 µl of the cell suspension was transferred into a new flask and supplemented with the corresponding cell culture medium. For detailed composition of the used media see material section.

Virus propagation

To passage LCMV, BHK cells were seeded into a cell culture flask and infected with a 'multiplicity of infection' (MOI) of 0.01 to 0.1. The corresponding amount of virus was diluted in 1 ml of BHK medium and left on the cells for 1h at 37° C. After this time, the 1 ml was removed and replaced by 20 ml fresh medium. Wild type LCMV was harvested after 48 h, attenuated LCMV (non-wild type) was harvested after 72h. For this, the cell culture supernatant was transferred into a 50 ml tube and centrifuged for 5 minutes at 1200 rpm to spin down residual cells and cell debris. After that, the supernatant was transferred into a fresh 50 ml tube, aliquotted and the virus titer measured by focus forming assay.

Concentration of viruses

For concentrating LCMV, Amicon Ultra 100 kDa Filters were used according to the manufacturers protocol until desired reduced volume was reached.

Viral déjà-vu

This animal model offers the unique opportunity to specifically investigate the molecular requirements of CTL-neuroaxonal interactions *in vivo* (Merkler et al. 2006). To establish a viral carrier status in CNS-neurons, newborn C57Bl/6 mice were infected with 10^5 to 10^6 PFU rLCMV intracerebrally using a 27-gauge needle (predisposing virus). The tip of the

protection cap was cut in a way that it forms a spacer to limit the depth of penetration of the injection needle to approximately 1.5 mm. The location of injection was 1 mm posterior to bregma and 2 mm lateral to the sagittal suture. A final volume of 30 μ l was injected. At 35 days of age, the mice receive a peripheral infection with 1×10^5 PFU LCMV-ARM in 200 μ l MEM into the tail vein (challenging virus). Voluntary running behavior was recorded until the end of the experiment.

Creation of bone marrow chimeric mice

Mice were lethally irradiated at the age of five to six weeks. IFNGR^{-/-}, TNFR1/2^{-/-} or FAS^{-/-} mice were reconstituted with C57BL/6 bone marrow and splenocytes, thus limiting the deficiency to the non-lymphohematopoietic compartment. Infecting mice with LCMVwt four to eight weeks after bone marrow reconstitution induced viral déjà vu.

Neutralization of IFN- γ

Mice were either injected i.p. with 2 mg anti-IFN- γ monoclonal rat antibody (clone XMG1.2) or 2 mg rat IgG1 isotype control five days after LCMVwt i.v. challenge.

Rotarod

Mice were placed on a rotating rod (rotarod) constantly accelerating from 10 to 80 rounds per minute for a maximum of 180 seconds. Animals were habituated and trained to the rotarod daily from day -3 to day 0 (day of LCMVwt i.v. challenge) and tested on day 3, 5 and 7-10. The time for mice to drop from the rotarod was monitored, and the two best runs out of three at each day were averaged for analysis. Values are displayed as percentage of healthy non-carrier controls on day 10.

Tissue asservation using 'HOPE' fixation

"HEPES-Glutamic Acid Buffer Mediated Organic Solvent Protection Effect" (HOPE) conservation is a alcohol and aldehyde (e.g. formalin) free tissue fixation method utilizing a HEPES/glutamic-acid buffer (Olert et al. 2001). Since macro molecular structures (e.g. proteins, nucleic acids) are not cross linked, their native structures are retained. Therefore, many antibodies validated for cryo sections work on HOPE tissue and analysis by PCR or qPCR is possible.

Protocol:

Mice were transcardially perfused with cold PBS and tissues taken and cut before transferring them into a glass containing 4 ml of HOPE I solution. After an overnight incubation at 4 °C, HOPE I solution was replaced by HOPE II solution diluted 1:1000 in ice cold molecular grade acetone and incubated for 2 h at 4°C. The acetone / HOPE II solution was replaced by pure ice-cold acetone and incubated for 2h. This step was repeated for 2 more times. Finally, the tissue samples were transferred into a plastic tissue capsule and embedded in low melting paraffin overnight at 60 °C. The final blocs were stored at 4 °C. Tissues subject to qPCR measurements were transcardially perfused with PBS before HOPE asservation.

Transcardial perfusion of mice

Mice were transcardially perfused with cold PBS and fixed with 4% PFA if not noted otherwise. Organs were removed and post-fixed 24 hours in 4% PFA at 4°C after which the organs were embedded in paraffin.

Running wheel

To assess the voluntary motor performance, mice were transferred into individual cages containing a running wheel with regularly spaced crossbars (Liebetanz and Merkler 2006). A sensor in the axis of each running wheel allows the following performance parameters to be recorded by a computer:

- 1) Maximum running velocity in rotations/min (V_{max})
- 2) Accumulated distance in meters ($Dist_{ac}$)
- 3) Number of individual runs (N_{run})
- 4) Accumulated running time (T_{total})
- 5) Maximum distance in one run ($Dist_{max}$)

Flow cytometry of blood and brain tissue

Flow cytometry was performed on full blood or isolated brain lymphocytes. For both sample types the same staining protocol was used.

Blood withdrawal:

Blood was withdrawn by submandibular bleeding (Golde, Gollobin, and Rodriguez 2005) and collected into EDTA-containing tubes to prevent clotting. Staining was performed using 50 µl of blood.

Percoll lymphocyte isolation:

To assess the frequencies of encephalitogenic cytotoxic T cells, mice were transcranially perfused using ice cold PBS and brains removed and stored in PBS on ice. The tissue was homogenized using a metal strainer and filtered with a 40µm strainer into a 50 ml tube. After centrifugation of 5 min at 1500rpm, the PBS was removed and the pellet resuspended in 70% Percoll. This solution was layered underneath a 37% Percoll layer, which in turn was layered underneath a 30% Percoll layer. After 25 min of centrifugation, the myelin layer was discarded and the cloudy interphase above the 70% Percoll containing the lymphocytes transferred into a fresh 50 ml tube and washed with FACS-buffer for 10 min at 1000 rpm.

70% Percoll, 5 ml / sample: 3.5 ml Percoll + 1.5 ml DMEM (2% FCS)

37% Percoll, 4 ml / sample: 1.48 ml Percoll + 2.58 ml DMEM (2% FCS)

70% Percoll, 4 ml / sample: 1.2 ml Percoll + 2.8 ml DMEM (2% FCS)

Staining protocol:

Cells were washed in FACS-buffer by centrifugation at 1200rpm for 5min at 4°C. FACS-buffer was removed and 50 µl antibody mix was added and incubated for 30min at 4°C. Antibodies were removed by washing two times with FACS-buffer followed by centrifugation. Lysis of erythrocytes and fixation of the cells was achieved by using Fix/Lyse solution according to the manufacturers protocol.

Immunohistochemistry

CNS tissue was either fixed with 4% PFA or in HOPE fixative and embedded in paraffin as described previously (Bergthaler et al. 2007). For light microscopy, endogenous peroxidases were neutralized with 3% H₂O₂ in PBS and unspecific binding blocked with 10%FCS in PBS. Sections were stained with the indicated primary antibodies. Bound primary antibodies were visualized either by an avidin-biotin technique with 3,3'-diaminobenzidine or alkaline phosphatase/anti-alkaline phosphatase as chromogens. For light microscopy, nuclei were visualized via haemalaun counterstaining. For fluorescence

microscopy, the appropriate species-specific Cy2-, Cy3- or Cy5-conjugated secondary antibodies were used. Nuclei and Nissl counterstaining was performed using DAPI or Neurotrace.

RNA extraction

30µm thick sections of HOPE fixed paraffin embedded tissue were cut and collected in 1.5 ml tubes. Paraffin was removed by isopropanol and the tissue dissolved in Trizol. The RNA was extracted using Guanidinium thiocyanate-phenol-chloroform extraction followed by isopropanol precipitation.

Quantitative real-time PCR

Quantitative real-time PCR (qPCR) was performed using an iCycler (Bio-Rad) using SYBR-green and the reaction protocol in table 4. Samples were normalized against GAPDH. Melting curve analysis was performed to exclude primer dimer formation and amplicon specificity.

Table 4: qPCR protocol for NP and GAPDH

1	Initial denaturation	15 min	98 °C
2	Denaturation	2 min	98 °C
3	Annealing	1 min	55 °C
4	Elongation	1 min	72 °C
5	Melting curve	2 min	60 – 98 °C in 0.5 °C steps

Plasmid preparations

Plasmid DNA was isolated using plasmid purification kits from Qiagen based on alkaline lysis following manufacturer's instructions.

Quantification of cerebral CD8⁺ cell infiltrates

Brain and organ samples were cut in 1µm thick sections and stained for CD8. Slides were then scanned using a MIRAX Midi slide scanner (ZEISS, Germany) at 200x magnification. CD8 signals (DAB-positive) were quantified using a custom ruleset in Definiens eCognition Network language on Definiens Developer XD (Definiens, Munch, Germany).

Quantification of inflammatory infiltrates and P-STAT1⁺ neurons and densitometry

For each animal a total brain area of at least $15 \times 10^6 \mu\text{m}^2$ was analyzed at 200x magnification to calculate the average number of CD8⁺ cells per mm^2 . Inflammatory foci in the deep cerebellar nuclei (DCN) were defined as areas with more than ten CD8⁺ T cells per high-power visual field. Average T cell densities within inflammatory foci were also assessed. The number of perisomatic synatophysin-positive boutons and the length of the somatic circumference of DCN neurons were quantified at 1000x magnification using the 'analySIS' software (Olympus GmbH) to calculate the density of boutons per μm . Human biopsies were scanned using the MIRAX Midi slide scanner at 200x magnification. P-STAT1⁺ neurons were counted manually within a cerebral cortical area of at least $17 \times 10^6 \mu\text{m}^2$.

Generation of CD8 density map of RE biopsy

Human biopsies were co-immunostained for CD8, P-STAT1 and DAPI and acquired at 200x magnification using the 'Pannoramic 250 Flash' slide scanner (3DHistech, Budapest, Hungary). To analyze the distribution patterns of CD8 T cells in the human RE biopsy, a custom image analysis ruleset based on the Definiens Cognition Network Language® (Definiens Developer XD 2.0, Definiens AG, Munich, Germany) was developed (Fig. 6). Briefly, the area of the tissue was detected and separated from background by its higher brightness (brightness value > 20 in all image layers). Detected tissue was then segmented using a multi-threshold segmentation calculating the threshold dividing the selected set of pixels into two subsets, so that heterogeneity is increased to a maximum. This segmentation was performed on the red as well as on the green image channel. P-STAT1 positive cells were then detected by the 8-bit brightness values of the red layer above 85, CD8 positive signals by values of the green channel above 70. Autofluorescence signal was detected based on the ratio of spatially overlapping red/green signal (ratio between 0.4 and 2) and excluded from further analysis. Next, an additional image layer was created containing the pixel-distances between neighboring CD8⁺ cells as gray values using the distance map algorithm. For this purpose, the borders of image objects classified as CD8 cells were grown along a distance gradient until establishing contact with the growing signal of neighboring CD8 cell. Growing of CD8 signal was limited to maximal distance of 30 pixels. The mean distance values at the border of two neighboring CD8 signals was calculated and CD8 cells were classified as follows: class I: distance value of < 20 pixels (light green), class II: distance value between 10-15 pixels (yellow), class III: distance values <10 pixels (red) and class

IV: distance value of 30 pixels (dark green). The latter class was considered as having no close neighbors. CD8 cluster were defined as groups of more than five CD8 cells belonging to either of the aforementioned class I – III. Furthermore, CD8 T cells situated within the perivascular, ependymal or meningeal space were excluded from further analysis. The detected CD8 clusters were then superimposed onto the stained tissue to correlate the spatial distribution with detected P-STAT1 signals.

Statistical analysis

ANOVA with Bonferroni posttest was used for the comparison of individual values from multiple groups. Viral RNA units were log-transformed for statistical analysis. Differences in individual values between two groups were analyzed by t-tests (unpaired, two-tailed). These analyses were performed using GraphPad Prism software version 5.04d. P-values ≤ 0.05 were considered statistically significant (*) and P-values ≤ 0.01 were considered highly significant (**), whereas P-values > 0.05 were considered statistically not significant.

Figure 6 (next page): Schematic description of the algorithm utilized to create a CTL density map of a Rasmussen encephalitis brain biopsy.

(A) A brain biopsy from a patient with Rasmussen Encephalitis (RE) was co-immunostained for CD8 (green), P-STAT1 and DAPI (blue). Pictures were recorded using a slide scanner at 200-fold magnification. (B) The different steps for the generation of a CD8 T cell density map are illustrated. (I) The raw image shows CD8 (green), P-STAT1+ cells (red) and yellow autofluorescence structures (mostly erythrocytes within vessels). (II) Detected structures were first classified according to their spectral characteristics into CD8+ T cells (turquoise), P-STAT1 (pink) and autofluorescence (yellow). The latter class of structures was excluded from further analysis. (III) An additional image layer was created in which the numeric distance (in pixels) to the classified CD8+ cell (turquoise) was coded as gray values (IV). The signal of CD8+ T cells were then grown along this distance gradient until they impinged the growing signal of the neighboring CD8 cell (the contact zones are depicted as turquoise line). (V) The mean distance values at the border of two neighboring CD8 signals were calculated and the CD8+ T cells were categorized into “no close neighbors” (dark green), “close neighbors” (light green), “closer neighbors” (yellow) and “very close neighbors” (red). (VI) The layer of color-coded density map was then superimposed onto the immunostained biopsy for the spatial correlation with P-STAT1 cells. Scale bars in A = 2 mm (overview) and 500 μm (inset), B = 100 μm (Kreutzfeldt et al. in revision).

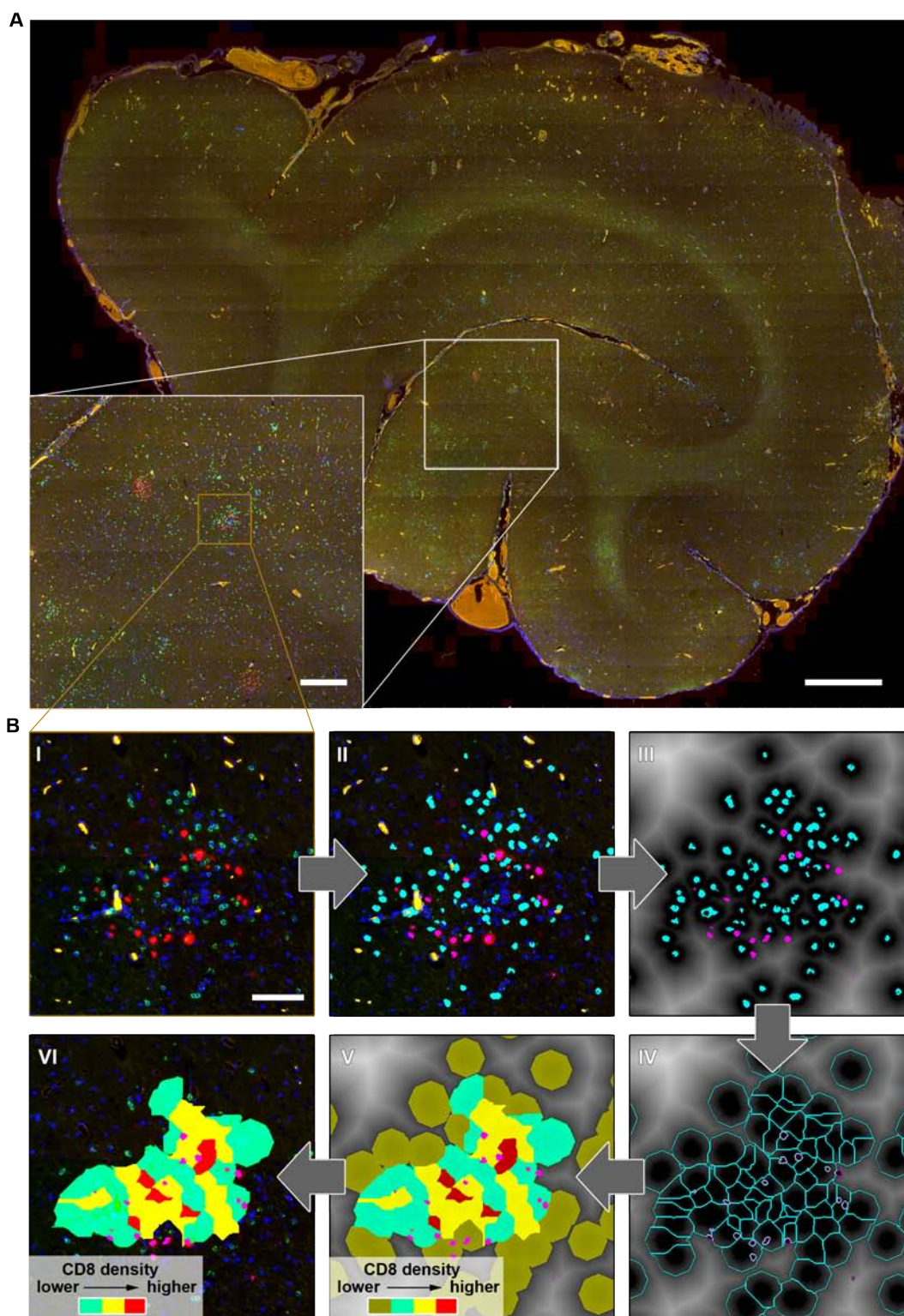


Figure 6: Schematic description of the algorithm utilized to create a CTL density map of a Rasmussen encephalitis brain biopsy.

Results – Aim 1

To investigate the influence and dependency of the viral déjà vu disease on epitopes with different affinities to MHC class I, different LCMV epitope mutants were created using a reverse genetics approach. This work focused on manipulating two immunodominant epitopes of LCMV in C57Bl/6 mice, NP396-404 and GP33-41. To minimize the influence of other epitopes contained in LCMV-GP, the leader sequence of LCMV-GP carrying the GP33 epitope was fused to VSV-GP (Fig. 5). All viruses were used to infect newborn C57Bl/6 mice intracerebrally on postnatal day 0 (p0) and challenged with LCMVwt i.v. at 5 weeks of age. (for details about the déjà vu setting see also introduction)

The GP33 epitope alone does not cause déjà vu disease

First, neonatal (p0) mice were infected i.c. with either rLCMV N5S/V3A (lacking both immunodominant epitopes NP396 and GP33) or N5S/GP33 (lacking NP396 but not GP33) or NP396/V3A (expressing NP396 but not GP33). Virus load in the CNS were measured by RT-PCR on day p16 revealing comparable virus load between the experimental groups (Fig. 7A). At the age of 5 weeks, virus carrier mice were challenged i.v. with LCMV-ARM (LCMVwt). Running performance was recorded and normalized for each mouse to the individual performance of day 3 post challenge. Carrier mice of the N5S/V3A mutant did not show any signs of disease, demonstrating that other subdominant epitopes have no major role for déjà vu disease onset (Fig. 7B, downward triangle). Similarly, the addition of the immunodominant GP33-41 epitope in N5S/GP33 rLCMV carrier mice, did not elicit déjà vu disease, neither (Fig. 7B, upright triangle). Only virus carriers expressing the immunodominant epitope NP396 in neurons (rLCMV NP396/V3A) showed déjà vu disease (Fig. 7B, squares). Quantification of the antiviral CD8 T cell population specific against NP396 and GP33 within the blood of these carriers confirmed efficient priming of both populations 10 days after LCMVwt i.v. challenge (Fig. 7C and D, black bars). Mice infected with rLCMV encoding the NP396 or GP33 epitopes, respectively, showed higher percentages of epitope specific CTLs. This might be due to subliminal priming (that evades detection by flow cytometry in carrier mice before LCMVwt challenge) of the particular antiviral CTL population. The NP396 specific CTL frequencies within the brain parenchyma of diseased NP/V3A carriers were doubled when compared to blood and 4-5x higher compared to the other rLCMV carrier groups (Fig. 7C, white bars).

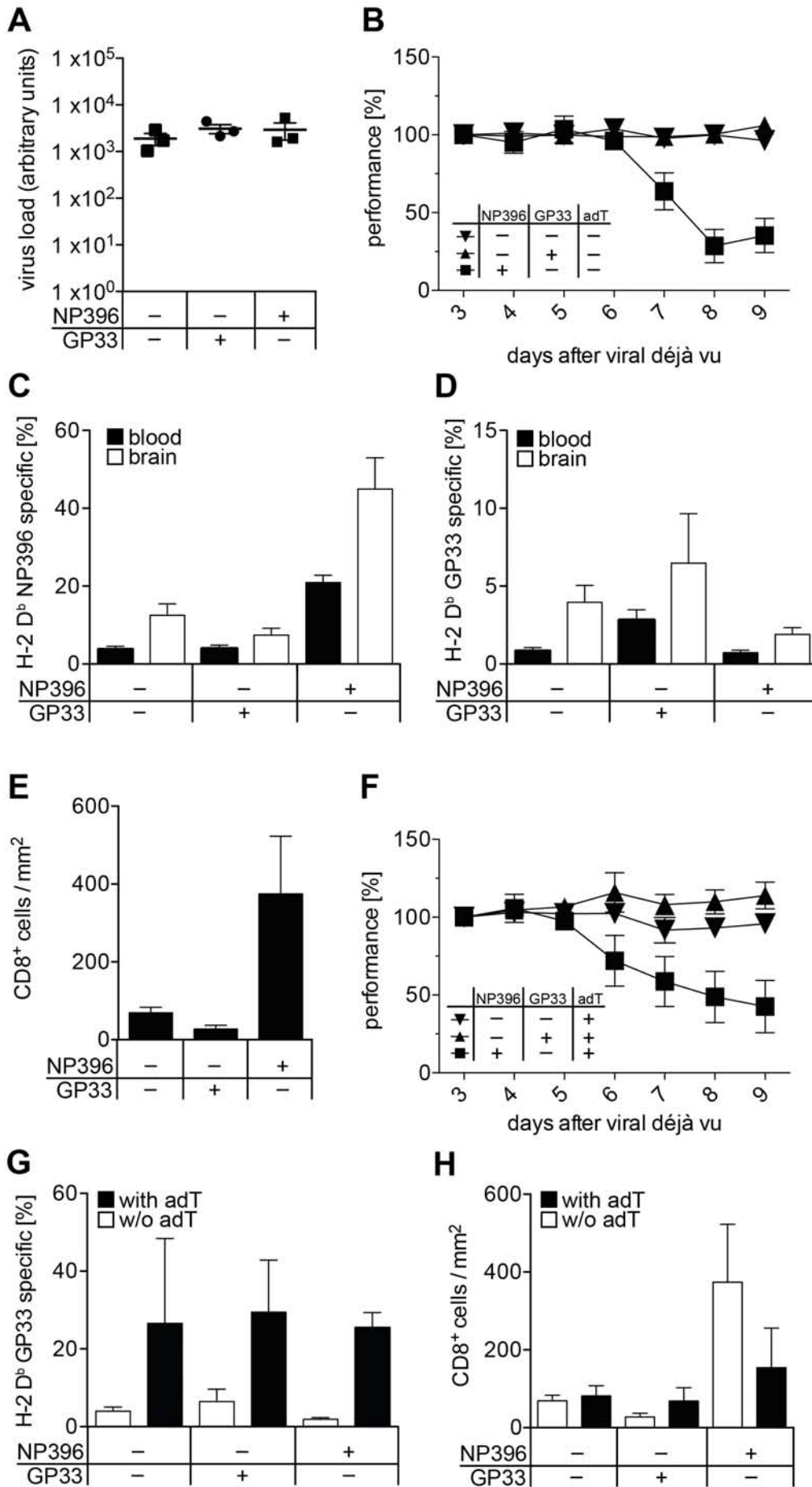


Figure 7 (previous page): GP33 epitope alone does not cause viral déjà vu disease.

(A) Virus load was quantified via qPCR for LCMV-NP and normalized against GAPDH (n=3 per group). (B) Running wheel performance (V_{max}) of C57Bl/6 rLCMV carrier mice. Performance on day 3 after LCMVwt challenge was set as baseline (n=8-10 per group). (C) H-2D^b restricted NP396 specific CD8⁺ T cells in blood and brain parenchyma were quantified using flow cytometry (n=8-10 for blood, n=4 for brain). (D) H-2D^b restricted GP33 specific CD8⁺ T cells in blood and brain parenchyma were quantified using flow cytometry (n=8-10 for blood, n=4 for brain). (E) Total CD8⁺ cell numbers in brain parenchyma were quantified using a custom ruleset in the tissue studio software (Definiens) (n=5). (F) Same experimental setup as in A but carrier mice received 1×10^3 adoptively transferred P14 cells one day before challenge with LCMVwt (n=10 per group). (G) H-2D^b restricted GP33 specific CD8⁺ T cells brain parenchyma were quantified using flow cytometry (n=4 per group). (H) Total CD8⁺ cell numbers in brain parenchyma were quantified as in E (n=5).

This effect was not evident in the GP33-specific CTL population (Fig. 7D, white bars). When the general CD8⁺ T cell infiltration density in the brain parenchyma was quantified, the diseased NP/V3A carrier group shows higher infiltration density within the brain parenchyma (Fig. 7E). The other two carrier groups, while showing no signs of déjà vu disease, still revealed heightened CD8⁺ T cell densities (Fig. 7E). Reduced frequencies of GP33-specific (as compared to NP396-specific) T cells could be a limiting factor for the absence of disease precipitation in rLCMV N5S/GP33 carrier mice. To address this possibility, we artificially increased the number of GP33 specific T cells by adoptive transfer of 1×10^5 TCR transgenic P14 cells directed against the GP33 epitope into carrier mice one day before challenge. However, déjà vu disease could not be observed following the adoptive transfer (Fig. 7F) although GP33 specific T cell frequencies were raised to comparable levels to NP396 specific T cells in the brains of these carrier mice (Fig. 7G, black bars and Fig. 7C, white bars). The adT of P14 cells had minor effects on the total infiltration of CD8⁺ cells in N5S/V3A as well as N5S/GP33 carrier mice and numbers did not reach the densities in NP/V3A carriers (Fig. 7H).

GP33 epitope variants with higher MHC class I affinity

The aforementioned results indicated that disease in the déjà vu setting seems not be caused by the total numbers or frequencies of antiviral CTLs in the brains of carrier mice, but may depend also on the affinity of the CTL epitope to the pMHC-complex. The affinity of GP33-41 to H-2D^b is considered as intermediate compared to the high affinity NP396-404 peptide (Van der Most et al. 1998). Nevertheless, the affinity of the GP33-41 peptide KAVYNFATC to H-2D^b can be strongly increased by exchanging the cysteine at position 9 for a methionine (C9M, Wang et al. 2002) or isoleucine (C9I, Utzschneider and Zehn, unpublished). Importantly, these GP33 variants are recognized by the same TCR. When P14 cells are cocultured with antigen presenting cells loaded with C9M or C9I *in vitro*, similar IFN- γ release could be measured at approximately 1 magnitude lower peptide concentrations compared to wild type GP33 (Fig. 8A). To test the expression and presentation of the GP33 epitope mutants *in vivo*, naïve mice were infected i.v. with 1×10^5 PFU GP33 variants (GP33, V3A, C9M and C9I). Eight days later, antiviral GP33-specific CTL frequencies in the blood were measured (Fig. 8B). The mean of GP33-specific antiviral CTL response was highest with 5.95 in the C9M mutant infected mice, followed by C9I with 2.20% compared to the response against wild type GP33 of 1.09%. The frequencies measured in V3A mutants correspond to the baseline GP33 specific T cell frequencies of naïve mice. Interestingly, the different potential of C9M vs. C9I was not resolvable using the *in vitro* stimulation assay.

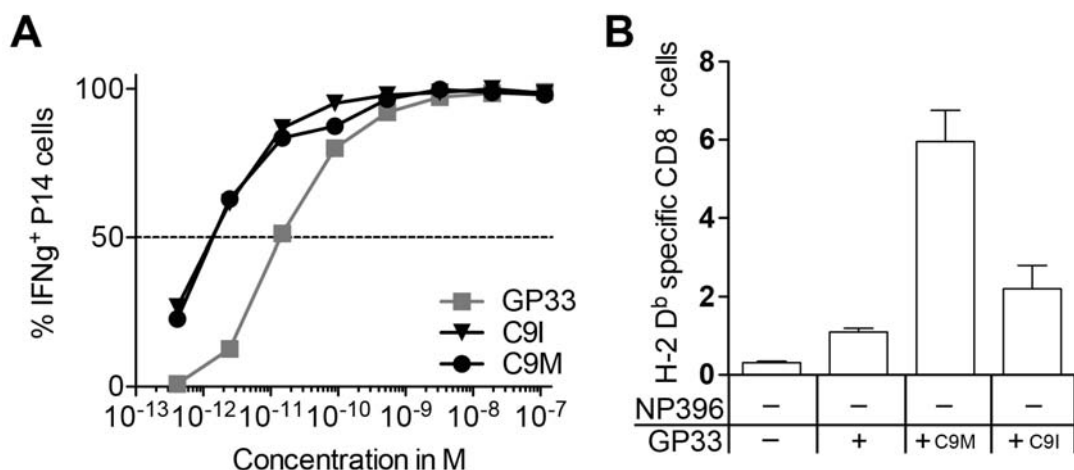


Figure 8: GP33 epitope mutants with increased H-2D^b binding capacity.

(A) Numbers of IFN- γ ⁺ GP33 specific P14 cells were measured by an *in vitro* stimulation assay. The affinity of C9I and C9M to H-2D^b is higher than the wild type GP33 epitope. (B) Naïve C57Bl/6 mice were infected with 1×10^5 PFU rLCMV carrying one GP33 epitope mutant. H-2D^b restricted GP33 specific CD8⁺ T cell response was quantified using flow cytometry (n=4 per group).

To test whether increasing the affinity to MHC class I of a given epitope (GP33) presented by infected neurons would be sufficient to induce déjà vu disease we infected p0 mice i.c. with rLCMV mutants encoding either for C9M (rLCMV N5S/C9M) or C9I (rLCMV N5S/C9I) mutations. Virus levels in the CNS were comparable at p16 (Fig. 9A) as measured by RT-PCR. However, after challenge with LCMVwt, no déjà vu disease could be observed until the end in all the experimental groups tested (Fig. 9B). NP396 specific T cell frequencies were comparable between the groups and no accumulation in the brain could be detected (Fig. 9C). The frequencies for GP33 specific T cells were comparable as well and again no accumulation in the brain was apparent (Fig. 9D). The total numbers of CD8⁺ cells in the brains were comparable to the numbers observed in N5S/GP33 carrier mice (see Fig. 7E). This data demonstrated that the increased MHC class I-affinity of the GP33 C9-mutants used, is still not sufficient to trigger viral déjà vu disease.

The results so far have shown that the CTL response to the GP33 epitope alone seems insufficient to trigger déjà vu disease. Neither rLCMV carrier mice with the wild type GP33 peptide, nor carrier mice infected with the high affinity GP33 variants develop disease but carriers of the NP396 epitope do. We next tested the influence of the different GP33 variants on déjà vu disease course in the presence of the NP396 epitope using CNS carrier mice of NP/V3A, NP/GP33, NP/C9M and NP/C9I. After challenge with LCMVwt, all groups developed locomotor impairments (Fig. 10A). Of note, in the higher affinity GP33 groups NP/C9M and NP/C9I, disease course was accentuated forcing to sacrifice animals already on day 7 post challenge (Fig. 10A, bottom row), 2 days before the other diseased carrier groups (Fig. 10A, upper row). The frequencies of NP396 specific T cells were increased in the brains of all groups compared to blood (Fig. 10B). Accumulation of GP33 specific T cells was detectable in all GP33 carrier mice, but was most apparent in the C9I carriers (Fig. 10C). The initial viral load was comparable between the groups (Fig. 10D) as was the total CD8⁺ cell infiltration (Fig. 10E).

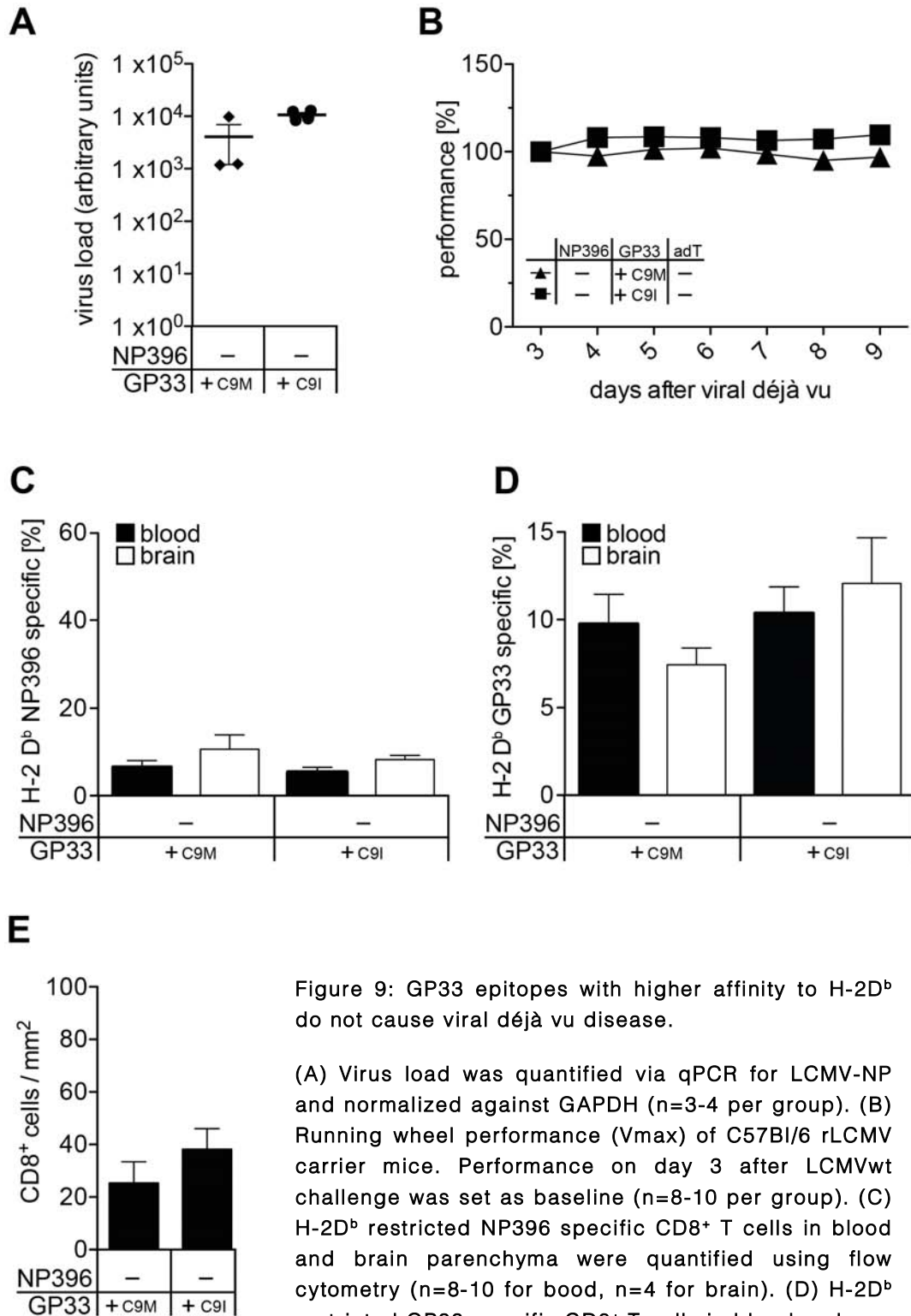


Figure 9: GP33 epitopes with higher affinity to H-2D^b do not cause viral déjà vu disease.

(A) Virus load was quantified via qPCR for LCMV-NP and normalized against GAPDH (n=3-4 per group). (B) Running wheel performance (Vmax) of C57BI/6 rLCMV carrier mice. Performance on day 3 after LCMVwt challenge was set as baseline (n=8-10 per group). (C) H-2D^b restricted NP396 specific CD8⁺ T cells in blood and brain parenchyma were quantified using flow cytometry (n=8-10 for blood, n=4 for brain). (D) H-2D^b restricted GP33 specific CD8⁺ T cells in blood and brain parenchyma were quantified using flow cytometry (n=8-10 for blood, n=4 for brain). (E) Total CD8⁺ cell numbers in brain parenchyma were quantified using a custom ruleset in the tissue studio software (Definiens) (n=5).

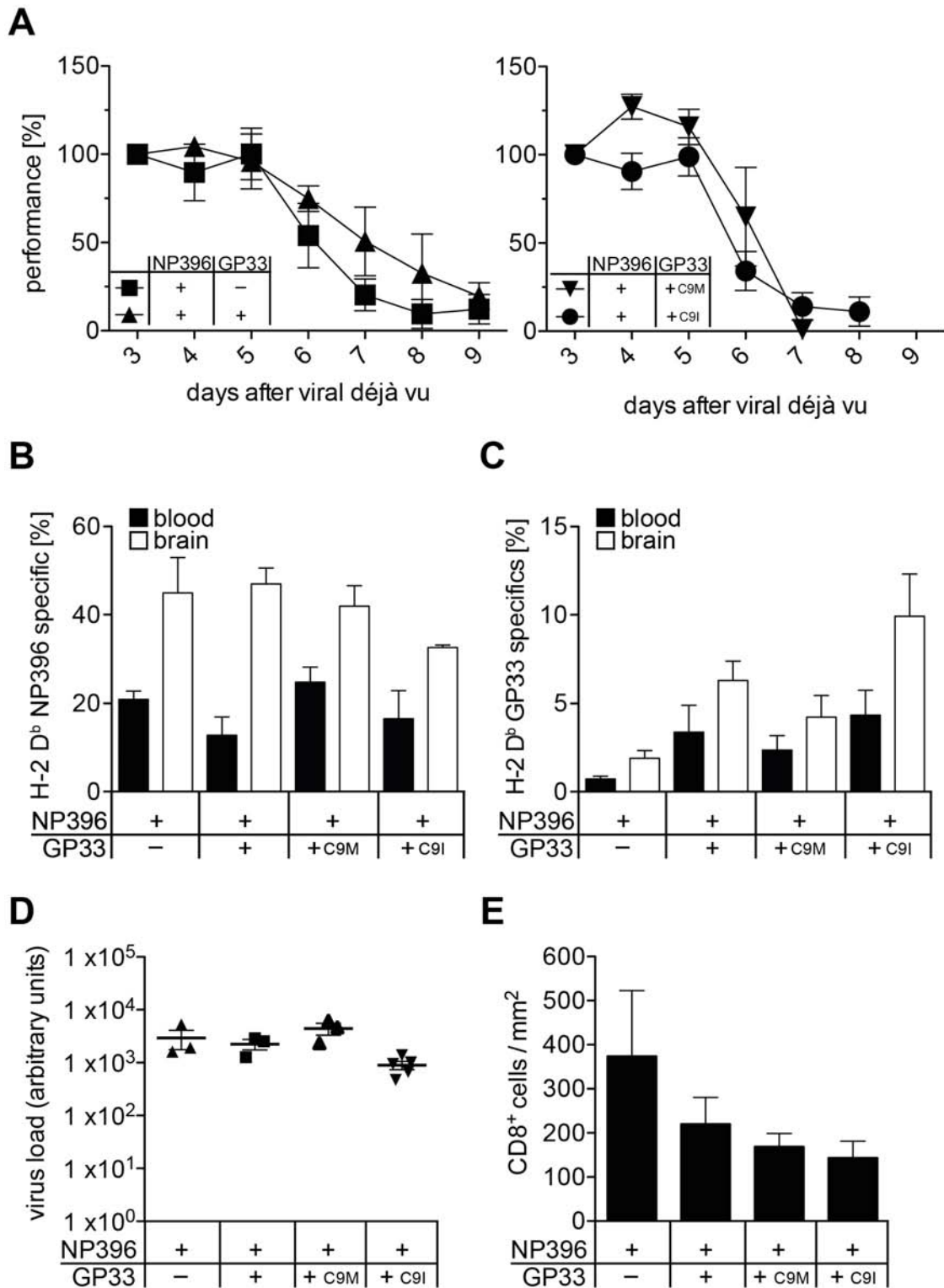


Figure 10: NP396 epitope induces viral déjà vu disease which can be influenced by GP33.

(A) Running wheel performance (Vmax left, DistMean right) of C57Bl/6 rLCMV carrier mice. Performance on day 3 after LCMVwt challenge was set as baseline (n=8-10 per group). (B) H-2D^b restricted NP396 specific CD8⁺ T cells in blood and brain parenchyma were quantified using flow cytometry (n=8-10 for blood, n=4 for brain). (C) H-2D^b restricted GP33 specific CD8⁺ T cells in blood and brain parenchyma were quantified using flow cytometry (n=8-10 for blood, n=4 for brain). (D) Virus load was quantified via

qPCR for LCMV-NP and normalized against GAPDH (n=3-4 per group). (E) Total CD8⁺ cell numbers in brain parenchyma were quantified using a custom ruleset in the tissue studio software (Definiens) (n=5).

The finding that a GP33 epitope with higher MHC class I affinity can worsen the disease, but is not sufficient to induce déjà vu disease in the absence of the NP396 epitope lead to the question if this outcome is caused by limited GP33 T cell frequencies. Hence, 1×10^5 GP33 specific P14 cells were adoptively transferred into C9M carrier mice carrying either the NP396 epitope or the N5S mutation in addition. One day after the adT, mice were challenged with LCMVwt. The disease course did not differ between mice that received P14 cells and those left untreated. The decisive factor for disease was again solely the presence of the NP396 epitope in the carrier mice (Fig. 11A). The frequencies of GP33 specific T cells were drastically increased in the brains of P14-recipients (Fig. 11B). However, this increase was not reflected in the total CD8⁺ cell infiltration of the brain, which was basically left unaffected by the higher GP33-specific T cell frequencies (Fig. 11C).

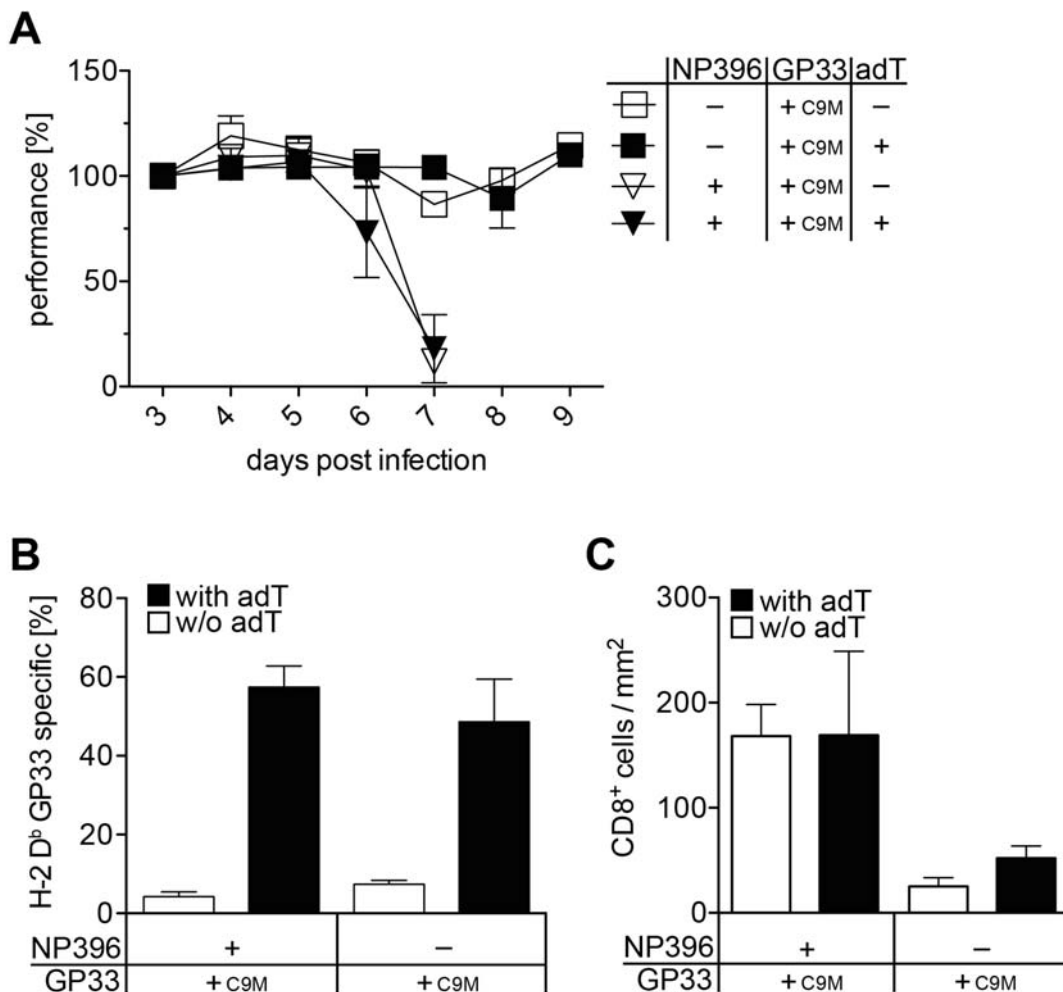


Figure 11: Viral déjà vu disease is not influenced by higher numbers of GP33 specific CTLs.

(A) Running wheel performance (Vmax) of C57Bl/6 rLCMV carrier mice. Indicated groups received 1×10^3 adoptively transferred P14 cells one day before LCMVwt challenge. Performance on day 3 after challenge was set as baseline (n=8-10 per group). (B) H-2D^b restricted GP33 specific CD8⁺ T cells brain parenchyma were quantified using flow cytometry (n=4 per group). (C) Total CD8⁺ cell numbers in brain parenchyma were quantified using a custom ruleset in the tissue studio software (Definiens) (n=5).

Results - Aim 2

Using the viral déjà vu model, it has been demonstrated that CNS-infiltrating CTLs are found preferentially in immediate vicinity to rLCMV/INDG-infected neurons, which suggests an antigen-specific interaction causing clinical disease (Merkler et al. 2006). Here, we addressed the morphological correlate for the observed neurological impairments in the viral déjà vu disease. More specific, we investigated the impact with regard to neuronal cell loss and/or subcellular neuronal alterations that are mediated by CTLs attacking antigenic neurons *in vivo*.

First, p0 mice were infected i.c. with rLCMV/INDG and challenged with LCMVwt at 5 weeks of age. Infiltrates of CTLs were regularly found in the cerebral cortex, basal ganglia, thalamic and hypothalamic nuclei, hippocampus, cerebellum and in some segments of the spinal cord. Three and eight weeks after challenge, neuronal cell densities were quantified in the aforementioned anatomical areas on immunohistochemically stained brain and spinal cord slides using the neuronal marker NeuN (Fig. 12). Quantification revealed that neuronal cell densities were unaltered even 2 weeks after disease onset. However, a minor reduction of neuronal cell bodies could be found in tissue samples of mice 7 weeks after disease onset. No reduction was seen within cortical and dentate gyrus structures. Thus, these analyses indicated that neuronal loss was unlikely the cause for the noted rapid and severe neurological impairments in viral déjà vu disease commencing at day 6-7 after challenge.

Since neurons are integrated in complex synaptic networks, CTL-induced neuronal decoupling could result in similar symptoms than neuronal ‘drop-out’. Thus, subcellular alterations in neurons of the deep cerebellar nuclei (DCN) were investigated. This structure was chosen due to its integration in important functional networks and its defined cytological features (Garin and Escher 2001). Furthermore, this structure can also be affected in human inflammatory CNS diseases (Dalmau and Rosenfeld 2008; Gilmore et al. 2009). The DCN-neurons receive input via synapses covering their soma, so called axosomatic boutons. By staining for the presynaptic component synaptophysin, these structures were visualized and enumerated. In healthy non-carrier mice, the boutons are visible as punctuate synaptophysin-positive areas, which are significantly reduced in diseased carrier mice (Fig. 13A). Furthermore, bouton density was found preferentially decreased on infected neurons in close contact with T cells (Fig. 13B).

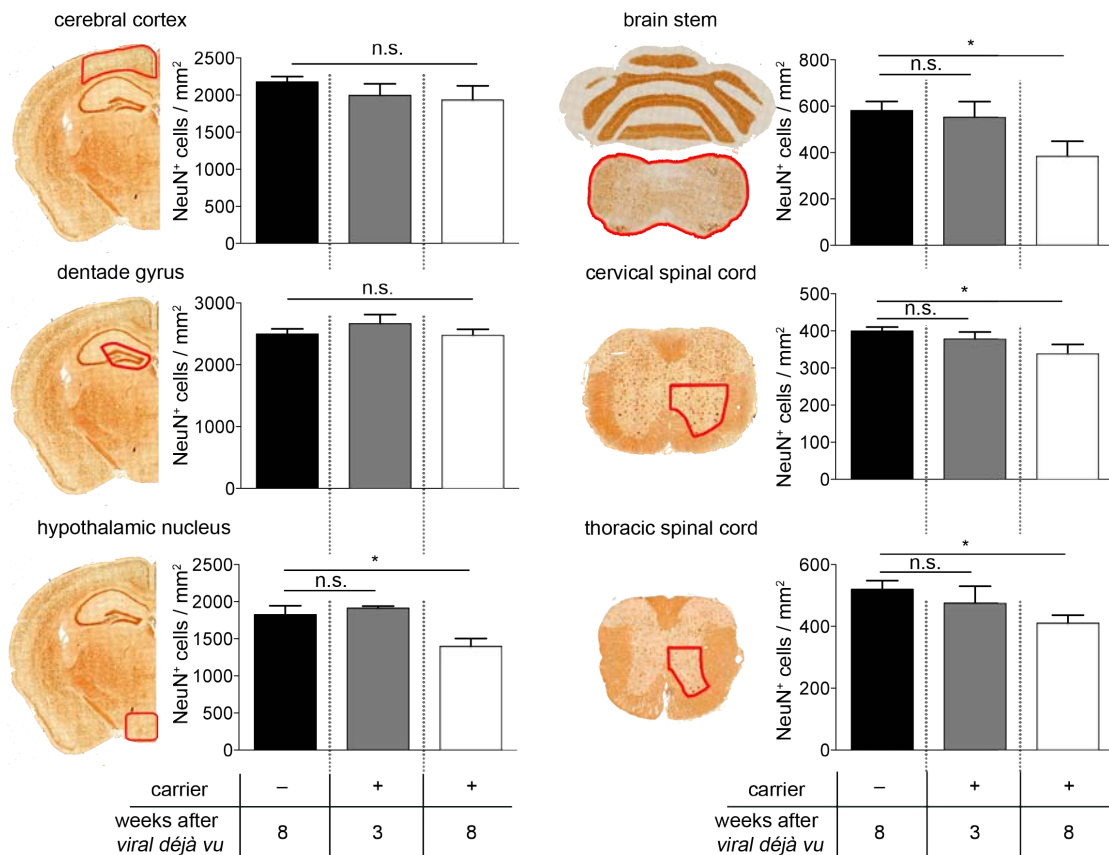


Figure 12: Neuronal loss is only observed in late stages of viral déjà vu disease.

Carrier mice and non-carrier controls were subject to viral déjà vu (day 0). At the indicated time points, the density of neurons (NeuN⁺) was quantified in various areas of brain and spinal cord. Red lines delimit the anatomical areas under study. (n=4–12 mice per anatomical area and group. Bars represent the mean+SEM (Kreutzfeldt et al. in revision).

This observation indicates that the loss of somatic synaptic input was a consequence of epitope-specific CTL engagement. We furthermore investigated the role of different CTL effector pathways, namely FAS, perforin, IFN- γ and TNF- α for the precipitation of déjà vu disease. Since defective FAS-, IFN- γ or TNF- α signaling pathways negatively impact the induction, expansion or maturation phases of CTLs, bone marrow chimeric mice were used. Carrier mice of TNFR1/2^{-/-}, FAS^{-/-}, IFNGR^{-/-}, and C57Bl/6 genotype were lethally irradiated and substituted with C57Bl/6 bone marrow. The resulting mice had a wild type immune system, but non-lymphohematopoietic cells (e.g. neurons) with the respective deficiency. It turned out that IFNGR^{-/-} or TNFR1/2^{-/-} deficiencies protect from viral déjà vu disease (Fig. 14A). Additionally, perforin deficiency did not protect from déjà vu disease (Fig. 14B). To control for impaired CTL responses in deficient mice, NP396-specific T cell frequencies were measured using flow cytometry. The frequencies were comparable between the different groups (Fig. 14C). When synaptic bouton densities were measured

in the different knockout lines, the absence of CD8⁺ cell infiltrates in TNFR1/2^{-/-} mice was observed. This can most likely be explained by the necessary TNF- α depended activation of vascular endothelium for immune cell transmigration (Kallmann et al. 2000). Due to this effect, the TNFR1/2^{-/-} carrier mice were excluded from further analyses centering the resistance of IFNGR^{-/-} neurons to CTL mediated attack, reflected in the unaltered bouton density after viral déjà vu (Fig. 14D and Fig. 14E).

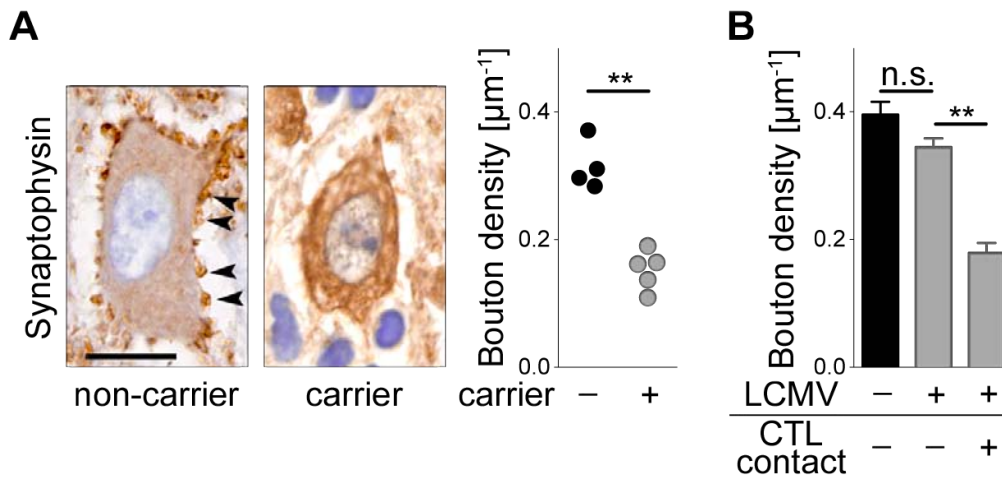


Figure 13: Deafferentation in viral déjà vu disease requires CTL contact with infected neurons.

(A) Left panel: Representative section stained for synaptophysin⁺ perisomatic boutons (arrowheads) in the deep cerebellar nuclei (DCN) of carrier and non-carrier mice 10 days after viral déjà vu. Right panel: quantification of axosomatic bouton density. Symbols represent individual animals. (B) On day 8, triple immuno-stained sections for T cells, synaptophysin and LCMV-NP antigen were analyzed (n=4), revealing a preferential reduction of bouton density on antigenic (LCMV-NP⁺) neurons in juxtaposition to infiltrating T cells. Bars represent the mean+SEM. “***” p < 0.01; “n.a.” not applicable; “n.s.” not significant (p > 0.05). Scale bar in A = 20 μm (Kreutzfeldt et al. in revision).

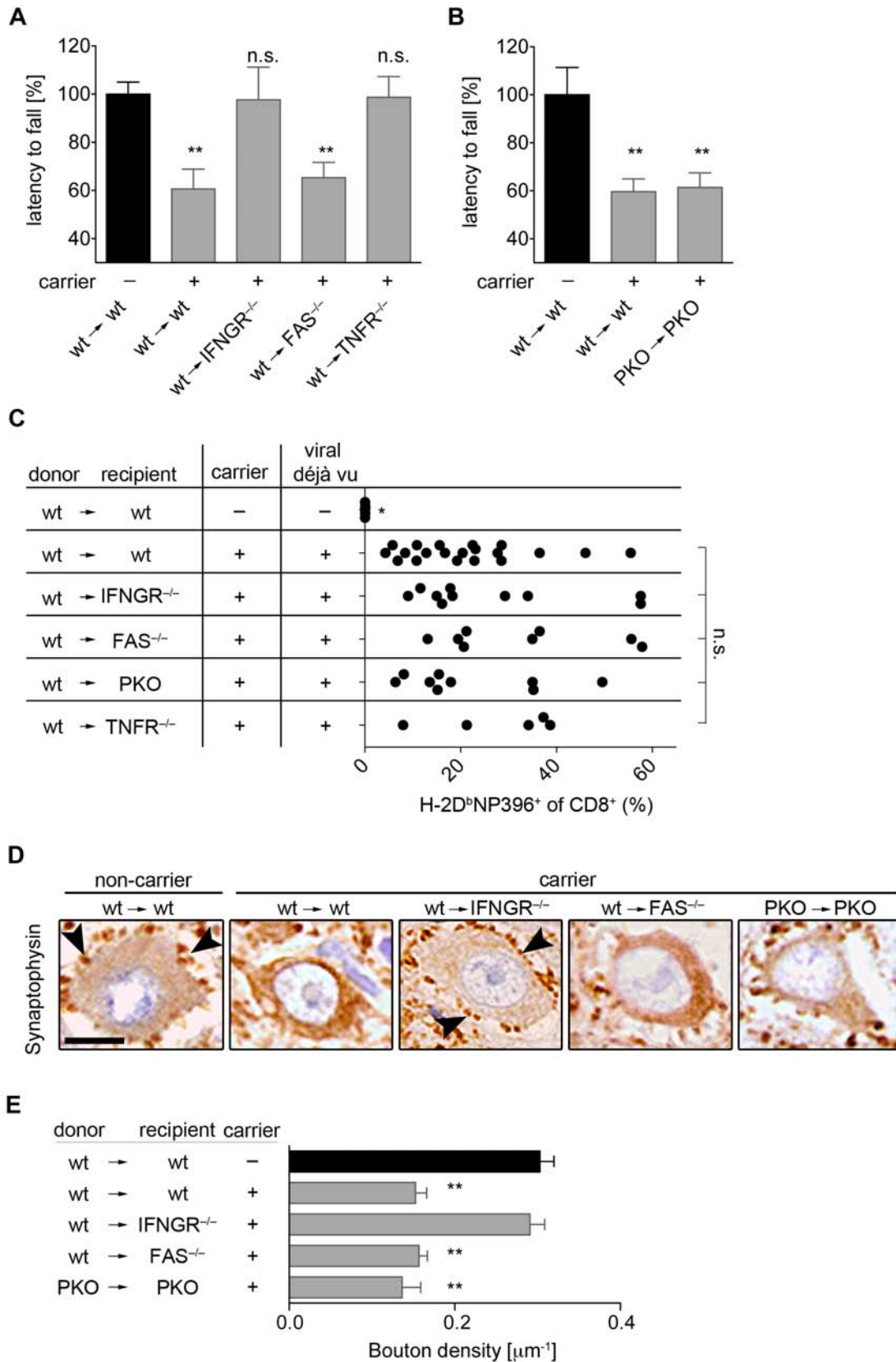


Figure 14: Viral déjà vu disease depends on non-hematopoietic IFN- γ receptor.

Viral déjà vu was induced in the indicated bone marrow-chimeric mice. (A,B) Rotarod performance was analyzed at the peak of disease. (A) Bars represent the mean+SEM of

19-31 mice per group from five independent experiments. (B) All groups received 1×10^4 P14 splenocytes by adoptive transfer on day -1. Bars represent the mean+SEM of 4-8 mice per group (D) Representative picture of synaptophysin⁺ boutons in DCN of the various experimental groups. Arrowheads indicate perisomatic boutons of wt→wt non-carrier control animals (do not develop CNS inflammation upon *viral déjà vu*) and on neurons of wt→IFNGR^{-/-}mice, which were found resistant to clinical disease. (E) Quantitative analysis of perisomatic bouton density. Bars indicate the mean+SEM of 3-7 mice per group. Scale bar in D = 10 μm (Kreutzfeldt et al. in revision).

IFN-γ has immunoregulatory and antiviral properties (Schroder et al. 2004) and can induce neuronal pathology when acting as effector cytokine *in vitro* (Kim et al. 2002). A key step in IFN-γ signaling is its binding to IFNGR, which activates the transcription factor STAT1 (signal transducer and activator of transcription) by phosphorylation (Ramana et al. 2002). The phosphorylated STAT1 homodimer then translocates into the nucleus where it binds to IFN-γ activation sites (GAS), initiating or suppressing the transcription of IFN-γ regulated genes. Having seen that IFNGR^{-/-} mice were protected from *déjà vu* disease, the STAT1 expression, phosphorylation and nuclear translocation was measured in neurons under CTL attack. For this, bone marrow chimeras were generated as described. STAT1 mRNA was significantly upregulated within brains of diseased wild type mice, but not in IFNGR^{-/-} mice (Fig. 15A). Likewise, phosphorylated STAT1 (P-STAT1) with nuclear location could be observed in diseased wt mice but were absent in IFNGR^{-/-} mice (Fig. 15B). P-STAT1⁺ neuronal nuclei were only found in inflamed areas and frequently associated closely with infiltrating T cells (Fig. 15C). More than seventy percent of P-STAT1⁺ neurons expressed viral antigen (Fig. 15D), suggesting antigen specific CTL interactions with infected neurons evoked targeted IFN-γ release.

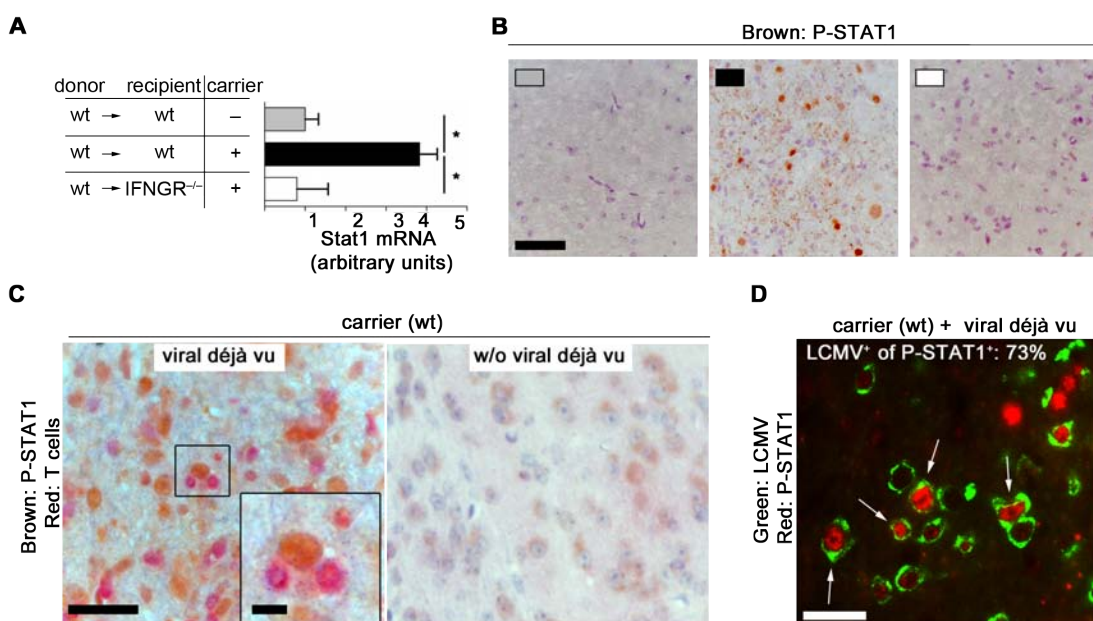


Figure 15 (previous page): STAT1 upregulation, phosphorylation and nuclear translocation reflect the neuronal signature of IFN- γ signaling.

(A–D): *Viral déjà vu* experiments were analyzed on day 10. (A) STAT1 mRNA levels. Bars indicate the mean+SEM of 4-6 mice. (B) STAT1 phosphorylation (P-STAT1) and nuclear translocation in neurons of diseased wt \rightarrow wt animals (black rectangle) but neither in wt \rightarrow IFNGR $^{-/-}$ carriers (white rectangle, infiltration but absence of disease) nor in non-carriers (grey rectangle, devoid of inflammation or disease). Representative pictures from 4-6 mice are shown. (C) Juxtaposition of P-STAT1 $^{+}$ (brown) neurons and CD3 $^{+}$ (red) T cells is only observed upon *viral déjà vu*. (D) Colocalization of LCMV-NP $^{+}$ (green) and P-STAT1 (red). Arrows indicated double-positive neurons. Within P-STAT1 $^{+}$ neurons 73% were LCMV-NP $^{+}$. Scale bars indicate 50 μ m (B,C overview), 10 μ m (C, inset), 20 μ m (D). “**” p < 0.05 (Kreutzfeldt et al. in revision).

To further support the role of IFN- γ in viral déjà vu disease pathology, it was assessed next whether neutralizing anti-IFN- γ antibody (Abrams et al. 1992) has any protective effect in this setting. Carrier mice received i.p. injections of IFN- γ neutralizing (XMG1.2) or isotype control (HRPN) antibodies 5 days after LCMVwt challenge. Neutralization of IFN- γ protected carrier mice from viral déjà vu disease (Fig. 16A). XMG1.2 treatment did neither alter the magnitude of NP396-specific CTL response in peripheral blood (Fig. 16B) nor total CTL invasion in to the CNS (Fig. 16C and D). However, the treatment protected neurons from deafferentation (Fig. 16E) and P-STAT1 was not elevated in XMG1.2 treated mice compared to non-carrier controls (Fig. 16F), consistent with a successfully blocked IFN- γ signaling pathway.

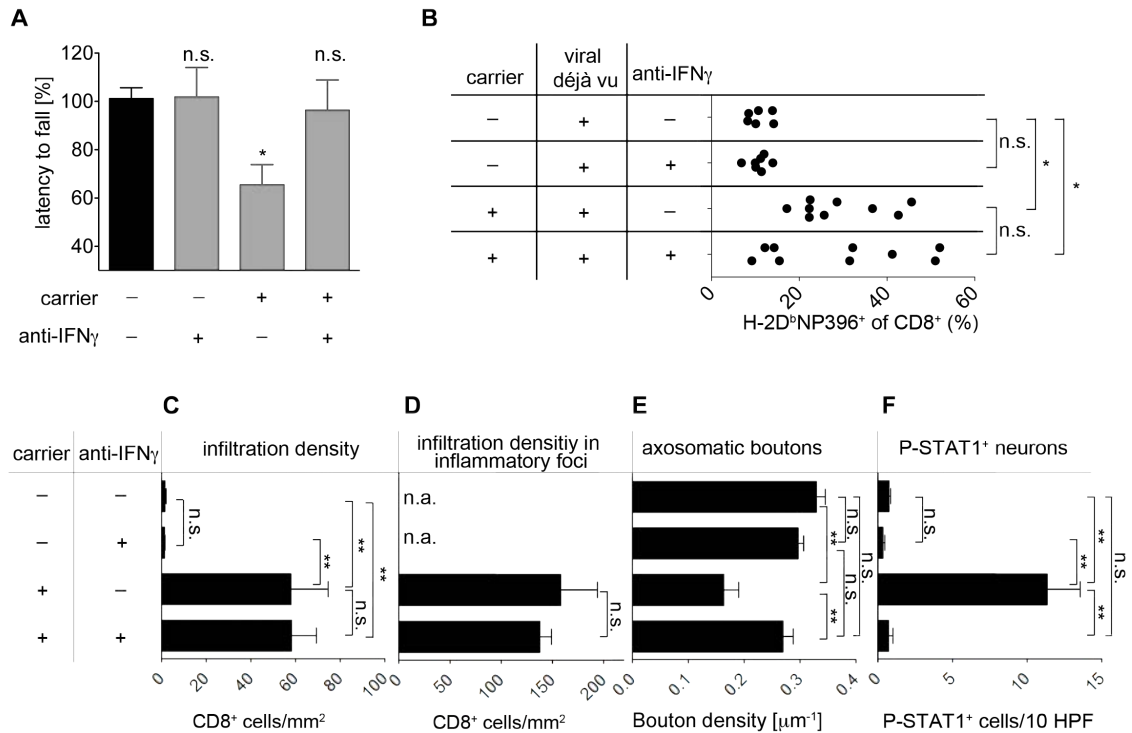


Figure 16: Antibody-mediated block of IFN- γ signaling protects from viral déjà vu disease and neuronal deafferentation.

Five days after LCMVwt i.v. challenge, anti-IFN- γ antibody (indicated as “+”) or isotype control (indicated as “-”) was injected i.p. into carrier mice (“+”) or non-carrier (“-”), respectively. (A) Rotarod performance. (B) The frequency of (pathogenic) NP396-specific CD8⁺ T cells in blood at day 10 measured using MHC class I tetramers. (C and D) Quantification of brain-infiltrating CTLs. (E) Axosomatic densities in the DCN and (F) the density of cerebellar P-STAT1⁺ neurons. Bars represent the mean+SEM (n=6-10 animals per group for A-D, F and 3-6 animals per group for E). “**” p < 0.05, “***” p < 0.01; “n.s.” not significant (p > 0.05); “n.a.” not applicable (Kreutzfeldt et al. in revision).

To test whether the IFN- γ -STAT1-pathway may also be involved in CTL-mediated neuroimmunological diseases in humans, six brain biopsies from Rasmussen encephalitis (RE) patients were examined for their CTL and neuronal PSTAT1 distribution (Fig. 17).

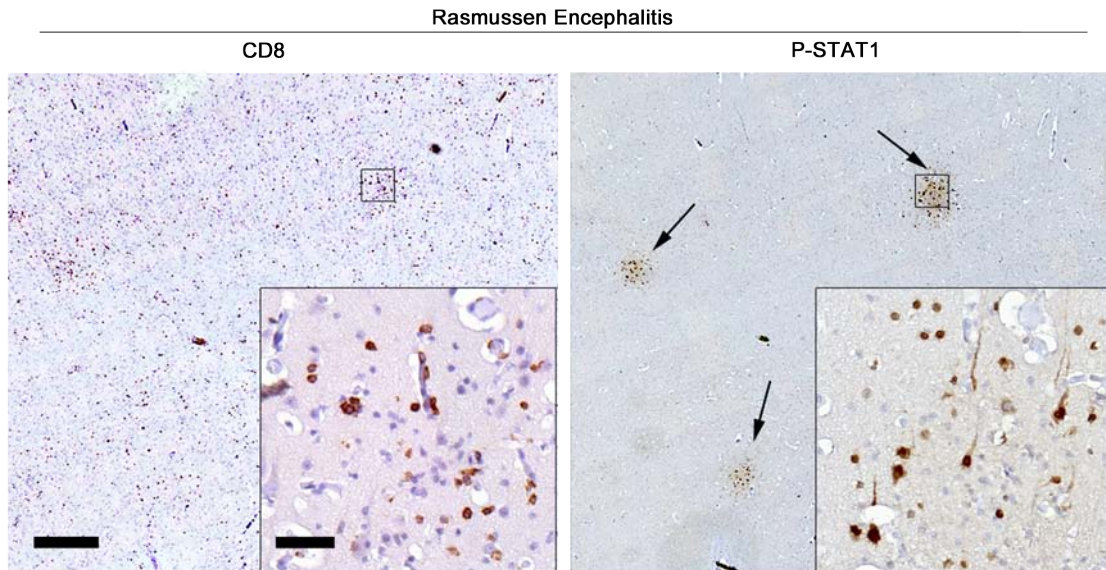


Figure 17: RE biopsies are characterized by widespread CD8⁺ T cell infiltrates and clusters of cortical P-STAT1⁺ neurons.

Representative image of RE biopsy stained for CD8 (left image) or P-STAT1 (right image) on adjacent brain sections. Note the widespread CD8⁺ T cell infiltrates in the entire parenchyma, and the groups of P-STAT1⁺ cortical neurons (arrows). Scale bars = 500 μ m (overview) and 50 μ m (inset) (Kreutzfeldt et al. in revision).

RE, a rare CTL-mediated neurological disease with unknown etiology, is very similar to viral déjà vu disease on the histopathological level in that many putatively antigen-specific CTL infiltrates can be found in close association with CNS neurons (Schwab et al. 2009) (Fig. 18A left). CTL infiltration densities correlated positively with the density of PSTAT1⁺ neurons (Fig. 18A right, $p < 0.05$, $r^2 = 0.76$). While CTLs could be found widely distributed throughout the specimen, PSTAT1⁺ neurons appeared to form clusters within the cerebral cortex. This raised the question, whether STAT1 phosphorylation can be associated with different CTL infiltration patterns at these areas. To assess this, a CTL density map from a representative RE biopsy was created (Fig. 18B left) and aligned with the observed P-STAT1 clusters (Fig. 18B right). This computational analysis revealed uneven CTL distribution with denser CTL ‘hot-spots’ at 70% of the PSTAT1⁺ clusters. The density of axosomatic synapses on PSTAT1⁺ neurons was significantly reduced as compared to PSTAT1⁻ neurons (Fig. 18C), reflecting the findings from the viral déjà vu model (see Fig. 13A).

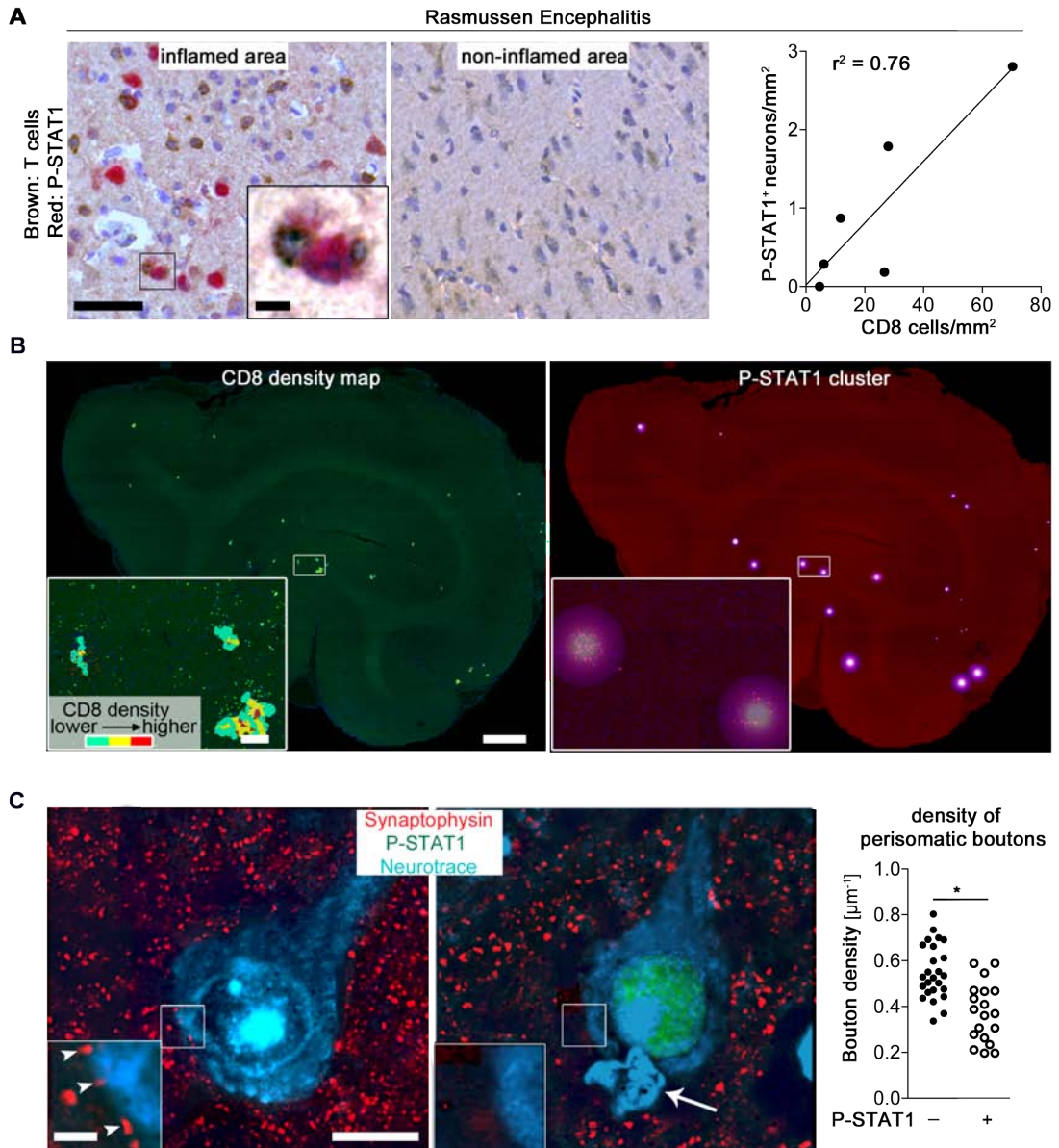


Figure 18: Neuronal STAT1 phosphorylation and reduced synaptic boutons in CD8⁺ T cell clusters of human Rasmussen encephalitis.

(A–C) Brain specimen from human Rasmussen encephalitis patient. (A) Left: Proximity of CD8⁺ T cell infiltrates (brown) and P-STAT1 neurons (red). P-STAT1⁺ neurons were only detected in inflamed areas. Right: Positive correlation between P-STAT1⁺ neurons and CD8⁺ T cell infiltration density. Symbols represent individual patients. (B) Left: CD8 density map visualizes CTL “hot spots” in a temporal lobe (left image). Right: P-Stat1⁺ neurons (visualized as pink spheres) within the same biopsy. (C) Left: Coimmunostaining of synaptophysin (red), P-STAT1 (green) and Neurotrace (cyan). Synaptophysin⁺ (red) perisomatic bouton density (arrowheads) on P-STAT1⁺ (green) is reduced as compared to P-STAT1⁻ neurons. Arrow points to a T cell found in contact with a P-STAT1⁺ neuron. Right: Symbols represent individual neurons. Scale bars indicate 50 μm (A; overview), 10 μm (A; inset), 2 mm (B, overview), 500 μm (B, inset), 10 μm (C; overview) and 2 μm (C; inset) (Kreutzfeldt et al. in revision).

Discussion

Many inflammatory diseases of the CNS cause permanent neurological deficits in the affected individuals. In addition to CNS-resident microglia and infiltrated T helper cells, the involvement of cytotoxic CD8⁺ T lymphocytes in inflammatory CNS diseases has become increasingly evident (Willing and Friese 2012). The recruitment of CTLs to the brain can be observed in autoimmune diseases like MS (Hauser et al. 1986) and Rasmussen encephalitis (C G Bien et al. 2005) as well as in many viral infections and paraneoplastic disorders (Albert and Darnell 2004). To become a targets for CTLs, cells need to present matching antigenic peptides bound to MHC class I (pMHC) on the cell surface. After recognition of their cognate pMHC complex, CTLs can utilize different effector mechanisms. The eponymous cytotoxic mechanisms induce apoptosis via perforin/granzymeB and Fas/FasL. But CTLs can also secrete immunomodulatory cytokines like IFN- γ and TNF- α (Stinchcombe and Griffiths 2007). The relative contribution of each of these pathways to tissue damage varies greatly and depends on the target cell type and tissue.

The CNS is considered as an immune specialized organ, able to actively regulate and inhibit local immune reactions by e.g. secretion of immunoregulatory TGF- β , expression of FasL and limited neuronal MHC class I expression. Neurons are post mitotic cells and possess only a limited regenerative capacity. They are furthermore integrated into a complex synaptic network and not easily replaceable. These factors might explain why many viruses infect and persist in neurons (Ter Meulen et al. 1984) thus minimizing detection by antiviral CTLs. Recent studies demonstrated, however, that this immune evasion is not absolute and CNS-infiltrating CTLs can engage virus infected neurons in a pMHC restricted manner.

Most of the experimental data about CTL-neuron interactions were generated *in vitro*. Using neuronal cultures and explants, CTL interactions with neuronal somata and axons have been shown and lysis or electrical silencing of targeted neurons has been described (Meuth et al. 2009; Rensing-Ehl et al. 1996). Due to the inevitable and deliberate simplifications made in neuronal *in vitro* cultures, the cellular composition, media conditions and external stimuli can never completely recreate the *in vivo* situation. All of these factors and manipulations can influence the fitness of the neurons by itself and their susceptibility to CTL-attack.

To gain insight into how CTLs damage neurons *in vivo* and which consequences this interaction has for the target cell, the recently established viral déjà vu model (Merkler et al. 2006) was used in this work. This model allows studying CTL-mediated neuronal damage and the resulting disease *in vivo*. Shortly outlined, neonatal mice were infected intracranial with attenuated LCMV (rLCMV), resulting in viral persistence selectively in CNS neurons. Importantly, rLCMV is not cytolytic and the infected mice were clinically healthy, with no increase in antiviral CTLs detectable by TCR-specific MHC-tetramers. These mice were exposed to a second infection with wild type LCMV in adulthood (déjà vu), inducing a strong antiviral CTL response. Because rLCMV and wild type LCMV shared some immunodominant H-2D^b restricted epitopes (e.g. NP396-404, GP33-41), CNS infiltrating CTLs caused severe disease within 7-10 days after viral déjà vu.

In the first part of this work, the viral déjà vu model was used to investigate the contribution of different LCMV-derived epitopes, displaying high, intermediate or low/no affinity to MHC class I, to precipitate disease. Herein it could be shown that the presentation of the high-affinity LCMV epitope NP396-404 on neuronal MHC class I was sufficient and necessary for the development of clinical symptoms, since the introduction of a non-presentable NP396-404 epitope (N5S) in the carrier virus abolished disease. Furthermore, other presented high-affinity GP33-41 variants (C9M, C9I) were not sufficient to induce disease themselves (Fig. 9B) but accelerated and enhanced disease severity in mice carrying the NP396-404 epitope (Fig.10A). First of all, the here presented work confirms that CD8⁺ T cells recognize their cognate antigen in the context of MHC class I expressed by neurons in an *in vivo* model and thereby extends the existing *in vitro* studies (Chevalier et al., 2011; Medana et al. 2001; Meuth et al., 2009). Albeit all neuroectoderm cell types in the CNS can express MHC class I and could thus become targets of CTLs (Höftberger et al. 2004). The MHC class I expression in healthy neurons is very low. This latter notion contributes to the CNS' immune privilege. However, MHC class I can be upregulated in response to inflammation, electrical disturbances or neuronal damage (Neumann et al. 1995).

The fact that solely carrier mice able to present the NP396-404 epitope developed déjà vu disease indicates that this epitope likely triggers a key response in this experimental setting. Notably, upon peripheral infection with wild type LCMV, the fraction of NP396-specific CD8⁺ T cell response is significantly higher than of GP33-specific CD8⁺ T cells (Fig.7C and Fig.8B). Moreover, NP396-specific CD8⁺ T cells also constitute the majority of

CNS-infiltrating CD8⁺ T cells (32.6% to 46.9%, Fig10B) in contrast to GP33-specific T cells (1.9% to 9.9%, Fig, 10C).

The affinity of the nonamer NP396-404 to H-2D^b has been reported in the range of IC₅₀=4.4 nM and those of wild type GP33-41 as IC₅₀=5429 nM (Van der Most et al. 1998). This difference in affinity was found to result in a 1000-fold better lysis of NP396-presenting cells in a chromium release assay (Gairin et al. 1995). It has to be considered that these results were obtained *in vitro* using MHC^{high} MC57 cells as CTL targets. And though both NP396-404 and GP33-41 epitopes are immunodominant in peripheral LCMV infection of C57Bl/6 mice (Kotturi, Scott, Wolfe, Peters, Cheroutre, et al. 2008), their different MHC affinity could shift their presentation in MHC^{low} neurons in favor of NP396, where both peptides compete for an even lower number of binding partners.

The disease-enhancing effect of GP33 variants with higher MHC class I affinity (C9M, C9I), if co-expressed with the NP396 epitope, further corroborate the importance of efficient CD8⁺ T cell engagements by pMHC complexes in neurons. This engagement elicits the effector functions leading to cellular damage and the development of clinical disease. The higher affinity of the C9M and C9I peptides to MHC class I could in principle influence the engagement of specific CD8⁺ T cells in two different ways. First, a higher-affinity binding of the presented peptide to the MHC likely prolongs the half-life of the respective pMHC molecules on the cell surface. It has been shown that peptide loaded MHC molecules remain longer on the cell surface than empty MHC molecules (Mahmutefendic et al. 2007). This could over time lead to an accumulation of similar pMHC complexes. It has been shown that pMHCs form clusters on the cell surface of antigen-presenting cells and that these clusters increase the avidity for TCR binding, resulting in a more efficient recognition (Lu et al. 2012). Second, although the mutations included in the presented peptide have been designed to mostly affect binding to MHC class I, an influence on the affinity of the T cell receptor (TCR) cannot be excluded. In general, how strong a TCR interacts with a pMHC complex depends on the number of amino acid residues of the TCR non-covalently interact with both the MHC molecule and the peptide. By using only mice on C57Bl/6 background, the MHC class I-sequence was kept constant in all the performed experiments. But it has been shown that the N- and C-termini of the loaded peptide contribute to the final conformation of pMHC complexes, thereby modulating the TCR-recognition (Wang et al. 2002). Data from *in vitro* studies showed indeed 10-fold higher affinity of P14 cells to C9M:MHC I complexes compared to wild type GP33 (Wang et al. 2002). The frequencies of GP33-specific CD8⁺ T cells are also higher after single intravenous infection with the high-affinity C9 rLCMV mutant (Fig.

8B), pointing towards better CTL priming due to more stable TCR:pMHC interaction. Therefore it is likely that both factors, a higher number of pMHC complexes on the neuronal surface as well as an increased TCR-pMHC affinity, contribute to a more efficient CD8⁺ T cell engagement and accelerated disease onset in carrier mice infected with virus co-expressing GP33-C9 mutant epitopes.

Irrespective of the occurrence of clinical disease, CTL infiltrates were present in all carrier-mice, although to a lesser extent in carrier brains of the MHC-non-binding variant of NP396-401, (Fig.7E, Fig.9E and Fig.10E). A reduced survival and expansion of NP396-specific CTLs in the absence of matching pMHC molecules in N5S carrier mice could explain the difference. The CD8⁺ T cells present in the CNS parenchyma of N5S carrier mice could be a mix of CTLs specific for GP33-41 and epitopes of the wild type LCMV that are not part of the predisposing rLCMV and thus not presented.

Depletion of immune cell fractions including CD8⁺ T cells and inhibition of migration have been associated with beneficial clinical outcomes in CD8⁺ T cell driven CNS disease, e.g. in multiple sclerosis (Coles et al. 2008; Polman et al. 2006). However, these treatments harbor considerable side effects due to their general immunosuppressive effects. The here-presented work in the viral déjà vu model now identifies the antigen-specific interaction between CD8⁺ T cells and neurons as key trigger of clinical disease in the CNS. This could set the cornerstone for further investigations of this interaction, leading to identify a more specific treatment for CD8⁺ T cell driven diseases.

In the second part of this work, the necessities of antigen specific CTL-neuron interactions and the consequences for the target cell were evaluated. Of note, no neuronal loss was observable in the acute phase of the viral déjà vu disease. FAS^{-/-} or Perforin-deficient carrier mice were neither protected, which seems to contradict earlier reports (Medana et al. 2000; Meuth et al. 2009; Sobottka et al. 2009). Nevertheless, this might be explainable by the present focus on the early phase of CTL-mediated disease.

Neurons have been reported to also actively regulate responses of incoming CTLs via cell adhesion molecules, FasL or release of soluble molecules (Tian, Rauvala, and Gahmberg 2009). On closer examination of sick animals it became clear that neuronal deafferentation was an important consequence of CTL attack. This was the case in the murine viral déjà vu model and found mirrored in human Rasmussen encephalitis patients. The changes in a neuronal soma under CTL-attack, which led to the retraction of axosomatic synapses, have to be identified. The findings that IFNGR^{-/-} mice were protected from déjà vu disease and that phosphorylated (=activated) STAT1 was found in

neurons of diseased mice and RE patients frequently in close association with CTLs, permits the assumption of a directed IFN- γ release towards target cells. It is known that IFN- γ enhances the production reactive oxygen species in microglia (Possel et al. 2000) and TNF- α release (Lafortune, Nalbantoglu, and Antel 1996). Thus, microglia were thought to be the main mediators of neurotoxicity during CNS inflammation. Until now, the direct effects of IFN- γ on neurons, as described in this work, are poorly understood. The IFNGR may form a neuron-specific, calcium permeable receptor complex with the AMPA receptor, as described in cultures of cortical neurons (Mizuno et al. 2008). Activation of the IFNGR leads to phosphorylation of the AMPA-subunit GluR1 via the Jak1-STAT1 pathway, leading to neurotoxic Ca²⁺ influx (Aarts et al. 2003) and subsequent inhibition of the mitochondrial respiratory chain by nNOS-derived nitric oxide (Mizuno et al. 2008). In fact, neurons within MS lesions show a reduced ATP production (Campbell and Mahad 2012) and this might be one reason why INF-g treatment in MS patients enhances disease progression (Panitch et al. 1987). The increased neuronal vulnerability to glutamate cytotoxicity might be connected to the observation that IFN- γ sensitizes inflamed brain regions to epileptic seizures, the earliest and most striking feature in Rasmussen encephalitis (Bien et al. 2005; Rasmussen, Olszewski, and LLoydsmith 1958).

In the viral déjà vu model, neuronal deafferentation was found to be the main correlate of disease. This could reduce electrical potential within affected neurons. Electrical silencing renders cultured neurons susceptible to CTL lysis *in vitro* (Neumann et al. 1995), but the consequences of electrical silencing *in vivo* are still unclear. It is important to note that the majority of deafferented neurons were virus infected and present in areas of high CTL-density. CTL-clusters in turn were found to be associated with nuclear P-STAT1 signals in neurons. This distribution pattern might be influenced by the formation of a local reticular fiber network in infected CNS-areas (Wilson et al. 2009), which could guide CD8⁺ cell migration towards infected, CXCL10-producing neurons in a CXCL10:CXCR3 dependent manner, as was shown for West Nile virus (Klein et al. 2005). How the IFN- γ release by CTLs induces the retraction of axosomatic boutons is not known. Retrograde IFN- γ signaling from axon-terminals to distal somata has been described (Kim et al. 2002) and could be important in conveying information about local injury or inflammation to distal brain regions.

It can be assumed that deafferentation and neuronal loss by cytolysis represent sequential steps, since loss was observed at later time points in viral déjà vu disease and is a dominant feature in chronic but not acute stages of RE (Bien et al. 2002; Pardo et al.

2004). IFN- γ is not only the mediator of the aforementioned deafferentation, but can also increase MHC class I expression (Joly and M B Oldstone 1992; Neumann et al. 1997) ultimately enhancing the probability of Fas- or perforin-mediated lysis by CTLs. Certainly, efficient CTL-mediated killing of virus-infected neurons would be detrimental for the host and more subtle mechanisms could have been selected for during phylogenesis. The importance of IFN- γ for non-cytolytic viral clearance from neurons has been described before (Binder and Griffin 2001). Reports on stroke (Zhang et al. 2005) and experimental autoimmune encephalomyelitis models (Nikić et al. 2011) illustrated the outstanding ability of neurons for recuperating from neurite damage. The direct role of IFN- γ and the Jak1–STAT1 pathway as a regulator of cellular immunity and inflammatory responses are well known. In addition IFN- γ and STAT1 can indirectly regulate cellular responses to other cytokines and inflammatory factors (e.g. TLR, pro- and anti-inflammatory cytokines, TH1 vs. TH2 T helper cell differentiation) (Hu and Ivashkiv 2009). Much less is known about the ways IFN- γ acts in antiviral responses, especially within the CNS. The involvement of the JAK1–STAT1 pathway in CTL-mediated neuronal damage opens potential opportunities for therapeutic approaches in various CNS diseases (Neumann et al. 2002). As a proof of principle, the present study demonstrated the neuroprotective effect of IFN- γ neutralization by antibody treatment in the viral déjà vu disease.

Summary

Although CD8⁺ T cells have been identified as important contributors to the pathogenesis of several inflammatory diseases such as virus-induced encephalitis, Rasmussen's encephalomyelitis, and more recently multiple sclerosis. The mechanism by which CD8⁺ T cells interact with target cells in the CNS *in vivo* and contribute to tissue damage and disease manifestation are so far unclear.

Here, the viral déjà vu model was exploited to investigate immunological prerequisites, molecular pathways as well as clinical and histomorphological consequences of CTL attack on neurons *in vivo*. This work identified CD8⁺ T cell derived IFN- γ , a non-cytolytic immunomodulatory effector molecule, as key mediator of inducing neuronal deafferentation and thereby contributing to acute déjà vu disease. Since no neuronal loss was evident during the early disease phase, the clinical symptoms were potentially caused by disturbances in deafferented neuronal networks. In addition, disease precipitation was independent of other effector pathways namely Perforin, FasL or TNF- α . Instead, this work identified IFN- γ as the key effector molecule by which CNS-infiltrating CD8⁺ T cells induce synaptic alterations in an epitope specific manner. In line with these findings, IFN- γ dependent phosphorylation and nuclear translocation of STAT1 was found in both the murine viral déjà vu model and human Rasmussen encephalitis, indicating similar underlying mechanisms in the human disease.

Moreover, by introducing NP396 and GP33 LCMV-epitope variants with different MHC class I-binding affinities into the viral genome, this study evaluated the contribution of these MHC class I restricted epitopes to CD8⁺ T cell infiltration and disease development in carrier mice. The epitope variants had the following relative H-2D^b affinities: NP396 > GP33_{C9M} \approx GP33_{C9I} > GP33 and non-binding epitope mutants NP396_{N5S} and GP33_{V3A}. Of the different NP and GP epitope combinations tested, it became evident that the presentation of the high-affinity epitope NP396 was essential for full disease precipitation. The numbers of total CTL infiltration in the brain parenchyma, as well as the frequencies of NP396 specific CD8⁺ cells were significantly reduced in carriers of the N5S mutation. In the absence of NP396 presentation, déjà vu disease could not be induced by artificially increasing GP33-specific CD8⁺ cells to match NP396-specific CD8⁺ numbers. Moreover, the introduction of GP33 high affinity mutants (C9M and C9I) into carrier mice did not induce disease in absence of NP396 presentation, confirming the importance of this epitope.

This work sheds new light on the interactions of the CNS with the immune system and describes a novel way of how antiviral CTLs specifically induce antiviral responses in infected neurons by inducing the neuronal Jak-STAT1 pathway using a directed cell-to-cell IFN- γ release. The fact that therapeutic IFN- γ blockade could protect mice from disease may have useful implications for the development of new neuroprotective strategies in CTL-driven viral and autoimmune CNS diseases.

References

- Aarts, Michelle, Koji Iihara, Wen-Li Wei, Zhi-Gang Xiong, Mark Arundine, Waldy Cerwinski, John F MacDonald, and Michael Tymianski. 2003. "A key role for TRPM7 channels in anoxic neuronal death." *Cell* 115(7): 863–77. <http://www.ncbi.nlm.nih.gov/pubmed/14697204> (January 11, 2013).
- Abrams, J S, M G Roncarolo, H Yssel, U Andersson, G J Gleich, and J E Silver. 1992. "Strategies of anti-cytokine monoclonal antibody development: immunoassay of IL-10 and IL-5 in clinical samples." *Immunological reviews* 127: 5–24. <http://www.ncbi.nlm.nih.gov/pubmed/1387110> (January 11, 2013).
- Adachi, M, S Suematsu, T Kondo, J Ogasawara, T Tanaka, N Yoshida, and S Nagata. 1995. "Targeted mutation in the Fas gene causes hyperplasia in peripheral lymphoid organs and liver." *Nature genetics* 11(3): 294–300. <http://www.ncbi.nlm.nih.gov/pubmed/7581453> (January 12, 2013).
- Albert, Matthew L, and Robert B Darnell. 2004. "Paraneoplastic neurological degenerations: keys to tumour immunity." *Nature reviews. Cancer* 4(1): 36–44. <http://www.ncbi.nlm.nih.gov/pubmed/14708025> (November 25, 2012).
- Andersen, I H, O Marker, and A R Thomsen. 1991. "Breakdown of blood-brain barrier function in the murine lymphocytic choriomeningitis virus infection mediated by virus-specific CD8+ T cells." *Journal of neuroimmunology* 31(2): 155–63. <http://www.ncbi.nlm.nih.gov/pubmed/1704015> (January 11, 2013).
- Barton, L L, and M B Mets. 2001. "Congenital lymphocytic choriomeningitis virus infection: decade of rediscovery." *Clinical infectious diseases : an official publication of the Infectious Diseases Society of America* 33(3): 370–4. <http://www.ncbi.nlm.nih.gov/pubmed/11438904>.
- Bergthaler, Andreas, Lukas Flatz, Ahmed N Hegazy, Susan Johnson, Edit Horvath, Max Löhning, and Daniel D Pinschewer. 2010. "Viral replicative capacity is the primary determinant of lymphocytic choriomeningitis virus persistence and immunosuppression." *Proceedings of the National Academy of Sciences of the United States of America* 107(50): 21641–6. <http://www.pubmedcentral.nih.gov/articlerender.fcgi?artid=3003068&tool=pmcentrez&rendertype=abstract> (November 5, 2012).
- Bergthaler, Andreas, Doron Merkler, Edit Horvath, Lukas Bestmann, and Daniel D Pinschewer. 2007. "Contributions of the lymphocytic choriomeningitis virus glycoprotein and polymerase to strain-specific differences in murine liver pathogenicity." *The Journal of general virology* 88(Pt 2): 592–603. <http://www.ncbi.nlm.nih.gov/pubmed/17251578> (November 30, 2012).
- Bien, C G, T Granata, C Antozzi, J H Cross, O Dulac, M Kurthen, H Lassmann, R Mantegazza, J-G Villemure, R Spreafico, and C E Elger. 2005. "Pathogenesis, diagnosis and treatment of Rasmussen encephalitis: a European consensus statement." *Brain : a journal of neurology* 128(Pt 3): 454–71. <http://www.ncbi.nlm.nih.gov/pubmed/15689357> (October 31, 2012).
- Bien, C G, H Urbach, M Deckert, J Schramm, O D Wiestler, H Lassmann, and C E Elger. 2002. "Diagnosis and staging of Rasmussen's encephalitis by serial MRI and histopathology." *Neurology* 58(2): 250–7. <http://www.ncbi.nlm.nih.gov/pubmed/11805253> (January 11, 2013).
- Binder, G K, and D E Griffin. 2001. "Interferon-gamma-mediated site-specific clearance of alphavirus from CNS neurons." *Science (New York, N.Y.)* 293(5528): 303–6. <http://www.ncbi.nlm.nih.gov/pubmed/11452126> (January 11, 2013).
- Bitsch, A, J Schuchardt, S Bunkowski, T Kuhlmann, and W Brück. 2000. "Acute axonal injury in multiple sclerosis. Correlation with demyelination and inflammation." *Brain : a journal of neurology* 123 (Pt 6): 1174–83. <http://www.ncbi.nlm.nih.gov/pubmed/10825356> (November 13, 2012).

- Boulter, Jonathan M, Nicole Schmitz, Andrew K Sewell, Andrew J Godkin, Martin F Bachmann, and Awen M Gallimore. 2007. "Potent T cell agonism mediated by a very rapid TCR/pMHC interaction." *European journal of immunology* 37(3): 798–806. <http://www.pubmedcentral.nih.gov/articlerender.fcgi?artid=2435421&tool=pmcentrez&rendertype=abstract> (December 6, 2012).
- Brown, S M, J H Subak-Sharpe, K G Warren, Z Wroblewska, and H Koprowski. 1979. "Detection by complementation of defective or uninducible (herpes simplex type 1) virus genomes latent in human ganglia." *Proceedings of the National Academy of Sciences of the United States of America* 76(5): 2364–8. <http://www.pubmedcentral.nih.gov/articlerender.fcgi?artid=383601&tool=pmcentrez&rendertype=abstract> (January 10, 2013).
- Camenga, D L, D H Walker, and F A Murphy. 1977. "Anticonvulsant prolongation of survival in adult murine lymphocytic choriomeningitis. I. Drug treatment and virologic studies." *Journal of neuropathology and experimental neurology* 36(1): 9–20. <http://www.ncbi.nlm.nih.gov/pubmed/833620> (January 11, 2013).
- Campbell, Graham R, and Don J Mahad. 2012. "Mitochondrial changes associated with demyelination: consequences for axonal integrity." *Mitochondrion* 12(2): 173–9. <http://www.ncbi.nlm.nih.gov/pubmed/21406249> (November 4, 2012).
- Campbell, Sandra J, V Hugh Perry, Fernando J Pitossi, Angus G Butchart, Mariela Chertoff, Sara Waters, Robert Dempster, and Daniel C Anthony. 2005. "Central nervous system injury triggers hepatic CC and CXC chemokine expression that is associated with leukocyte mobilization and recruitment to both the central nervous system and the liver." *The American journal of pathology* 166(5): 1487–97. <http://www.pubmedcentral.nih.gov/articlerender.fcgi?artid=1606402&tool=pmcentrez&rendertype=abstract> (January 12, 2013).
- Cao, W, M B Oldstone, and J C De La Torre. 1997. "Viral persistent infection affects both transcriptional and posttranscriptional regulation of neuron-specific molecule GAP43." *Virology* 230(2): 147–54. <http://www.ncbi.nlm.nih.gov/pubmed/9143270> (January 11, 2013).
- Carson, Monica J, Jonathan M Doose, Benoit Melchior, Christoph D Schmid, and Corinne C Ploix. 2009. "CNS immune privilege : hiding in plain sight." 48–65.
- Chevalier, Grégoire, Elsa Suberbielle, Céline Monnet, Valérie Duplan, Guillaume Martin-Blondel, Fanny Farrugia, Gwendal Le Masson, Roland Liblau, and Daniel Gonzalez-Dunia. 2011. "Neurons are MHC Class I-Dependent Targets for CD8 T Cells upon Neurotropic Viral Infection." *PLoS pathogens* 7(11): e1002393. <http://www.pubmedcentral.nih.gov/articlerender.fcgi?artid=3219726&tool=pmcentrez&rendertype=abstract> (November 30, 2011).
- Christensen, Jeanette Erbo Jan Pravsgaard, Anneline Nansen, Torben Moos, Bao Lu, Craig Gerard, and Allan Randrup Thomsen. 2004. "Efficient T-cell surveillance of the CNS requires expression of the CXC chemokine receptor 3." *The Journal of neuroscience : the official journal of the Society for Neuroscience* 24(20): 4849–58. <http://www.ncbi.nlm.nih.gov/pubmed/15152045> (October 5, 2012).
- Christensen, Jeanette Erbo, Carina de Lemos, Torben Moos, Jan Pravsgaard Christensen, and Allan Randrup Thomsen. 2006. "CXCL10 is the key ligand for CXCR3 on CD8+ effector T cells involved in immune surveillance of the lymphocytic choriomeningitis virus-infected central nervous system." *Journal of immunology (Baltimore, Md. : 1950)* 176(7): 4235–43. <http://www.ncbi.nlm.nih.gov/pubmed/16547260> (January 13, 2013).
- Coles, Alasdair J, D Alastair S Compston, Krzysztof W Selmaj, Stephen L Lake, Susan Moran, David H Margolin, Kim Norris, and P K Tandon. 2008. "Alemtuzumab vs. interferon beta-1a in early multiple sclerosis." *The New England journal of medicine* 359(17): 1786–801. <http://www.ncbi.nlm.nih.gov/pubmed/18946064> (January 13, 2013).

- Corriveau, R A, G S Huh, and C J Shatz. 1998. "Regulation of class I MHC gene expression in the developing and mature CNS by neural activity." *Neuron* 21(3): 505–20. <http://www.ncbi.nlm.nih.gov/pubmed/9768838> (January 10, 2013).
- Cserr, H F, and P M Knopf. 1992. "Cervical lymphatics, the blood-brain barrier and the immunoreactivity of the brain: a new view." *Immunology today* 13(12): 507–12. <http://www.ncbi.nlm.nih.gov/pubmed/1463583> (January 12, 2013).
- Dalmau, Josep, and Myrna R Rosenfeld. 2008. "Paraneoplastic syndromes of the CNS." *Lancet neurology* 7(4): 327–40. <http://www.pubmedcentral.nih.gov/articlerender.fcgi?artid=2367117&tool=pmcentrez&rendertype=abstract> (January 11, 2013).
- Ehrlich, Paul. 1885. "Das Sauerstoff-Bedürfnis des Organismus. Eine farbenanalytische Studie. [On the oxygen consumption of the body. A study using intravital dyes.]" Verlag von August Hirschwald, Berlin.
- Farina, Cinthia, Francesca Aloisi, and Edgar Meinl. 2007. "Astrocytes are active players in cerebral innate immunity." *Trends in immunology* 28(3): 138–45. <http://www.ncbi.nlm.nih.gov/pubmed/17276138> (November 5, 2012).
- Flatz, Lukas, Andreas Bergthaler, Juan Carlos de la Torre, and Daniel D Pinschewer. 2006. "Recovery of an arenavirus entirely from RNA polymerase I/II-driven cDNA." *Proceedings of the National Academy of Sciences of the United States of America* 103(12): 4663–8. <http://www.pubmedcentral.nih.gov/articlerender.fcgi?artid=1450228&tool=pmcentrez&rendertype=abstract> (January 11, 2013).
- Friese, Manuel a, and Lars Fugger. 2005. "Autoreactive CD8+ T cells in multiple sclerosis: a new target for therapy?" *Brain : a journal of neurology* 128(Pt 8): 1747–63. <http://www.ncbi.nlm.nih.gov/pubmed/15975943> (January 10, 2013).
- Gairin, J E, H Mazarguil, D Hudrisier, and M B Oldstone. 1995. "Optimal lymphocytic choriomeningitis virus sequences restricted by H-2Db major histocompatibility complex class I molecules and presented to cytotoxic T lymphocytes." *Journal of virology* 69(4): 2297–305. <http://www.pubmedcentral.nih.gov/articlerender.fcgi?artid=188900&tool=pmcentrez&rendertype=abstract>.
- Garin, N, and G Escher. 2001. "The development of inhibitory synaptic specializations in the mouse deep cerebellar nuclei." *Neuroscience* 105(2): 431–41. <http://www.ncbi.nlm.nih.gov/pubmed/11672609> (December 23, 2012).
- Gilmore, C P, I Donaldson, L Bö, T Owens, J Lowe, and N Evangelou. 2009. "Regional variations in the extent and pattern of grey matter demyelination in multiple sclerosis: a comparison between the cerebral cortex, cerebellar cortex, deep grey matter nuclei and the spinal cord." *Journal of neurology, neurosurgery, and psychiatry* 80(2): 182–7. <http://www.ncbi.nlm.nih.gov/pubmed/18829630> (January 11, 2013).
- Glynn, Marian W, Bradford M Elmer, Paula A Garay, Xiao-Bo Liu, Leigh A Needleman, Faten El-Sabeawy, and A Kimberley McAllister. 2011. "MHCI negatively regulates synapse density during the establishment of cortical connections." *Nature Neuroscience* 14(4): 442–451. <http://www.pubmedcentral.nih.gov/articlerender.fcgi?artid=3251641&tool=pmcentrez&rendertype=abstract> (November 16, 2012).
- Golde, WT, Peter Gollobin, and LL Rodriguez. 2005. "A rapid, simple, and humane method for submandibular bleeding of mice using a lancet." *Lab animal* 34(9): 39–43. <http://ukpmc.ac.uk/abstract/MED/16195737> (January 11, 2013).
- Goldmann, E. 1913. "Vitalfärbungen am Zentralnervensystem. Beitrag zur Physio-Pathologie des Plexus Choroideus und der Hirnhäute. [Intravital labelling of the central nervous system. A study on the pathophysiology of the choroid plexus and the meninges.]" *Physikalisch-Mathematische Classe 1*: 1–64.

- Guidotti, L G, T Ishikawa, M V Hobbs, B Matzke, R Schreiber, and F V Chisari. 1996. "Intracellular inactivation of the hepatitis B virus by cytotoxic T lymphocytes." *Immunity* 4(1): 25–36.
<http://www.ncbi.nlm.nih.gov/pubmed/8574849> (January 10, 2013).
- Hanisch, Uwe-Karsten, and Helmut Kettenmann. 2007. "Microglia: active sensor and versatile effector cells in the normal and pathologic brain." *Nature neuroscience* 10(11): 1387–94.
<http://www.ncbi.nlm.nih.gov/pubmed/17965659> (November 3, 2012).
- Hauser, S L, A K Bhan, F Gilles, M Kemp, C Kerr, and H L Weiner. 1986. "Immunohistochemical analysis of the cellular infiltrate in multiple sclerosis lesions." *Annals of neurology* 19(6): 578–87.
<http://www.ncbi.nlm.nih.gov/pubmed/3524414> (January 13, 2013).
- Hu, Xiaoyu, and Lionel B Ivashkiv. 2009. "Cross-regulation of signaling pathways by interferon-gamma: implications for immune responses and autoimmune diseases." *Immunity* 31(4): 539–50.
<http://www.pubmedcentral.nih.gov/articlerender.fcgi?artid=2774226&tool=pmcentrez&rendertype=abstract> (October 30, 2012).
- Huang, S, W Hendriks, A Althage, S Hemmi, H Bluethmann, R Kamijo, J Vilcek, R M Zinkernagel, and M Aguet. 1993. "Immune response in mice that lack the interferon-gamma receptor." *Science (New York, N.Y.)* 259(5102): 1742–5. <http://www.ncbi.nlm.nih.gov/pubmed/8456301> (January 12, 2013).
- Höftberger, R, F Aboul-Enein, W Brueck, C Lucchinetti, M Rodriguez, M Schmidbauer, K Jellinger, and H Lassmann. 2004. "Expression of major histocompatibility complex class I molecules on the different cell types in multiple sclerosis lesions." *Brain pathology (Zurich, Switzerland)* 14(1): 43–50.
<http://www.ncbi.nlm.nih.gov/pubmed/14997936>.
- Joly, E, L Mucke, and M B Oldstone. 1991. "Viral persistence in neurons explained by lack of major histocompatibility class I expression." *Science (New York, N.Y.)* 253(5025): 1283–5.
<http://www.ncbi.nlm.nih.gov/pubmed/1891717> (January 10, 2013).
- Joly, E, and M B Oldstone. 1992. "Neuronal cells are deficient in loading peptides onto MHC class I molecules." *Neuron* 8(6): 1185–90. <http://www.ncbi.nlm.nih.gov/pubmed/1610569> (January 11, 2013).
- Kallmann, B A, V Hummel, T Lindenlaub, K Ruprecht, K V Toyka, and P Rieckmann. 2000. "Cytokine-induced modulation of cellular adhesion to human cerebral endothelial cells is mediated by soluble vascular cell adhesion molecule-1." *Brain : a journal of neurology* 123 (Pt 4): 687–97.
<http://www.ncbi.nlm.nih.gov/pubmed/10734000> (January 11, 2013).
- Khanna, Kamal M, Robert H Bonneau, Paul R Kinchington, and Robert L Hendricks. 2003. "Herpes simplex virus-specific memory CD8+ T cells are selectively activated and retained in latently infected sensory ganglia." *Immunity* 18(5): 593–603.
<http://www.pubmedcentral.nih.gov/articlerender.fcgi?artid=2871305&tool=pmcentrez&rendertype=abstract> (January 10, 2013).
- Kim, In-Jung, Hiroko Nagasawa Beck, Pamela J Lein, and Dennis Higgins. 2002. "Interferon gamma induces retrograde dendritic retraction and inhibits synapse formation." *The Journal of neuroscience : the official journal of the Society for Neuroscience* 22(11): 4530–9.
<http://www.ncbi.nlm.nih.gov/pubmed/12040060>.
- Klein, Robyn S, Eugene Lin, Bo Zhang, Andrew D Luster, Judy Tollett, Melanie A Samuel, Michael Engle, and Michael S Diamond. 2005. "Neuronal CXCL10 directs CD8+ T-cell recruitment and control of West Nile virus encephalitis." *Journal of virology* 79(17): 11457–66.
<http://www.pubmedcentral.nih.gov/articlerender.fcgi?artid=1193600&tool=pmcentrez&rendertype=abstract> (January 11, 2013).
- Kotturi, Maya F, Iain Scott, Tom Wolfe, Bjoern Peters, Hilde Cheroutre, Matthias G Von Herrath, J Buchmeier, Howard Grey, Alessandro Sette, John Sidney, and Michael J Buchmeier. 2008. "the Degree of Epitope Diversity Shape CD8 T Cell."

- Kotturi, Maya F, Iain Scott, Tom Wolfe, Bjoern Peters, John Sidney, Hilde Cheroutre, Matthias G von Herrath, Michael J Buchmeier, Howard Grey, and Alessandro Sette. 2008. "Naive precursor frequencies and MHC binding rather than the degree of epitope diversity shape CD8+ T cell immunodominance." *Journal of immunology* (Baltimore, Md. : 1950) 181(3): 2124–33. <http://www.pubmedcentral.nih.gov/articlerender.fcgi?artid=3319690&tool=pmcentrez&rendertype=abstract> (January 10, 2013).
- Kuhlmann, Tanja, Gueanelle Lingfeld, Andreas Bitsch, Jana Schuchardt, and Wolfgang Brück. 2002. "Acute axonal damage in multiple sclerosis is most extensive in early disease stages and decreases over time." *Brain : a journal of neurology* 125(Pt 10): 2202–12. <http://www.ncbi.nlm.nih.gov/pubmed/12244078> (January 11, 2013).
- Kägi, D, B Ledermann, K Bürki, P Seiler, B Odermatt, K J Olsen, E R Podack, R M Zinkernagel, and H Hengartner. 1994. "Cytotoxicity mediated by T cells and natural killer cells is greatly impaired in perforin-deficient mice." *Nature* 369(6475): 31–7. <http://www.ncbi.nlm.nih.gov/pubmed/8164737> (December 6, 2012).
- Kägi, D, B Odermatt, P S Ohashi, R M Zinkernagel, and H Hengartner. 1996. "Development of insulinitis without diabetes in transgenic mice lacking perforin-dependent cytotoxicity." *The Journal of experimental medicine* 183(5): 2143–52. <http://www.pubmedcentral.nih.gov/articlerender.fcgi?artid=2192591&tool=pmcentrez&rendertype=abstract> (January 10, 2013).
- Lafortune, L, J Nalbantoglu, and J P Antel. 1996. "Expression of tumor necrosis factor alpha (TNF alpha) and interleukin 6 (IL-6) mRNA in adult human astrocytes: comparison with adult microglia and fetal astrocytes." *Journal of neuropathology and experimental neurology* 55(5): 515–21. <http://www.ncbi.nlm.nih.gov/pubmed/8627341> (January 11, 2013).
- Leist, T P, and R M Zinkernagel. 1990. "Treatment with anti-tumor necrosis factor alpha does not influence the immune pathological response against lymphocytic choriomeningitis virus." *Cytokine* 2(1): 29–34. <http://www.ncbi.nlm.nih.gov/pubmed/2129499> (January 13, 2013).
- Liebetanz, David, and Doron Merkler. 2006. "Effects of commissural de- and remyelination on motor skill behaviour in the cuprizone mouse model of multiple sclerosis." *Experimental neurology* 202(1): 217–24. <http://www.ncbi.nlm.nih.gov/pubmed/16857191> (October 11, 2012).
- Little, C C, and E E Tyzzer. 1916. "Further experimental studies on the inheritance of susceptibility to a Transplantable tumor, Carcinoma (J. W. A.) of the Japanese waltzing Mouse." *The Journal of medical research* 33(3): 393–453. <http://www.pubmedcentral.nih.gov/articlerender.fcgi?artid=2083849&tool=pmcentrez&rendertype=abstract> (January 10, 2013).
- Liu, Yawei, Ingrid Teige, Bryndis Birnir, and Shohreh Issazadeh-Navikas. 2006. "Neuron-mediated generation of regulatory T cells from encephalitogenic T cells suppresses EAE." *Nature medicine* 12(5): 518–25. <http://www.ncbi.nlm.nih.gov/pubmed/16633347> (December 12, 2012).
- Lu, Xiujun, James S Gibbs, Heather D Hickman, Alexandre David, Brian P Dolan, Yetao Jin, David M Kranz, Jack R Bennink, Jonathan W Yewdell, and Rajat Varma. 2012. "Endogenous viral antigen processing generates peptide-specific MHC class I cell-surface clusters." *Proceedings of the National Academy of Sciences of the United States of America* 109(38): 15407–12. <http://www.ncbi.nlm.nih.gov/pubmed/22949678> (November 6, 2012).
- Mahmutefendic, H, G Blagojevic, N Kucic, and P Lucin. 2007. "Constitutive internalization of murine MHC class I molecules." *Journal of cellular ...* 455(April 2006): 445–455. <http://onlinelibrary.wiley.com/doi/10.1002/jcp.20877/full> (January 11, 2013).

- Manning, P T, E M Johnson, C L Wilcox, M A Palmatier, and J H Russell. 1987. "MHC-specific cytotoxic T lymphocyte killing of dissociated sympathetic neuronal cultures." *The American journal of pathology* 128(3): 395–409.
<http://www.pubmedcentral.nih.gov/articlerender.fcgi?artid=1899668&tool=pmcentrez&rendertype=abstract> (January 10, 2013).
- Matloubian, M, S R Kolhekar, T Somasundaram, and R Ahmed. 1993. "Molecular determinants of macrophage tropism and viral persistence: importance of single amino acid changes in the polymerase and glycoprotein of lymphocytic choriomeningitis virus." *Journal of virology* 67(12): 7340–9.
<http://www.pubmedcentral.nih.gov/articlerender.fcgi?artid=238198&tool=pmcentrez&rendertype=abstract> (January 11, 2013).
- Matloubian, M, T Somasundaram, S R Kolhekar, R Selvakumar, and R Ahmed. 1990. "Genetic basis of viral persistence: single amino acid change in the viral glycoprotein affects ability of lymphocytic choriomeningitis virus to persist in adult mice." *The Journal of experimental medicine* 172(4): 1043–8.
<http://www.pubmedcentral.nih.gov/articlerender.fcgi?artid=2188602&tool=pmcentrez&rendertype=abstract> (January 11, 2013).
- McDole, Jeremiah R, Steve C Danzer, Raymund Y K Pun, Yi Chen, Holly L Johnson, Istvan Pirko, and Aaron J Johnson. 2010. "Rapid formation of extended processes and engagement of Theiler's virus-infected neurons by CNS-infiltrating CD8 T cells." *The American journal of pathology* 177(4): 1823–33.
<http://www.pubmedcentral.nih.gov/articlerender.fcgi?artid=2947278&tool=pmcentrez&rendertype=abstract> (January 11, 2013).
- McGavern, Dorian B, and Phi Truong. 2004. "Rebuilding an immune-mediated central nervous system disease: weighing the pathogenicity of antigen-specific versus bystander T cells." *Journal of immunology (Baltimore, Md. : 1950)* 173(8): 4779–90. <http://www.ncbi.nlm.nih.gov/pubmed/15470017> (January 13, 2013).
- Medana, I, Z Li, A Flügel, J Tschopp, H Wekerle, and H Neumann. 2001. "Fas ligand (CD95L) protects neurons against perforin-mediated T lymphocyte cytotoxicity." *Journal of immunology (Baltimore, Md. : 1950)* 167(2): 674–81. <http://www.ncbi.nlm.nih.gov/pubmed/11441070> (January 10, 2013).
- Medana, I M, A Gallimore, A Oxenius, M M Martinic, H Wekerle, and H Neumann. 2000. "MHC class I-restricted killing of neurons by virus-specific CD8+ T lymphocytes is effected through the Fas/FasL, but not the perforin pathway,." *European journal of immunology* 30(12): 3623–33.
<http://www.ncbi.nlm.nih.gov/pubmed/11169405> (January 10, 2013).
- Medana, I, M A Martinic, H Wekerle, and H Neumann. 2001. "Transection of major histocompatibility complex class I-induced neurites by cytotoxic T lymphocytes." *The American journal of pathology* 159(3): 809–15.
<http://www.pubmedcentral.nih.gov/articlerender.fcgi?artid=1850471&tool=pmcentrez&rendertype=abstract> (December 19, 2012).
- Medana, Isabelle, and MA Martinic. 2001. "Transection of major histocompatibility complex class I-induced neurites by cytotoxic T lymphocytes." *The American journal of ...* 159(3): 809–815.
<http://www.sciencedirect.com/science/article/pii/S0002944010617555> (October 11, 2012).
- MEDAWAR, P B. 1948. "Immunity to homologous grafted skin; the fate of skin homografts transplanted to the brain, to subcutaneous tissue, and to the anterior chamber of the eye." *British journal of experimental pathology* 29(1): 58–69.
<http://www.pubmedcentral.nih.gov/articlerender.fcgi?artid=2073079&tool=pmcentrez&rendertype=abstract> (January 10, 2013).
- Melzer, Nico, Sven G Meuth, and Heinz Wiendl. 2009. "CD8+ T cells and neuronal damage: direct and collateral mechanisms of cytotoxicity and impaired electrical excitability." *FASEB journal : official publication of the Federation of American Societies for Experimental Biology* 23(11): 3659–73.
<http://www.ncbi.nlm.nih.gov/pubmed/19567369> (October 11, 2012).

- Merkler, Doron, Edit Horvath, Wolfgang Bruck, Rolf M Zinkernagel, Juan Carlos, De Torre, and Daniel D Pinschewer. 2006. “Viral déjà vu ’ elicits organ-specific immune disease independent of reactivity to self.” *Seven* 116(5).
- Ter Meulen, V, M J Carter, H Wege, and R Watanabe. 1984. “Mechanisms and consequences of virus persistence in the human nervous system.” *Annals of the New York Academy of Sciences* 436: 86–97. <http://www.ncbi.nlm.nih.gov/pubmed/6398025> (January 10, 2013).
- Meuth, Sven G, Alexander M Herrmann, Ole J Simon, Volker Siffrin, Nico Melzer, Stefan Bittner, Patrick Meuth, Harald F Langer, Stefan Hallermann, Nadia Boldakowa, Josephine Herz, Thomas Munsch, Peter Landgraf, Orhan Aktas, Manfred Heckmann, Volkmar Lessmann, Thomas Budde, Bernd C Kieseier, Frauke Zipp, and Heinz Wiendl. 2009. “Cytotoxic CD8+ T cell-neuron interactions: perforin-dependent electrical silencing precedes but is not causally linked to neuronal cell death.” *The Journal of neuroscience : the official journal of the Society for Neuroscience* 29(49): 15397–409. <http://www.ncbi.nlm.nih.gov/pubmed/20007464> (December 19, 2012).
- Mizuno, Tetsuya, Guiqin Zhang, Hideyuki Takeuchi, Jun Kawanokuchi, Jinyan Wang, Yoshifumi Sonobe, Shijie Jin, Naoki Takada, Yukio Komatsu, and Akio Suzumura. 2008. “Interferon-gamma directly induces neurotoxicity through a neuron specific, calcium-permeable complex of IFN-gamma receptor and AMPA GluR1 receptor.” *FASEB journal : official publication of the Federation of American Societies for Experimental Biology* 22(6): 1797–806. <http://www.ncbi.nlm.nih.gov/pubmed/18198214> (November 28, 2012).
- Van der Most, R G, K Murali-Krishna, J L Whitton, C Oseroff, J Alexander, S Southwood, J Sidney, R W Chesnut, A Sette, and R Ahmed. 1998. “Identification of Db- and Kb-restricted subdominant cytotoxic T-cell responses in lymphocytic choriomeningitis virus-infected mice.” *Virology* 240(1): 158–67. <http://www.ncbi.nlm.nih.gov/pubmed/9448700>.
- Neumann, H, A Cavalié, D E Jenne, and H Wekerle. 1995. “Induction of MHC class I genes in neurons.” *Science (New York, N.Y.)* 269(5223): 549–52. <http://www.ncbi.nlm.nih.gov/pubmed/7624779> (January 11, 2013).
- Neumann, H, H Schmidt, A Cavalié, D Jenne, and H Wekerle. 1997. “Major histocompatibility complex (MHC) class I gene expression in single neurons of the central nervous system: differential regulation by interferon (IFN)-gamma and tumor necrosis factor (TNF)-alpha.” *The Journal of experimental medicine* 185(2): 305–16. <http://www.pubmedcentral.nih.gov/articlerender.fcgi?artid=2196130&tool=pmcentrez&rendertype=abstract> (January 11, 2013).
- Neumann, Harald, Isabelle M Medana, Jan Bauer, and Hans Lassmann. 2002. “Cytotoxic T lymphocytes in autoimmune and degenerative CNS diseases.” *Trends in neurosciences* 25(6): 313–9. <http://www.ncbi.nlm.nih.gov/pubmed/12086750>.
- Nikić, Ivana, Doron Merkler, Catherine Sorbara, Mary Brinkoetter, Mario Kreutzfeldt, Florence M Bareyre, Wolfgang Brück, Derron Bishop, Thomas Misgeld, and Martin Kerschensteiner. 2011. “A reversible form of axon damage in experimental autoimmune encephalomyelitis and multiple sclerosis.” *Nature medicine* 17(4): 495–9. <http://www.ncbi.nlm.nih.gov/pubmed/21441916> (November 6, 2012).
- Oldstone, M B. 1985. “An old nemesis in new clothing: viruses playing new tricks by causing cytopathology in the absence of cytolysis.” *The Journal of infectious diseases* 152(4): 665–7. <http://www.ncbi.nlm.nih.gov/pubmed/3876393> (January 11, 2013).
- Oldstone, M, and KP Campbell. 2011. “Decoding arenavirus pathogenesis: Essential roles for alpha-dystroglycan-virus interactions and the immune response.” *Virology* 411(2): 170–179. <http://www.sciencedirect.com/science/article/pii/S0042682210007415> (October 11, 2012).
- Olert, J, K H Wiedorn, T Goldmann, H Kühl, Y Mehraein, H Scherthan, F Niketeghad, E Vollmer, A M Müller, and J Müller-Navia. 2001. “HOPE fixation: a novel fixing method and paraffin-embedding technique for human soft tissues.” *Pathology, research and practice* 197(12): 823–6. <http://www.ncbi.nlm.nih.gov/pubmed/11795830> (January 11, 2013).

- Panitch, H S, R L Hirsch, A S Haley, and K P Johnson. 1987. "Exacerbations of multiple sclerosis in patients treated with gamma interferon." *Lancet* 1(8538): 893–5. <http://www.ncbi.nlm.nih.gov/pubmed/2882294> (January 6, 2013).
- Pardo, Carlos A, Eileen P G Vining, Liping Guo, Richard L Skolasky, Benjamin S Carson, and John M Freeman. 2004. "The pathology of Rasmussen syndrome: stages of cortical involvement and neuropathological studies in 45 hemispherectomies." *Epilepsia* 45(5): 516–26. <http://www.ncbi.nlm.nih.gov/pubmed/15101833> (January 5, 2013).
- Penn, Dustin J. 2002. "Major Histocompatibility."
- Peschon, J J, D S Torrance, K L Stocking, M B Glaccum, C Otten, C R Willis, K Charrier, P J Morrissey, C B Ware, and K M Mohler. 1998. "TNF receptor-deficient mice reveal divergent roles for p55 and p75 in several models of inflammation." *Journal of immunology (Baltimore, Md. : 1950)* 160(2): 943–52. <http://www.ncbi.nlm.nih.gov/pubmed/9551933> (January 12, 2013).
- Pinschewer, Daniel D, Mar Perez, and Juan Carlos de la Torre. 2005. "Dual role of the lymphocytic choriomeningitis virus intergenic region in transcription termination and virus propagation." *Journal of virology* 79(7): 4519–26. <http://www.pubmedcentral.nih.gov/articlerender.fcgi?artid=1061552&tool=pmcentrez&rendertype=abstract> (January 10, 2013).
- Pinschewer, Daniel D, Mar Perez, Ana B Sanchez, and Juan Carlos de la Torre. 2003. "Recombinant lymphocytic choriomeningitis virus expressing vesicular stomatitis virus glycoprotein." *Proceedings of the National Academy of Sciences of the United States of America* 100(13): 7895–900. <http://www.pubmedcentral.nih.gov/articlerender.fcgi?artid=164684&tool=pmcentrez&rendertype=abstract>.
- Pinschewer, Daniel D, Mariann Schedensack, Andreas Bergthaler, Edit Horvath, Wolfgang Brück, Max Löhning, and Doron Merkler. 2010. "T cells can mediate viral clearance from ependyma but not from brain parenchyma in a major histocompatibility class I- and perforin-independent manner." *Brain : a journal of neurology* 133(Pt 4): 1054–66. <http://www.ncbi.nlm.nih.gov/pubmed/20354003> (October 11, 2011).
- Pircher, H, K Bürki, R Lang, H Hengartner, and R M Zinkernagel. 1989. "Tolerance induction in double specific T-cell receptor transgenic mice varies with antigen." *Nature* 342(6249): 559–61. <http://www.ncbi.nlm.nih.gov/pubmed/2573841> (January 12, 2013).
- Polman, Chris H, Paul W O'Connor, Eva Havrdova, Michael Hutchinson, Ludwig Kappos, David H Miller, J Theodore Phillips, Fred D Lublin, Gavin Giovannoni, Andrzej Wajgt, Martin Toal, Frances Lynn, Michael A Panzara, and Alfred W Sandrock. 2006. "A randomized, placebo-controlled trial of natalizumab for relapsing multiple sclerosis." *The New England journal of medicine* 354(9): 899–910. <http://www.ncbi.nlm.nih.gov/pubmed/16510744> (January 3, 2013).
- Possel, H, H Noack, J Putzke, G Wolf, and H Sies. 2000. "Selective upregulation of inducible nitric oxide synthase (iNOS) by lipopolysaccharide (LPS) and cytokines in microglia: in vitro and in vivo studies." *Glia* 32(1): 51–9. <http://www.ncbi.nlm.nih.gov/pubmed/10975910> (January 11, 2013).
- Ramana, Chilakamarti V, M Pilar Gil, Robert D Schreiber, and George R Stark. 2002. "Stat1-dependent and -independent pathways in IFN-gamma-dependent signaling." *Trends in immunology* 23(2): 96–101. <http://www.ncbi.nlm.nih.gov/pubmed/11929133> (November 11, 2012).
- Rammensee, H G, T Friede, and S Stevanović. 1995. "MHC ligands and peptide motifs: first listing." *Immunogenetics* 41(4): 178–228. <http://www.ncbi.nlm.nih.gov/pubmed/7890324> (January 13, 2013).
- Ransohoff, Richard M, Pia Kivisäkk, and Grahame Kidd. 2003. "Three or more routes for leukocyte migration into the central nervous system." *Nature reviews. Immunology* 3(7): 569–81. <http://www.ncbi.nlm.nih.gov/pubmed/12876559> (November 12, 2012).

- Rasmussen, T, J Olszewski, and D LLOYDSMITH. 1958. "Focal seizures due to chronic localized encephalitis." *Neurology* 8(6): 435–45. <http://www.ncbi.nlm.nih.gov/pubmed/13566382> (January 11, 2013).
- Reboldi, Andrea, Caroline Coisne, Dirk Baumjohann, Federica Benvenuto, Denise Bottinelli, Sergio Lira, Antonio Uccelli, Antonio Lanzavecchia, Britta Engelhardt, and Federica Sallusto. 2009. "C-C chemokine receptor 6-regulated entry of TH-17 cells into the CNS through the choroid plexus is required for the initiation of EAE." *Nature immunology* 10(5): 514–23. <http://www.ncbi.nlm.nih.gov/pubmed/19305396> (November 3, 2012).
- Rensing-Ehl, A, U Malipiero, M Irmeler, J Tschopp, D Constam, and A Fontana. 1996. "Neurons induced to express major histocompatibility complex class I antigen are killed via the perforin and not the Fas (APO-1/CD95) pathway." *European journal of immunology* 26(9): 2271–4. <http://www.ncbi.nlm.nih.gov/pubmed/8814277> (January 10, 2013).
- Rock, Kenneth L, and Lianjun Shen. 2005. "Cross-presentation: underlying mechanisms and role in immune surveillance." *Immunological reviews* 207: 166–83. <http://www.ncbi.nlm.nih.gov/pubmed/16181335> (November 26, 2012).
- Rowe, W P, P H Black, and R H Levey. 1963. "Protective Effect of Neonatal Thymectomy on Mouse LCM Infection." *Proceedings of the Society for Experimental Biology and Medicine. Society for Experimental Biology and Medicine (New York, N.Y.)* 114: 248–51. <http://www.ncbi.nlm.nih.gov/pubmed/14076900> (January 13, 2013).
- Salvato, M, P Borrow, E Shimomaye, and M B Oldstone. 1991. "Molecular basis of viral persistence: a single amino acid change in the glycoprotein of lymphocytic choriomeningitis virus is associated with suppression of the antiviral cytotoxic T-lymphocyte response and establishment of persistence." *Journal of virology* 65(4): 1863–9. <http://www.pubmedcentral.nih.gov/articlerender.fcgi?artid=239996&tool=pmcentrez&rendertype=abstract> (January 11, 2013).
- Scheikl, Tanja, Béatrice Pignolet, Cécile Dalard, Sabine Desbois, Danièle Raison, Masanori Yamazaki, Abdelhadi Saoudi, Jan Bauer, Hans Lassmann, Hélène Hardin-Pouzet, and Roland S Liblau. 2012. "Cutting edge: neuronal recognition by CD8 T cells elicits central diabetes insipidus." *Journal of immunology (Baltimore, Md. : 1950)* 188(10): 4731–5. <http://www.ncbi.nlm.nih.gov/pubmed/22504649> (November 8, 2012).
- Schroder, Kate, Paul J Hertzog, Timothy Ravasi, and David A Hume. 2004. "Interferon-gamma: an overview of signals, mechanisms and functions." *Journal of leukocyte biology* 75(2): 163–89. <http://www.ncbi.nlm.nih.gov/pubmed/14525967> (November 28, 2012).
- Schwab, Nicholas, Christian G Bien, Anne Waschbisch, Albert Becker, Giles H Vince, Klaus Dornmair, and Heinz Wiendl. 2009. "CD8+ T-cell clones dominate brain infiltrates in Rasmussen encephalitis and persist in the periphery." *Brain : a journal of neurology* 132(Pt 5): 1236–46. <http://www.ncbi.nlm.nih.gov/pubmed/19179379> (January 11, 2013).
- Sequiera, L W, L C Jennings, L H Carrasco, M A Lord, A Curry, and R N Sutton. 1979. "Detection of herpes-simplex viral genome in brain tissue." *Lancet* 2(8143): 609–12. <http://www.ncbi.nlm.nih.gov/pubmed/90272> (January 10, 2013).
- Sobottka, Bettina, Melanie Denise Harrer, Urs Ziegler, Katja Fischer, Heinz Wiendl, Thomas Hünig, Burkhard Becher, and Norbert Goebels. 2009. "Collateral bystander damage by myelin-directed CD8+ T cells causes axonal loss." *The American journal of pathology* 175(3): 1160–6. <http://www.pubmedcentral.nih.gov/articlerender.fcgi?artid=2731134&tool=pmcentrez&rendertype=abstract> (November 15, 2012).
- Steinman, L. 2001. "Myelin-specific CD8 T cells in the pathogenesis of experimental allergic encephalitis and multiple sclerosis." *The Journal of experimental medicine* 194(5): F27–30. <http://www.pubmedcentral.nih.gov/articlerender.fcgi?artid=2195937&tool=pmcentrez&rendertype=abstract> (January 11, 2013).

- Stephensen, C B, S R Blount, R E Lanford, K V Holmes, R J Montali, M E Fleenor, and J F Shaw. 1992. "Prevalence of serum antibodies against lymphocytic choriomeningitis virus in selected populations from two U.S. cities." *Journal of medical virology* 38(1): 27–31. <http://www.ncbi.nlm.nih.gov/pubmed/1402829> (January 12, 2013).
- Stinchcombe, Jane C, and Gillian M Griffiths. 2007. "Secretory mechanisms in cell-mediated cytotoxicity." *Annual review of cell and developmental biology* 23: 495–517. <http://www.ncbi.nlm.nih.gov/pubmed/17506701> (November 16, 2012).
- Storm, Pernille, Christina Bartholdy, Maria Rathman Sørensen, Jan Pravsgaard Christensen, and Allan Randrup Thomsen. 2006. "Perforin-deficient CD8+ T cells mediate fatal lymphocytic choriomeningitis despite impaired cytokine production." *Journal of virology* 80(3): 1222–30. <http://www.pubmedcentral.nih.gov/articlerender.fcgi?artid=1346958&tool=pmcentrez&rendertype=abstract> (January 13, 2013).
- Sullivan, Brian M, Sébastien F Emonet, Megan J Welch, Andrew M Lee, Kevin P Campbell, Juan C de la Torre, and Michael B Oldstone. 2011. "Point mutation in the glycoprotein of lymphocytic choriomeningitis virus is necessary for receptor binding, dendritic cell infection, and long-term persistence." *Proceedings of the National Academy of Sciences of the United States of America* 108(7): 2969–74. <http://www.pubmedcentral.nih.gov/articlerender.fcgi?artid=3041138&tool=pmcentrez&rendertype=abstract> (November 5, 2012).
- Tian, Li, Heikki Rauvala, and Carl G Gahmberg. 2009. "Neuronal regulation of immune responses in the central nervous system." *Trends in immunology* 30(2): 91–9. <http://www.ncbi.nlm.nih.gov/pubmed/19144568> (October 6, 2012).
- Traub, E. 1936. "Persistence of Lymphocytic Choriomeningitis Virus in Immune Animals and its Relation to Immunity." *The Journal of experimental medicine* 63(6): 847–61. <http://www.pubmedcentral.nih.gov/articlerender.fcgi?artid=2133407&tool=pmcentrez&rendertype=abstract> (January 13, 2013).
- Wang, Bo, Ashawni Sharma, Robert Maile, Mohamed Saad, Edward J Collins, and Jeffrey a Frelinger. 2002. "Peptidic termini play a significant role in TCR recognition." *Journal of immunology* (Baltimore, Md. : 1950) 169(6): 3137–45. <http://www.ncbi.nlm.nih.gov/pubmed/12218131>.
- Warkel, R L, C F Rinaldi, W H Bancroft, R D Cardiff, G E Holmes, and R E Wilsnack. 1973. "Fatal acute meningoencephalitis due to lymphocytic choriomeningitis virus." *Neurology* 23(2): 198–203. <http://www.ncbi.nlm.nih.gov/pubmed/4568992> (January 12, 2013).
- Willing, Anne, and Manuel a Friese. 2012. "CD8-mediated inflammatory central nervous system disorders." *Current opinion in neurology* 25(3): 316–21. <http://www.ncbi.nlm.nih.gov/pubmed/22547102> (November 21, 2012).
- Wilson, Emma H, Tajie H Harris, Paulus Mrass, Beena John, Elia D Tait, Gregory F Wu, Marion Pepper, E John Wherry, Florence Dzierzinski, David Roos, Philip G Haydon, Terri M Laufer, Wolfgang Weninger, and Christopher a Hunter. 2009. "Behavior of parasite-specific effector CD8+ T cells in the brain and visualization of a kinesis-associated system of reticular fibers." *Immunity* 30(2): 300–11. <http://www.pubmedcentral.nih.gov/articlerender.fcgi?artid=2696229&tool=pmcentrez&rendertype=abstract> (January 10, 2013).
- Zajac, Allan J, John M Dye, and Daniel G Quinn. 2003. "Control of lymphocytic choriomeningitis virus infection in granzyme B deficient mice." *Virology* 305(1): 1–9. <http://www.ncbi.nlm.nih.gov/pubmed/12504535> (January 13, 2013).
- Zhang, Shengxiang, Jamie Boyd, Kerry Delaney, and Timothy H Murphy. 2005. "Rapid reversible changes in dendritic spine structure in vivo gated by the degree of ischemia." *The Journal of neuroscience : the official journal of the Society for Neuroscience* 25(22): 5333–8. <http://www.ncbi.nlm.nih.gov/pubmed/15930381> (November 23, 2012).

Zinkernagel, R M, and P C Doherty. 1974. "Restriction of in vitro T cell-mediated cytotoxicity in lymphocytic choriomeningitis within a syngeneic or semiallogeneic system." *Nature* 248(450): 701-2.
<http://www.ncbi.nlm.nih.gov/pubmed/4133807> (January 10, 2013).

Acknowledgements

I would like to thank my supervisor Prof. D. Merkler for inviting me to his laboratory and giving me the opportunity to take part in a very interesting and challenging project. I am very grateful for his excellent support and guidance throughout the project. His cordiality and professional and personal integrity are of high value for me.

I would also like to thank Prof. W. Brück for his supervision and for giving me the opportunity to work in the department of neuropathology, Göttingen.

My sincere thanks go to Prof. J. Wienands and Prof. M. Simons for being members of my thesis committee.

Furthermore, I would like to thank our collaboration partners in Geneva (Prof. D. Pinschewer), Vienna (Dr. A. Bergthaler) and Lausanne (Prof. D. Zehn). Especially D. Utzschneider for his contribution to the epitope mutants.

My special thanks go out to all the people in the neuropathology in Göttingen, for always being a helpful, supportive and funny. You and all the after-work beers and 'Phrasenschwein' battles (thanks Tommy!) will always remain in good memory.

I would also like to thank my lab mates in Geneva Karin, Tanja and Ingrid for all her support and friendship. Special thanks to Karin, who only outspeeds her proofreading skills with her coffee-drinking skills ;)

Very special thanks go to my good friends from the Geneva-Crew Sandra, Fe, Meli, Ben and Praxi for great times inside and outside the lab.

A big 'thank you' to my parents for not stopping asking 'When are you going to finish' and not stopping supporting me.

And finally, my biggest thanks to Carmen, for all her support, help and understanding patience. You are the best!